HEWLETT-PACKARD
JOURNAL

HEWLETT-PACKARD
JOURNAL

February 1987 Volume 38 ● Number 2

Articles

Departments

© Hewlett-Packard Company 1987 Printed in U.S.A.

In this Issue

If "fiber optics" wasn't a household word before, it's about to become one. In the U.S.A., where several long-distance telephone companies compete, we're now seeing television commercials promising clearer, quieter communications thanks to fiber optic transmission. This is indicative of the explosive growth rate of fiber optic communication links in the last few years. Applications have expanded from multimode propagation at a wavelength of 850 nanometers to single-mode (more suitable for long distances) at 1300 and 1550 nanometers. To meet the need for versatile, precise instruments to test fiber optic receivers, transmitters, and components at these wavelengths, HP designers have come up with a new family of fiber optic test instruments (page 4). The family includes an optical average power meter (pages 8 and 12) that works with either of two optical heads (page 22), depending on the wavelength. The optical heads have individual calibration data stored in ROM and a high-precision optical interface. Two models of variable optical attenuator (page 31) cover the three wavelength windows; one model is distinguished by its usability in both single-mode and multimode applications. Three models of optical source (page 6) provide highly stable optical power for testing components and receivers. An optical switch (page 36) provides flexibility in building test setups. Because test instruments have to be connected and disconnected hundreds of times during their lifetimes, the new family is equipped with a special connector (page 28) designed for high stability, repeatability, and lifetime. A crucial design consideration for the optical heads was the choice of a detector to convert optical power to electric current. The article on page 16 presents a survey of detector characteristics that illuminates the reasoning behind the choice of different detectors for the two optical heads.

Accurate, repeatable device and component measurements become more difficult at frequencies in the microwave range. As a result, microwave designers have always had a problem getting circuits designed using measured data to work as expected. HP microwave designers have now addressed one aspect of this problem—the need for a standard fixture, capable of accurate calibration and high repeatability, for measuring transistors in a variety of package styles. Their solution uses the error-correction capabilities of the HP 8510 Microwave Network Analyzer, and consists of a specially designed transistor fixture and some software for an HP 9000 workstation. The article on page 39 explains the theory and applications of the HP 85014A Active Device Measurements Pac.

-R. P. Dolan

Cover

The detector assembly of the HP 81520A Optical Head.

What's Ahead

In March, we continue our series of issues on the new HP Precision Architecture. There'll be an article on the first two products based on the architecture—the HP 9000 Model 840 and HP 3000 Series 930 Computers. The terminal controller for the Series 930, the test system for both products, and compiler performance issues will also be covered.

A New Family of Precise, Reliable, and Versatile Fiber Optic Measurement Instruments

The family members are an average power meter, two optical heads, three LED sources, two optical attenuators, and an optical switch.

by Michael Fleischer-Reumann

SINCE THE FIRST CAREFUL STEPS in fiber optic communication techniques, it has taken only a short time for this fast-developing market to reach a 30% annual growth rate and an installed base of 500,000 km of fiber core in the U.S.A. in 1985. The shift from multimode first-window ($\lambda = 850$ nm) components to single-mode second-window (1.3 μm) and third-window (1.55 μm) components occurred earlier than expected, as soon as reliable and reasonably priced components became available. The end of this rapid development is not yet in sight.

Of course, the more that fiber optic links come into use replacing old copper communications links or opening new paths, and the more megabytes of information are transmitted, the more dependent we become on the reliability and serviceability of these systems. Systems and components manufacturers and telecommunications companies are demanding accurate, precise, and reliable measurement equipment to ensure this high reliability.

A new family of Hewlett-Packard fiber optic measurement instruments takes some new approaches to achieve the high goals of reliability and honest accuracy that customers expect and need. The family includes the HP 8152A Optical Average Power Meter (see article, page 8), which is used with the HP 81520A and 81521B Optical Heads (see article, page 22), the HP 8154B LED Sources (see article, page 6), the HP 8158B Optical Attenuators (see article, page 31), and the HP 8159A Optical Switch (see article, page 36).

The fiberless technique used in the HP 8158B Option 002 Optical Attenuator makes it, to our knowledge, the only variable optical attenuator usable in both single-mode and multimode systems. The HP 81520A and 81521B Optical Heads for the HP 8152A Power Meter feature individual wavelength calibration stored in EEPROM and a specially designed high-precision optical interface.

All of the instruments have HP-IB (IEEE 488/IEC 625) capability for computer-controlled operation in production, R&D, or maintenance.

Fig. 1. HP's new family of programmable, fully specified, fiber optic test instruments includes (clockwise from top left) the HP 8158B Optical Attenuator, the HP 8154B LED Source, the HP 8152A Optical Average Power Meter, the HP 8159A Optical Switch, and the HP 81521B Optical Head (two shown in foreground).

A Color-Coding Scheme for Fiber Optic Instruments and Accessories

Imagine you are working in R&D or a production environment and you are dealing with both 850-nm MM and 1300-nm SM components. You want to select the right accessories for your measurement setup (let's say patchcord cables, lens and connector adapters, a splitter, or attenuators). Many accessories and measurement instruments are only usable for a special wavelength or fiber core diameter. HP marks its accessories with a user-friendly color code to show the purpose of each device clearly. For example, in Fig. 1, the HP 81050BL Lens Adapter's color code reads as follows:

- Red/orange: second and third wavelength windows (1.3 μm and 1.55 μm)
- Green/blue: 50 to 62 μm core diameter.
  The complete code is listed below:

Wavelength:	brown	1st window
	red	2nd window
	orange	3rd window

Core Diameter:	white	9 μm (SI-SM)
	green	50 μm (GI-MM)
	blue	62 μm (GI-MM)
	gray	85 μm (GI-MM)
	black	>100 μm (SI-MM)

where:	SI	= step-index
	GI	= graded-index
	SM	= single-mode
	MM	= multimode.

Fig. 1. HP 81050BL Lens Adapter, showing color coding.

Measurement Standards Needed

The more communication networks expand, the more systems of different manufacturers have to work together. Here two problems can arise, both related to standardization issues.

First, it is important that everyone measure and specify according to the same standards. In developing the new family of fiber optic instruments, HP has worked extensively with standards laboratories such as NBS in the U.S.A. and PTB in Germany, and has installed its own state-of-the-art fiber optic standards laboratory. The goal has been to increase not only the relative accuracy of the instruments (many measurements in fiber optics are purely relative), but especially to increase their absolute accuracy, particularly that of the HP 8154B LED Source and the HP 8152A Power Meter. The HP 81520A and 81521B Optical Heads' flexible optical interface is an advantage in this effort, because it allows calibration with either parallel or divergent beams.

Second, there is a need for standardization in other areas, from seemingly trivial things like connectors to more sophisticated measurement procedures.

Because of the number of different fibers, wavelengths, and connectors in use, HP has adopted a color-code approach to help the user work with HP equipment and accessories (see box, this page).

Acknowledgments

To the family of instruments introduced in this article, many people contributed either directly as R&D engineers and project leaders, marketing engineers, or production and QA personnel, or indirectly, by offering their ideas as valuable inputs. I would especially like to mention Peter Aue, fiber optics section manager, and Christian Hentschel, who is a member of several committees that are involved with laser safety or standardization of measurement methods, tools, and terms.

Stable LED Sources for a Wide Range of Applications

by Michael Fleischer-Reumann

CHARACTERIZATION OF PASSIVE fiber optic components like connectors, splitters, patchcord cables, attenuators, and other devices usually requires a stable light source. The absolute value of its power output is not critical. Stability is the main feature. For fewer problems from interference or modal noise, a light-emitting diode (LED) is preferred over a laser diode.

The new HP 8154B Optical Sources (Fig. 1) provide stable optical power for testing fiber optic components. The HP 8154B Option 001 provides −17 dBm (20 μW) at 850 nm, the HP 8154B Option 002 provides −20 dBm (10 μW) at 1300 nm, and the HP 8154B Option 003 provides −23 dBm (5μW) at 1550 nm. Short-term stability is better than 0.02 dB within a ±2°C window for one hour. Stability for one year over the entire operating range of 0°C to 55°C is better than 0.3 dB. The HP 8154A/B/C output is CW, but can be externally modulated at frequencies up to 1 MHz. Each source also has a built-in 270-Hz square-wave generator. All of its functions can be controlled via the HP-IB (IEEE 488/IEC 625).

Factors Influencing Stability

Two major factors influence the stability of an optical source. The first, of course, is the stability of the light that is generated by the LED and launched into the internal fiber available at the connector on the front panel. The second factor, which is usually ignored, is the stability of the mechanism used for coupling the light into the fiber that the user connects to the light source. The user is generally interested in the amount and stability of the power at the end of the connected fiber. This means that a precise, reliable, very stable connector with low temperature dependence is required.

The Diamond® HMS-10/HP connector used in the HP 8154B and other HP fiber optic instruments, patchcords, and other accessories (see article, page 28) meets these requirements. The mechanics of this connector are independent of whether it is used with a 50/125-μm or 62/125-μm graded-index multimode fiber or a 9/125-μm step-index single-mode fiber. This means that without loss of stability one can couple light into a variety of fibers. Only the absolute power changes, for example from −20 dBm into a 50/125-μm fiber to −36 dBm into a 9/125-μm single-mode fiber for the long-wavelength sources (HP 8154B Options 002 and 003).

The HMS-10/HP connector offers high stability and repeatability and tolerates a large number of mating cycles. Another major advantage of the connector and the HP 8154B front-panel design is that the connector is easily cleaned. This is essential for reliability of the optical contact. No tools for opening the instrument are required. Simply unscrewing the outside part of the connector gives direct access to the instrument's inside connector for cleaning.

LED Stability

Fig. 2 shows the LED output power as a function of temperature relative to the power at 25°C, for a current of I_{LED} = 100 mA. The temperature coefficient (TC) for short-wavelength devices (850-nm) is rather small, about −0.02 dB/°C, which is not far from the design goal. It also does not vary much between individual devices, so that a typical amount of compensation is possible. This is provided in the HP 8154B Option 001. The TC of long-wavelength devices (1300-nm and 1550-nm) is much larger, about −0.05 dB/°C, which is far from the desired specification. It also

Fig. 1. *The HP 8154B LED Sources provide stable optical power at 850 nm (Option 001), 1300 nm (Option 002), and 1550 nm (Option 003).*
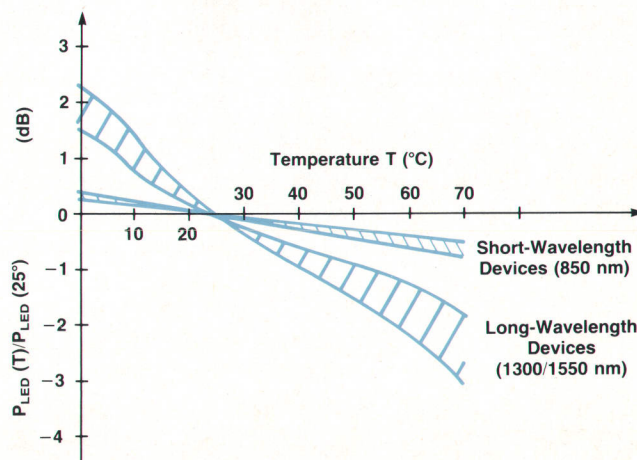

Fig. 2. *Typical temperature coefficient of LED output power as a function of temperature for I_{LED} = 100 mA.*

varies considerably from one device to another.

To create a stable long-wavelength source, there is no other way than to operate the LED at a controlled temperature. For this reason the LEDs in the HP 8154B Options 002 and 003 are mounted on a thermoelectric Peltier cooler and are regulated to about 25°C, so that the desired specifications are achieved over the full temperature range of 0°C to 55°C.

Holding the LED chip at a constant temperature, however, does not result in a zero TC because of two effects. First, there is a small but well-known TC of the front-panel HMS-10/HP connector. Second, the coupling efficiency from the LED into the fiber changes with temperature. Both effects together result in a positive TC of about 0.01 to 0.02 dB/°C. Since these effects are of the order of magnitude of the design goal, very well-known, and without large variations between individual devices, temperature compensation is possible. In the HP 8154B Options 002 and 003 it is implemented by measuring the ambient temperature with a negative temperature coefficient (NTC) sensor (see block diagram, Fig. 3). This sensor is outside the LED case, and supplements the primary NTC sensor which is inside the case, mounted on the Peltier cooler. The outside sensor's output is used to change the input value to the temperature regulator slightly, so that the LED chip temperature is not constant, but is a function of the ambient temperature. This results in excellent stability for the overall instrument.

In addition to these techniques, a five-turn mandrel wrap is used inside the instrument to achieve nearly ideal optical conditions (i.e., an equilibrium mode distribution) at the front-panel fiber connector.

Absolute Output Power and Its Calibration

Although many applications don't depend on knowledge of the absolute value of the output power, its calibration and the related accuracy are physical measurement problems of general interest.

Fig. 4 shows the typical power distribution of a 1300-nm LED and the responsivity of a germanium detector diode as functions of wavelength. The detector is a type commonly used by measurement instruments like the HP 81521B Optical Head.
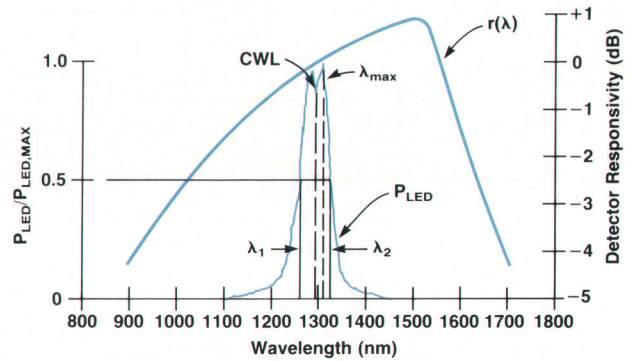

Fig. 4. *Typical power distribution of a 1300-nm LED and the responsivity of a germanium detector diode.*

The absolute amount of power represented by the LED curve in Fig. 4 is

$$P_{LED} = \int_0^\infty P(\lambda)d\lambda \qquad (1)$$

and the current output of the detector in use is

$$I_D = \int P(\lambda)r(\lambda)d\lambda \qquad (2)$$

where $r(\lambda)$ is the responsivity of the detector. There are two ways to make a correct measurement of the absolute power of this LED.

First, and this is the way the HP standards laboratory calibrates all HP 8154B LED Sources, one can use a wavelength independent detector, that is, $r(\lambda) = 1$, like a thermopile or a pyrometer. The second way is to do an integration according to equation 2. This is not a simple user-friendly method, although $r(\lambda)$ can be read out of the HP 8152A Optical Power Meter via the HP-IB and each LED can be measured with an optical spectrum analyzer.

Hewlett-Packard measures all LEDs in the factory. The wavelengths λ_1 and λ_2 where $P_{out} = \frac{1}{2}P_{out\,max}$ are measured (see Fig. 4), and FWHM $= \lambda_2 - \lambda_1$ and CWL $= \lambda_1 + \frac{1}{2}$FWHM are computed and supplied to the customer on a rear-panel label on each source. Note that CWL is not
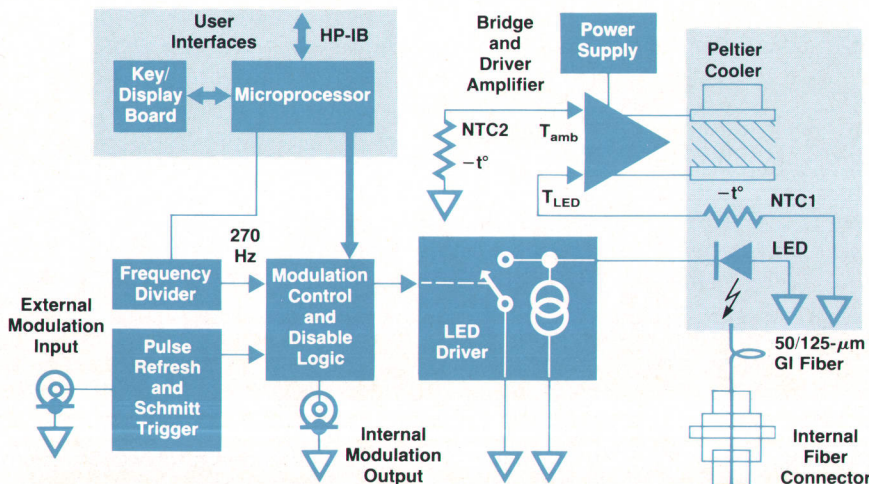

Fig. 3. *HP 8154B Option 002/003 block diagram.*

necessarily the wavelength of maximum peak output power.

If the HP 8154B is used in a stimulus/response test setup with the HP 8152A Optical Power Meter, and if the value of CWL supplied with the HP 8154B is entered into the HP 8152A as the wavelength of the source, the absolute power measurement error (depending on the symmetry of the LED's power distribution and the linearity of the detector's responsivity) is less than 1 to 2% (0.05 to 0.01 dB) compared with a measurement done in our standards laboratory. The error comes from the inaccuracy of the mathematical model, which assumes a Gaussian LED power distribution. This error is well below the tolerances in connector loss and is therefore negligible.

Versatile Modulation Capabilities

The HP 8154B LED Sources are not only CW light sources but also have internal and external modulation capabilities, easily selectable by a keystroke on the front panel or a simple HP-IB command. The internal 270-Hz modulator is useful if you have a large amount of attenuation in a system and your detector is not sensitive enough, so that you have to deal with a lock-in amplifier (a trigger signal is available at the front panel). External modulation with TTL signals up to 1 MHz is possible. Also, the light output can be disabled by a keystroke. This is helpful, for example, when zeroing an optical detector without a shutter (like the HP 81521B Optical Head), so that no optical disconnection is necessary.

Acknowledgments

An Accurate Two-Channel Optical Average Power Meter

by Horst Schweikardt

IN COMBINATION WITH the HP 81520A or 81521B Optical Head, the HP 8152A Optical Average Power Meter (Fig. 1) is useful for both absolute and relative power measurements over a wavelength range of 450 to 1700 nm. Two optical inputs are available for power measurements on two channels or for power ratio measurements. The two channels are useful for such applications as checking the insertion loss or attenuation of optical connectors or cables. For automatic test system use, the power meter is programmable via the HP-IB (IEEE 488/IEC 625). A flexible optical interface connects quickly and easily to all common optical connectors.

The HP 8152A is designed for both single-mode and multimode applications. With the HP 81521B Optical Head, it measures power levels between $+3$ dBm and -70 dBm with 10-pW resolution. ± 0.15-dB accuracy is achieved between $+3$ dBm and -50 dBm over the temperature range of 0 to 40°C. Accuracy derating is an additional ± 0.2 dB at 55°C. At 25 ± 5°C, the accuracy is ± 0.05 dB between $+3$ dBm and -60 dBm. To extend the measurement range beyond $+3$ dBm, additional attenuation filters can be inserted.

A high-performance optical splitter, the HP 81000BS, is a useful companion instrument. It provides a 1:10 power split ratio. The splitter works with fiber core diameters between 9 μm and 85 μm, and is mode independent within 1%.

Mainframe

This article describes the hardware design of the HP 8152A mainframe. The HP 8125A firmware is described in the article on page 12 and the optical head is the subject of the article on page 22. The main functions of the mainframe are to provide the interface for two optical heads and to serve as the user interface.

Head Interface

As the head interface, the mainframe delivers the power for the head electronics (5 lines) and the Peltier current for temperature stabilization of the detector chip (2 lines). Nine control lines are used for analog feedback of the chip temperature, feedback of head status, data and mode control, range control, head on/off information, and the read/write signal for the head EEPROM. There are two lines for signal and signal ground, for a total of 18 pins at each head input connector.

User Interface

On the front panel are LEDs for units indication of absolute average power (mW, μW, nW, pW), and to indicate an average power measurement relative to 1 mW (dBm) or relative to a user-defined reference value (dB). Switches are provided for setting the reference power and for setting the wavelength equal to the wavelength of the source. The
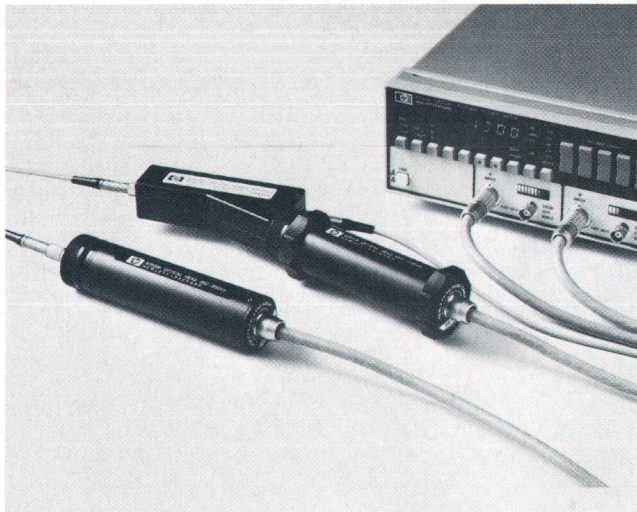
Fig. 1. *The programmable, two-channel HP 8152A Optical Average Power Meter has accuracy as high as ±0.15 dB for both absolute and relative power measurements. It operates with the HP 81520A Optical Head from 450 to 950 nm and with the HP 81521B Optical Head from 850 to 1700 nm.*

selected wavelength must be within the wavelength range of the connected head. Wavelength resolution is 1 nm. The user-defined reference power can be set in watts (mW, μW, nW, pW) or in dBm (−199.99 dBm to +199.99 dBm). A calibration factor can be set in dB (−199.99 dB to +199.99 dB). The **CLR** button clears the parameters to default values (λ = 1300 nm, calibration factor = 0.00 dB, and reference power = 0.00 dBm or 1000 μW).

The warning HEAD in the display indicates that no head is connected to the selected channel. CAL#0 indicates that the calibration factor is not 0.00 dB for the selected channel. REF#0 indicates that the reference value is not 0 dBm when making relative measurements on the selected channel. Overflow and underflow indications are also provided.

In measurement mode, the HP 8152A displays the abso-

lute or relative power at the selected channel, A or B:

$$P\,(dBm) = Measured\ Power + Calibration\ Factor$$

or

$$P\,(dB) = Measured\ Power + Calibration\ Factor + Reference\ Value$$

Alternatively, it displays the measured power at channel B relative to the power at channel A according to the reference setting and the specific channel settings for calibration factor and wavelength. The user can select autoranging, a filter (2 Hz or 8 Hz), and zeroing to compensate for offset errors in each range.

The **XDCR OUT** (transducer output) connector provides an analog head output signal with head dependent bandwidth and an output impedance of 600 ohms. 1999 display counts equals 2.00V into an open circuit, independent of the wavelength setting. This makes it easy to build a synchronous detection system by using an external chopper and a lock-in amplifier with the standard head (HP 81521B) and mainframe (HP 8152A). All modes and parameters are programmable via the HP-IB connector on the rear panel. HP-IB address information is displayed when the **LCL** button is pressed. The default address, 22, results in a display of A22.

Analog Section

Fig. 2 is a simplified block diagram of the HP 8152A mainframe showing one of the two channels. Fig. 3 is a block diagram of the analog section. The head input signal V_{IN} is fed to an input amplifier of gain G1 via the input switch. If no head is connected, the input switch is connected to signal ground. The output V1 of the input amplifier and the output of the offset DAC (0 volts before activation of the zero routine) are summed and fed to a variable-gain amplifier of gain $G2(\lambda)$ to compensate for the wavelength dependence of the detector signal. The output V2 of the λ DAC is buffered and sent to the front-panel **XDCR OUT** connector. After the mainframe offset and gain adjust switch, V2 goes to a fixed ×4 amplifier and then to
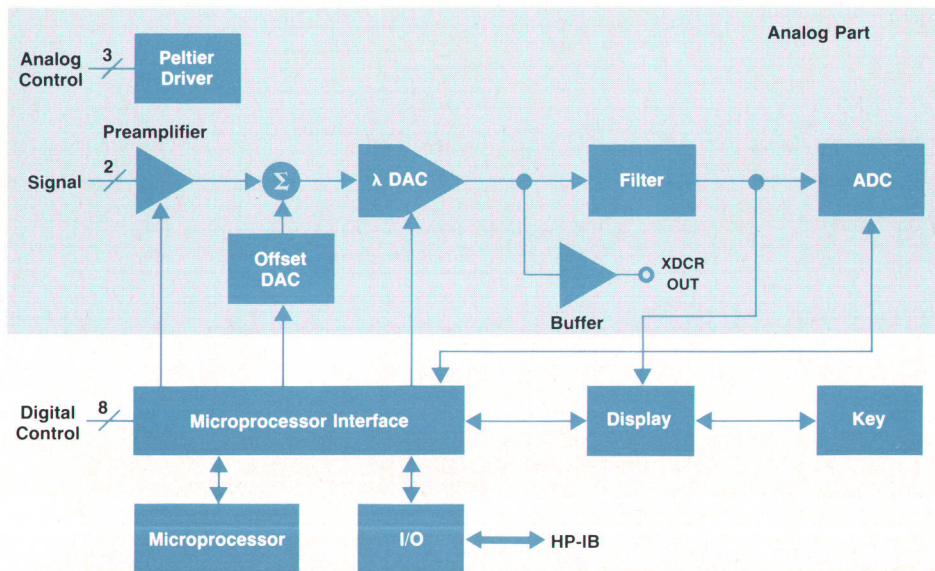

Fig. 2 *Simplified block diagram of one channel of the HP 8152A Optical Average Power Meter.*

one of two filters. Depending on the amount of averaging desired, either the 8-Hz or the 2-Hz filter can be selected.

The filter output signal goes to a CMOS switch, which selects one out of eight input signals (four for each channel). The switch output is shifted down by 3.901V to adapt the level to the requirements of the ADC. Reference voltages for the offset DAC and the gain and offset adjustment circuits for the ADC are taken from a reference IC, which delivers 10.00V.

For self-test and troubleshooting purposes, the analog outputs of the offset DACs and the attenuated head input signals are fed to inputs of the CMOS switch and thus can be measured with the ADC. For a visual indication of the power input level, the 8-Hz filter output controls an LED array on the front panel that acts as a trendmeter.

DAC

The responsivity of a detector is the ratio of output current to absorbed optical power and is a function of wavelength. For the germanium detector used in the HP 81521B Optical Head, Fig. 4 shows a typical curve of responsivity versus wavelength. If the responsivity at 1300 nm is defined to be 0 dB, typical relative responsivity is -5.5 dB at 850 nm, -4 dB at 1700 nm, and $+1.3$ dB at 1520 nm. To compensate for this variation, the HP 8152A mainframe should have a wavelength calibration range from -6 dB to $+2$ dB, and a calibration point at 1300 nm and 0.00 dB.

These requirements are met by a variable-gain amplifier—a multiplying DAC—in the signal path of the mainframe. The input signal of the λ DAC is related to the optical input power P_{opt} by the equation

$$V1 = G0 \times G1 \times R_f \times r(\lambda) \times P_{opt}$$

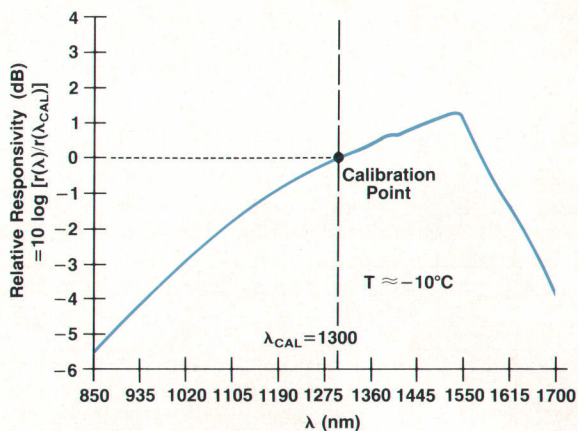where G0 is total head gain, R_f is the feedback resistor of the transimpedance amplifier, G1 is the input amplifier

Fig. 4. *Typical responsivity of the detector in the HP 81521B Optical Head.*

gain (1, 10, or 100), and $r(\lambda)$ is the responsivity of the detector in A/W. The output of the λ DAC is given by

$$V2 = G2 \times V1$$

which is independent of wavelength and equal to KP_{opt} if $G2(\lambda) = r(\lambda_{CAL})/r(\lambda)$.

Each head has individual G2 values stored in an EE-PROM. When a head is connected to the mainframe, these values are read into the mainframe RAM for wavelengths from 850 nm to 1700 nm in 10-nm steps for the HP 81521B. The wavelength resolution of the mainframe is 1 nm, and all values for wavelength settings not on the valid 10-nm grid are calculated by linear interpolation.

The resolution of the λ DAC should be <0.01 dB for all wavelength settings. This means that the minimum number of λ-DAC counts is 434. For a total compensation range of 8 dB, which corresponds to a gain factor $G2 = 10^{-0.8} =$
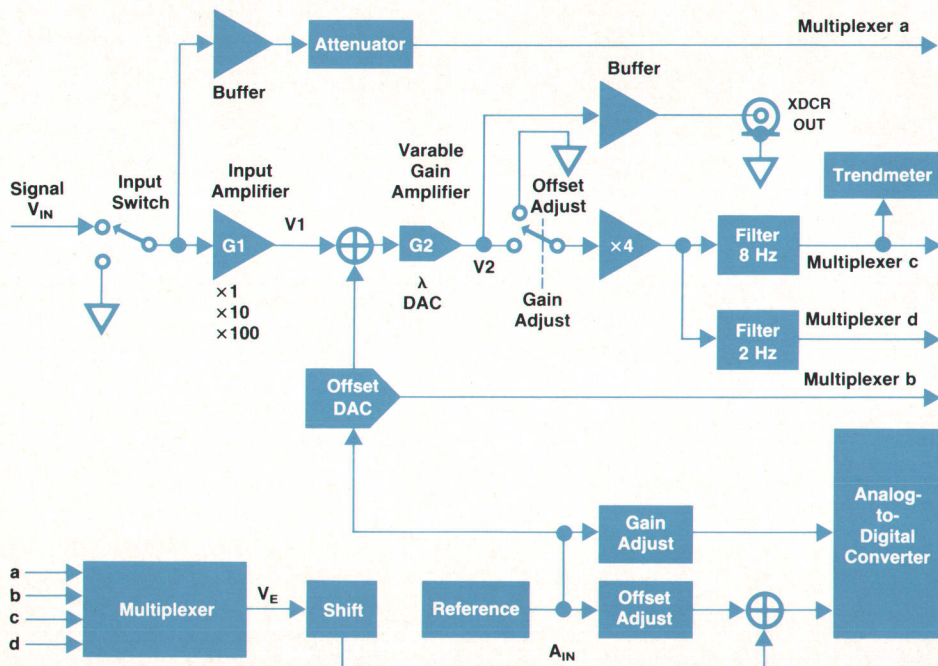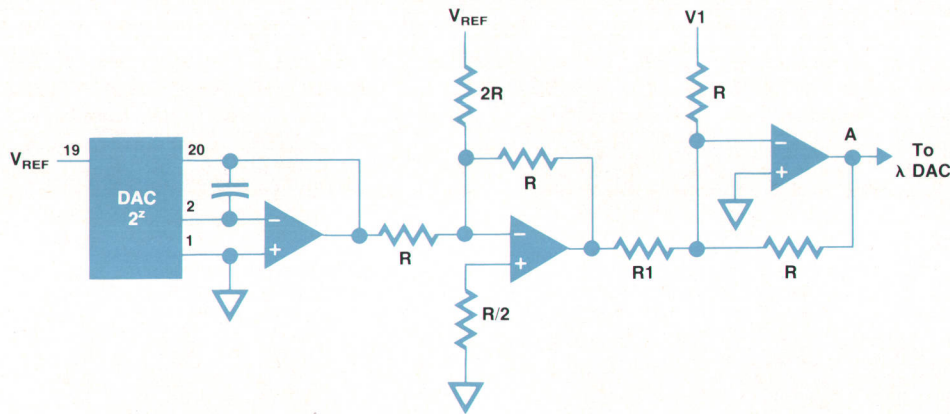

Fig. 3. *Block diagram of the analog signal path.*

(1) $\quad A = \dfrac{R}{R1} \times V_{REF} \times \left(\dfrac{1}{2} + \dfrac{1-X}{n}\right) - V1$

$\qquad\qquad\qquad\qquad\qquad 0 \leq X \leq n-1$
$\qquad\qquad\qquad\qquad\qquad n = 2^z$

(2) $\quad dA = \dfrac{-R \times V_{REF}}{R1 \times n} \times dX - dV1$

Fig. 5. *Head offset compensation circuitry.*

0.1585, the maximum number of counts must be greater than 434/0.1585 = 2739. Therefore, a 12-bit DAC is necessary. G2 at the calibration point (1300 nm) then should be $10^{-0.6} = 0.2512$. The actual value used is 0.2500 and a postamplifier with a gain of 4 reestablishes V1. The specifications of the operational amplifier limit the maximum dynamic input signal to 12.5V, so at the calibration point, a full-scale signal of $V_E = 12.5 \times 10^{-0.2} = 7.887V$ is allowed. The actual full-scale voltage of the input signal at the calibration point is +8.000V. Thus the actual upper limit of the compensation range is +1.94 dB (i.e., 10 log 12.5/8) and the actual lower limit is −6.02 dB (i.e., 10 log 2/8).

Analog-to-Digital Converter

For the ADC, better than 0.01-dB resolution at 1/10 of full scale is needed. This leads to n > 434/0.1 = 4340. The choice, therefore, was a 13-bit ADC, the AD7550 from Analog Devices (or equivalent). For the AD7550, the following equation holds:

$$n = A_{IN} \times 4096/V_{FS} + 4096,$$

where n is the number of ADC counts, A_{IN} is the analog input voltage, and V_{FS} is the full-scale input voltage. Thus n = 0 gives $A_{IN} = -V_{FS}$, and n = 4096 gives $A_{IN} = 0$. For convenience, the transfer function of the ADC should be 1 count per millivolt of V_E. From the equation

$$dn/dA_{IN} = 4096/V_{FS} = 1/1 \text{ mV}$$

we get $V_{FS} = +4.096V$. Therefore we have the following relations:

$V_E(V)$	$A_{IN}(V)$	ADC Counts	Display Counts
>7.996		overflow	+1
7.996	4.095	8191	1999
4.000	0.099	4195	1000
3.901	0.000	4096	975
0.000	−3.901	195	0
−0.195	−4.096	0	−49
<−0.195		underflow	−1

This is why V_E is shifted down by 3.901V as explained above.

Offset Compensation

For offset compensation, or zero adjustment, there were two requirements. First, the resolution had to be less than or equal to 1 display count at minimum responsivity (−6 dB from the calibration point). The full-scale value of V1 is 2.000V, so 1 display count equals dV1 = 1 mV.

Fig. 5 shows the head offset compensation circuitry. From equation 2 in Fig. 5, dA = 0 and dX = 1 gives

$$ndV1 = V_{REF} \times R/R1.$$

The second requirement was that the compensation range be at least 10% of full scale at maximum responsivity (1.94 dB from the calibration point). Here the full-scale value of V1 is 12.5V, and therefore 10% of full-scale equals $V_M \approx 1.3V$. From Fig. 5, equation 1, with A = 0 and X = 1, we get

$$2V_M = V_{REF} \times R/R1.$$

Combining these results gives

$$n > 2V_M/dV1 = 2600 < 2^{12}.$$

Thus the offset DAC is also a 12-bit DAC. With n = 4096, dV1 = 1 mV, and V_{REF} = 10.00V, R/R1 = 0.4096. With R = 10 kΩ, we get R1 = 24.3 kΩ and $V_M > 2.057V$. Thus the offset compensation range is >16% of full scale and the resolution is <1 mV.

Optical Power Meter Firmware Development

by Bernhard Flade and Michael Goder

OBJECTIVES FOR THE DEVELOPMENT of the HP 8152A Optical Power Meter firmware (which the design team thought of as software, since it was not yet installed in ROM) were as follows:

- To provide a human interface with a friendly operating concept, that is, it should be easy to program via the HP-IB, the front panel should be self-explanatory, and the operating modes should offer great flexibility.
- To provide effective software support for the hardware designers, without interfering with the software development.
- To complete the software with no known bugs in a very short time.

The software also had to meet a number of requirements. These included:

- Ability to work in a "dumb" mainframe until intelligence is provided by connected heads.
- Data processing in ranges not known by the mainframe until a head is connected in the active channel.
- Results in either linear or logarithmic units. Single-channel or ratio measurements with no or little difference in processing speed.
- Independence of the channel specific parameters for one channel from those of the other channel during ratio measurements.
- Production support for adjustments, troubleshooting and individual head calibration.
- Extensive self-test capabilities.

The HP 8152A processor system includes a Motorola 6809A microprocessor, a Texas Instruments 9914A HP-IB controller, an Intel 8279A keyboard and display controller, and the following memory:

     32K bytes of ROM
     8K bytes of static RAM
     8K bytes of I/O RAM
     16K bytes configurable as:
       8K bytes of ROM + 8K bytes of static RAM or
       8K bytes of ROM + 8K bytes of EEROM or
       16K bytes of ROM, etc.

The software development tools consisted of an HP 64000 Logic Development System and C, SPL, and assembly programming languages. SPL6809 is a dedicated compiler for the 6809 processor, developed for the HP 1630A Logic Analyzer project and later used in the HP 8175A Data Generator development project. SPL6809 runs on the HP 64000 system.

Meeting the Objectives

Once the first definition of the members of the new fiber optic instrument family was done, a complete external reference specification (ERS) was worked out, using as many inputs as possible from anyone knowledgeable in fiber optic measurements. Subsequently, a complete simulation of the front-panel functions, the resulting displays, and the signal processing was written on an HP 9000 Series 200 Computer. Working with this simulation, the last refinement of the ERS was done. From that time, the ERS was not altered in any detail.

A by-product of the simulation, in conjunction with a mini-HP-IB software driver, was the ability to access any hardware device directly. This turned out to be a very powerful tool. It could perform any front-panel function needed for testing or modifying any latch or DAC, or for reading out ADC values. Since no working front panel was available in the early project stages, this capability was invaluable. The only effort required to solve any hardware demand was to write a small sequence of direct-access commands and insert it after a simulated key recognition or replace a simulated data input with it. This software was so useful that it was still being used through the first environmental test and until the lab prototype was completed.

To save time and effort, software was leveraged from other projects as much as possible. For example, the operating system and the HP-IB kernel software were leveraged from the HP 8175A Data Generator project. The software was divided into independent modules that could be de-
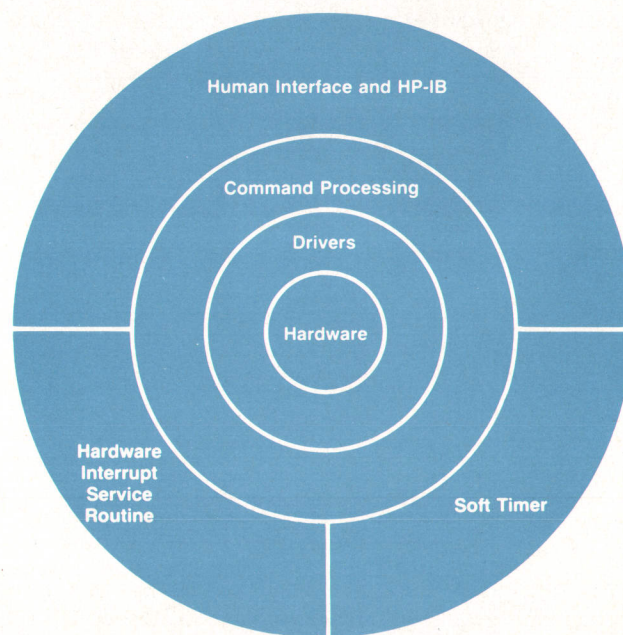

Fig. 1. *Layer model of the HP 8152A software. Interactions between modules are always in the radial direction.*

veloped without interfering with one another. Newly written software was shared among the members of the new instrument family as much as possible. Time was also saved by decoupling the hardware and software designs as long and as much as possible, and by working with good and easy-to-use software tools.

Using C

The motivation for using C was to get some experience to see how this language might meet our needs, and of course, the everlasting dream of universal, portable, and ready-to-use software packages. The results were different, depending on the assignment.

The tasks written in C are the keyboard and display management, the output data formatter, and the lin/log/lin conversions. The data formatter and the conversions were written, tested, and debugged on an HP-UX system and transferred to the HP 64000 after completion.

Writing a keyboard and display driver is an instrument specific and especially hardware-oriented task. It needs on-line debugging in the emulator environment with single-stepping, memory examination, and program tracing. The advantage of being freed from memory allocation, memory organization, problems of parameter passing, and other tasks during program development is paid for dearly in the debugging phase, because following all the steps the compiler did for you is a very tedious and bothersome job.

On the other hand, writing a conversion program is an instrument independent task, and commonly needs no debugging on the emulation level. Debugging this kind of software is more of a high-level job, where commands like WRITE, WRITELN, READ, or READLN from Pascal or a short test program allow easy tracing of program flow and data manipulation. In such cases, if you can remain in the C environment, we feel that C is a good tool for increasing the efficiency of software development.

Using SPL

During our search for a suitable operating system for the fiber optic instruments, we determined that the one used in the HP 8175A Data Generator, which is the same as the one in the HP 1630A Logic Analyzer, would meet our needs in a nearly ideal way. In addition, since the processor hardware is similar, adapting this system for the fiber optic instruments promised to be an easy task.

This operating system was written in SPL. SPL programs have the readability of Pascal programs. Also, SPL provides data structures and a modular program structure very similar to Pascal, and allows easy assembly code embedding (if the need for it is unavoidable). In conjunction with an optimizer, which is also available to reduce the amount of final code, it seemed to be an ideal tool, if only it had not been dedicated to a single processor (6809).

To get away from this processor dependence, and because of the resemblance with Pascal, we rewrote this operating system in Pascal with a very small amount of assembly code. A comparison between the SPL version and the Pascal version produced the following results:

	Pascal OS	SPL OS
Code Efficiency	4297 bytes code + 2533 bytes library	3109 bytes
Execution time for typical OS activities		
Interrupt processing:	6.5 ms	465 μs
Signal a semaphore:	1.7 ms	278 μs
Wait for a semaphore:	955 μs	294 μs

These results caused us to abandon plans to write a Pascal software system for the fiber optic family.
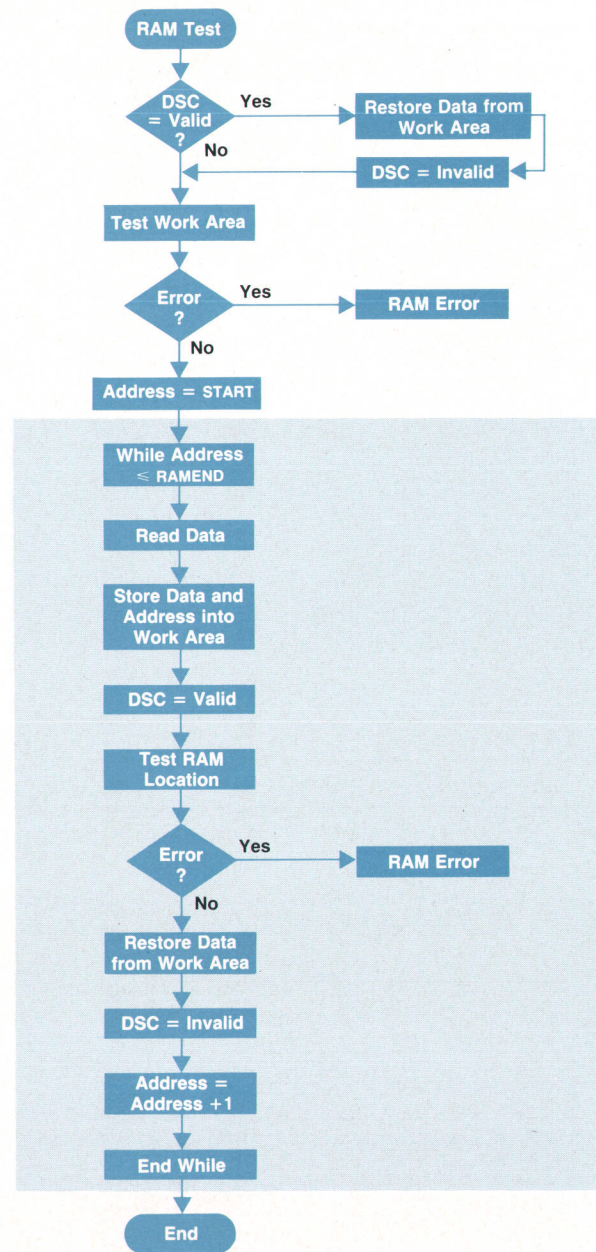

Fig. 2. RAM test algorithm. The test is not destructive although it overwrites the entire RAM with test patterns.

Using the Assembler

From our experience in assembly language programming in earlier projects we knew that it is best to avoid assembly language. The portion of assembly code in the HP 8152A software is less than 1%. It is only used for interfacing SPL with C and vice versa and for direct accessing of the processor's condition code register.

Structure of the Software

The heart of the HP 8152A software is the operating system leveraged from the HP 8175A and modified for the needs of the fiber optic instruments. The attributes of this operating system are control of nine competitive processes (multitasking), priority-controlled preemption by interrupt or signal and wait mechanism, no dynamic priorities, and no special task communication.

The tasks are:

- Idler process. Does the measurement if there is nothing else to do.
- Command processing. Synchronizes and schedules any activity or command initiated by an interrupt.
- Keybord management. Recognizes keystrokes, performs the autovernier function, and sends commands according to any keystroke.
- HP-IB I/O. Handles communication via the HP-IB and activates the command interpreter.
- HP-IB talker initialization. Loads the HP-IB output buffer with the instrument messages sent by the HP-IB I/O process if the instrument is addressed to talk.
- Measurement result processing. Works up measurement results and provides results display.
- Hardware interrupt handler. Recognizes hardware interrupts and sends commands accordingly.
- Hardware I/O. Driver routines manage data transfer to and from the hardware.
- Soft timer. Provides timer functions for time-outs, repetitive actions, etc.

Fig. 1 (page 12) shows the layered nature of the software.

Self-Test

A self-test procedure runs at power-on or whenever a TST? command is received via the HP-IB. The self-test includes testing RAM, the keyboard and display, the device bus, the offset and λ DACs, the filters, the ADC, and the optical heads if present. A SYSTEM FAILURE bit and an error number Exxx shown on the display indicate that a defect has been detected while testing the HP 8152A. This error number can be interrogated by a controller or thrown away by pressing a key or sending any command to the HP 8152A.
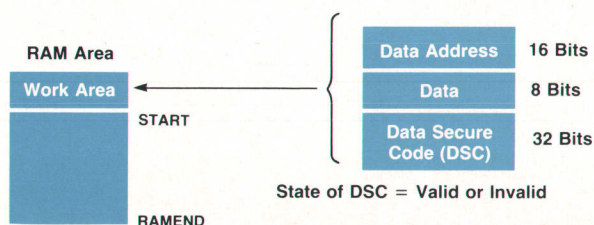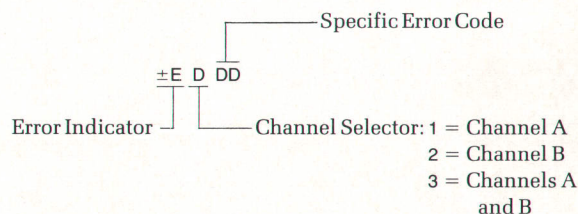

Fig. 3. *The RAM test is bytewise. A work area is used to save the data at each RAM location during testing.*

In the latter case the displayed error number is transferred into a LAST ERROR register which can be interrogated later. A 3-digit error number is used to indicate the error state. The coding is as follows:

For example, −E 1 50 means that zero calibration failed in the −50 dBm range of channel A.

An error track in the HP 8152A is used to save the complete hardware status of the defective state. A valuable feature for production and service is that this hardware status can be restored by sending a special HP-IB command, even if the error state has been left. Once this command is sent, the HP 8152A holds the defective hardware state as long as no key is pressed. Pressing a key causes the HP 8152A to do a power-on restart.

A special algorithm, shown in Fig. 2, is used in the RAM test. The test is not destructive, although the complete RAM is overwritten by test patterns, including the stack area. This is accomplished by a bytewise test: a work area (Fig. 3) is used to save the data and its corresponding address while testing each RAM location. A data secure code (DSC) is used to indicate that data in the work area is either valid or invalid. If there is a valid data byte in this area at the beginning of the test, it is restored before testing the RAM from address START. This could occur, for example, if the HP 8152A is powered off while a test pattern is being written into a RAM location.

Self-Calibration

The HP 8152A has a self-calibration procedure, which eliminates undesirable offset voltages caused by the optical head and/or other active and passive components in the mainframe. The calibration routine is activated by pressing the **ZERO** key or by the ZER 1 command on the HP-IB. After activation, the HP 8152A is either in autozero or single-zero mode. This is determined by the attached optical head. Autozero means that the calibration is repeated automatically after a time determined by the optical head. Single-zero means that the function has to be activated every time the user wants to calibrate the instrument.

The HP 8152A is capable of eliminating an offset of one quarter of full scale. The offset is measured in each range and the compensation values are stored in the internal memory. Each time the measurement range changes, the corresponding compensation values are applied to the offset DACs of both channels.

When the calibration is initiated while an optical head with internal shutter is connected, the shutter moves into the disable position so that incident light is blocked. This causes the offset to be the only signal remaining in the system. If an optical head without shutter is applied, the user has to darken the source to avoid an erroneous abort of the calibration. The offset compensation is done by
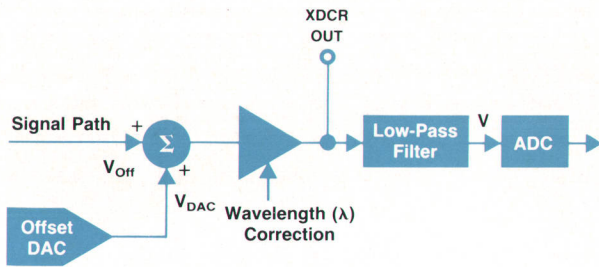
Fig. 4. *Block diagram for offset compensation.*

measuring the offset voltage twice with different settings of the offset DAC. The compensation value programmed into the offset DAC is the complement of the measured and calculated offset voltage.

The offset voltage is calculated by the following equation (see Fig. 4):

$$V = V_{DAC} + V_{Off}$$

where V = voltage measured by the ADC on the signal path, V_{DAC} = voltage of the offset DAC, and V_{Off} = offset voltage to be compensated.

The first measurement is done with the offset DAC set to its maximum output voltage. That leads to the first compensation value:

$$V_{Comp1} = -V_{Off1} = V_{DACmax} - V.$$

The second measurement is done with the offset DAC set to V_{Comp1}. This leads to the final compensation value:

$$V_{Comp} = V_{Comp1} - V.$$

The compensation error is less than 1 display count.

Mainframe Control by the Heads

Mainframe hardware control and parameter limiting depend on what optical-to-electrical transducer is connected to the mainframe. All of the head dependencies (center wavelength, range limits, etc.) are stored in a nonvolatile memory in every head. Problems of data loss protection (a head connection is never a controlled power-on to the head electronics because of contact bouncing, sequence of pin connections from mechanical tolerances, etc.) are solved by using a special write adapter when programming the head EEROM and then pulling the write enable input of the EEROM to V_{CC} during normal operation.

Each time a head is connected to the HP 8152A this data is read out and stored in a RAM copy of the head memory. After testing for a complete data transfer without errors, all the information the mainframe needs to modify its control software is transferred. In case of erroneous or invalid head data all specials are set to defaults, and an error message is initiated and sent to the display and the HP-IB.

The defaults are selected so that, despite the erroneous condition, the measurement can continue, although it may be out of specification.

Measurement Modes

The HP 8152A provides two different measurement modes, continuous and single. The single mode is available only under remote control. In this case, measurements are only done when a GROUP EXECUTE TRIGGER or the TRG command is received via the HP-IB.

This is a useful feature for synchronizing measurements by the HP 8152A with other operations within a measurement system. Another important feature is single mode in conjunction with autoranging. This ensures that erroneous measurement results such as overrange and underrange during ranging are suppressed and not output over the HP-IB.

Detectors for Optical Power Measurements

by Josef Becker

ALTHOUGH MOST OF TODAY'S intelligent optical power meters are found in fiber optic measurement setups, they are not generic fiber optic instruments. Design and characterization of an optical power meter detector are more easily understood if one considers that its parents are the photometer for chemical analysis and the radiation detector in physics labs or national bureaus of standards.

In a fiber optic communications link, the detector has to respond to fast and weak digital signals, so its speed and noise performance are optimized, while linearity and stability are of secondary interest. A typical detector for this application is the avalanche photodiode, mounted straight onto the fiber end.

A power meter, on the other hand, must give accurate information about the beam intensity radiating onto its detector from a fiber end, an LED, a laser diode, or any sort of freely propagating light beam. If the beam intensity is not constant with time, it is generally accepted that the power meter reads the average intensity. From this we see that, for a detector in a power meter, wide dynamic range with good linearity, low aging and temperature dependence, and spectral response are of primary interest, while speed is of no concern. For these reasons, typical detectors are large-area photodiodes (2-mm to 10-mm diameter), thermopiles, or pyroelectric detectors.

Detector Physics

All of the detectors mentioned above for optical radiation (ultraviolet, visible, infrared) are either tiny thermometers or make use of the photoeffect.

Thermal detectors measure the heat generated when radiation power is absorbed ($\Delta T = 1K$ for $P_r = 250\ \mu W$). The small temperature rise can be converted into a dc voltage by a *thermopile*, that is, a series array of 10 to 50 thin-film thermoelements (Fig. 1a). In a *bolometer*, the change of resistance of a gold film or a thermistor is measured. In a *pyroelectric detector*, a capacitor with temperature dependent electret material as dielectric produces a measurable charge/discharge current into a high-impedance load when it is struck by alternating or pulsed radiation. To measure constant light intensity, this type of detector needs a chopper (Fig. 1b).
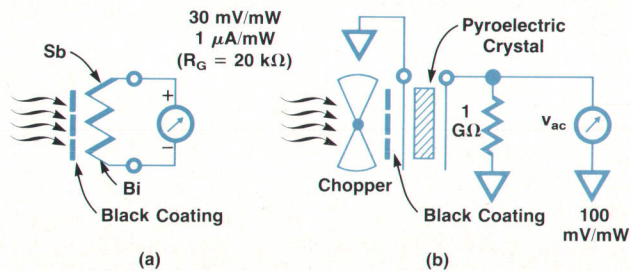
A black coating is applied to the thermal detector's surface to achieve a broad spectral range of constant sensitivity (Fig. 2). Spectral response is limited, and can be tailored by the window material in front of the detector.

Quantum detectors for measurement purposes are photodiodes, photoresistors, and photocathodes in photomultiplier tubes. Photocathodes are favorable in the ultraviolet and for very large-area detectors, while in the visible and near infrared parts of the spectrum, silicon, germanium, or ternary (GaInAs) photodiodes are the first choice.

In a quantum detector, an electron-hole pair is generated for every radiation energy quantum (hf) absorbed in the depletion layer (Fig. 3). If all quanta striking the detector surface were exploited, the ideal response (dashed line in Fig. 2) would be

$$r_{ideal}(\lambda) = \frac{i_p}{P_r} = \frac{nq/t}{nhf/t} = \frac{q\lambda}{hc} = 0.807\lambda \text{ A/W}$$

where λ is in μm.

$$\eta = \frac{r(\lambda)}{r_{ideal}(\lambda)} \quad \text{is called the quantum efficiency.}$$

Two effects cause η to be less than 100%: surface reflection (some 30%) and wavelength dependence of the absorption

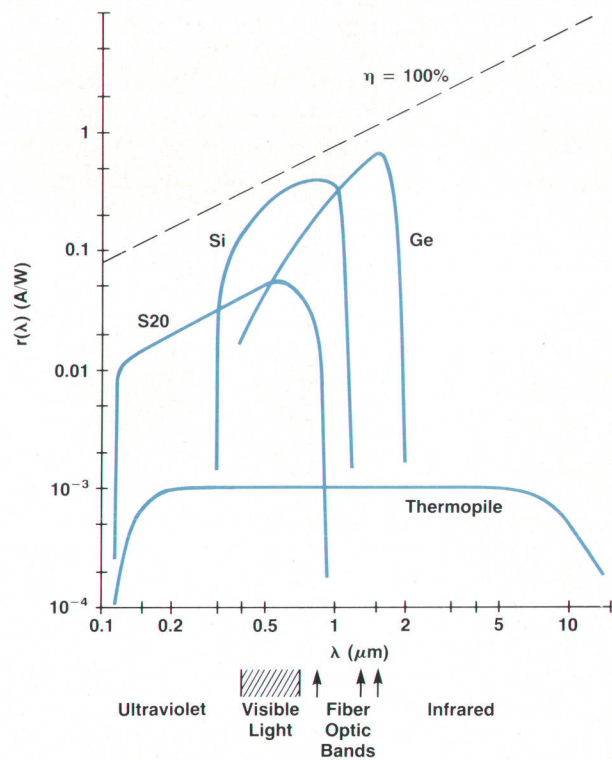**Fig. 1.** *Two types of thermal detectors. (a) Thermopile. (b) Pyroelectric detector.*

Fig. 2. *Spectral responses of silicon and germanium photodiodes, S20 photocathode with MgF$_2$ window, and thermopile with CaF$_2$ window.*

depth. Only carriers generated in the depletion layer d contribute to photocurrent i_p in the external circuit. At the short-wavelength end of the useful spectrum, most of the energy is absorbed in the front layer of the diode, where minority carriers are quickly lost by recombination.

At the long-wavelength end, there is a sharp cutoff when the quantum energy hf falls below the bandgap qV$_{BG}$ of the diode material. In Si, with V$_{BG}$ = 1.2V, λ_c = 1.05 μm. In Ge, V$_{BG}$ = 0.7V and λ_c = 1.8 μm. Photons of longer wavelength cannot provide the energy to release an electron into the conduction band. For them, the diode is a transparent window.

Spectral response is temperature dependent. Technological progress in the last three years has made it possible to design photodiodes for fiber optic applications with zero temperature coefficient at the wavelength of interest. In a power meter, however, where a broader spectral range is needed, Fig. 4 shows a clear demand for constant detector
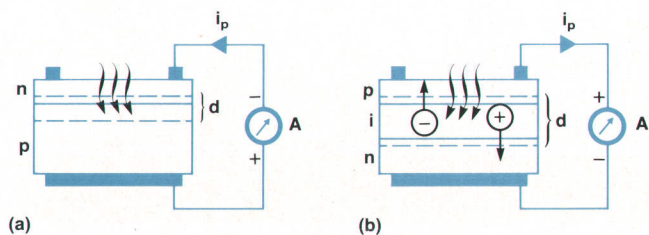
temperature.

Homogeneity and Angular Response

As a result mainly of passivation and antireflection coating imperfections, photocurrent will vary to some extent if a photodiode is scanned with a small light spot. It is common practice to adjust the scanning beam diameter and step size to 1/10 of the active detector diameter. Then, with Si diodes of 1-cm diameter, inhomogeneities in the detector response of less than ±0.5% can be expected over the central area or at least 70% of the active diameter. This causes no problems. But with Ge diodes, inhomogeneities of several percent are normally found (Fig. 5). Recently introduced SiO passivation on Ge can reduce the problem to ±0.5% or less. To reduce the influence of local inhomogeneities to a negligible level, the light beam should cover at least 50% of the detector diameter.

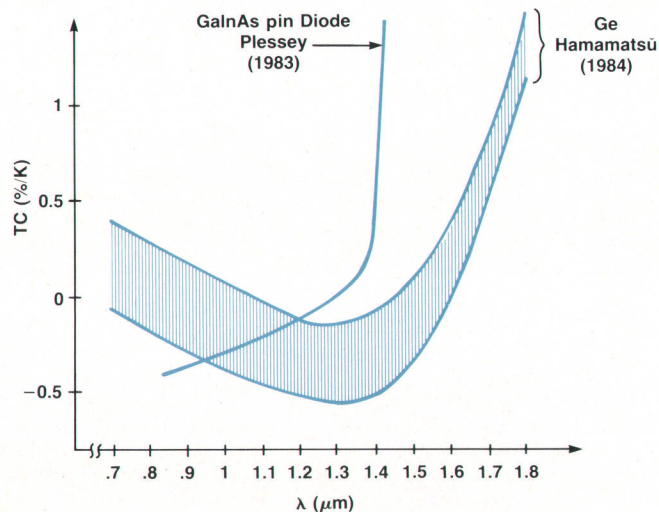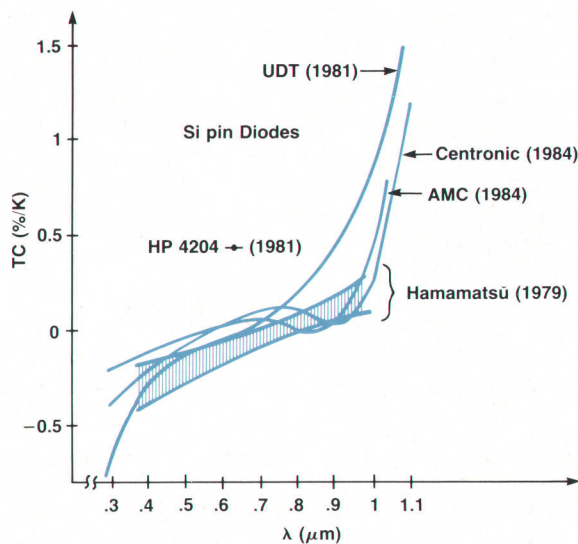

Fig. 3. *Two types of quantum detectors. (a) Germanium photodiode. (b) Silicon pin diode. d is the depletion layer.*

Fig. 4. *Temperature coefficient of the responsivity of silicon (top) and long-wavelength (bottom) photodiodes.*
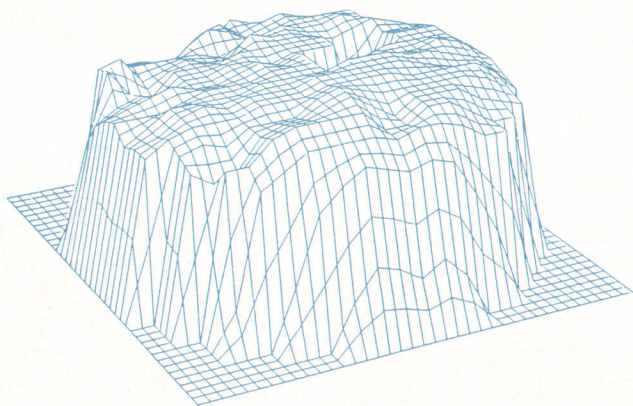
Fig. 5. *Responsivity map of a 5-mm diameter Ge photodiode with polyimide passivation, showing inhomogeneities of ±3%.*

Attention to the detector properties discussed so far is sufficient for accurate measurements of the intensity of a collimated (parallel) beam that is perpendicular to the detector surface. If divergent radiation out of a fiber is coupled to the detector, we have to consider the detector's responsivity for oblique rays. Surface reflection will increase with growing aperture angle according to Fresnel's formulas. On the other hand, the absorption path in the detector crystal is longer, thus giving better absorption efficiency. Both effects cancel to some extent. Therefore, in a Si diode at 850 nm, responsivity remains constant within ±0.3% for incident angles from 0 to ±15°, and is down 1% at ±20°. With Ge diodes, coating layers may introduce large errors (Fig. 6) and there is a distinct dependence on wavelength. However, technological progress in detector surface finishing within the last year has made it possible to reduce this effect to well below ±1%.

Optical Interface

To couple optical fibers to a detector head of the HP 8152A Optical Average Power Meter, a collimating lens adapter is used, eliminating possible inaccuracies caused by slanting rays. The required aperture of the lens—or of the detector itself, if no lens is used—depends on the angular radiation pattern (far field) of the optical fiber. Fig. 7 shows the collecting efficiency for a typical 50/125-μm graded-index fiber.

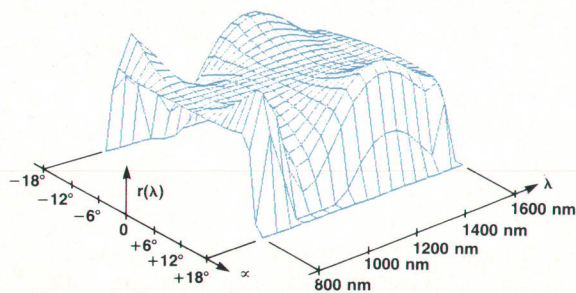The simplest optical collimator, a planoconvex lens, per-

forms nearly ideally with monomode fibers; a lens with NA = 0.2 is sufficient to collect all the light emitted from the fiber end. With multimode fibers, Fig. 7 shows that the collimator should have a useful aperture of 0.4 to 0.5. However, spherical aberration of a planoconvex lens produces marginal rays at NA = 0.4 that are inclined 7° to the axis. Therefore, the accuracy problem shown in Fig. 6 is only partly solved by the simple planoconvex lens.

Two collimators for higher apertures are shown in Fig. 8. The molded aspherical lens and the two ground spherical lenses have comparable price and aberration performance. The latter is preferred because of looser optical manufacturing tolerances, and because of smaller refraction angles for edge rays. This reduces variations in the spectral transmission of the lens coating with incident angle.

Photodiode Circuit

The irradiated pn or pin structure of Fig. 3 is described by the equivalent circuit of Fig. 9a. The diode symbol represents the pn junction's v-i characteristic, in parallel with the junction capacitance C_D.

$$i_D = I_s \left(\exp \frac{qV_D}{kT} - 1 \right)$$

R_s is the spreading resistance in the outer layer (10 to 100 ohms). R_l is the external load. Fig. 9b shows the v-i characteristics of this circuit. Irradiation, like thermal motion, generates electron-hole pairs that appear as reverse current i_p, driven by the inner diffusion voltage across the depletion layer.

For high-speed applications, an additional reverse bias voltage is applied in series with R_l to reduce diode capacitance and speed up carrier collection, at the expense of added dark current noise. For wide dynamic range down to the lowest possible noise level, no bias should be applied. The diode then operates in the photovoltaic mode ($V_D \geqslant 0$).

Fig. 6. *Responsivity of a coated Ge photodiode varies up to ±5% with wavelength and beam incidence angle.*
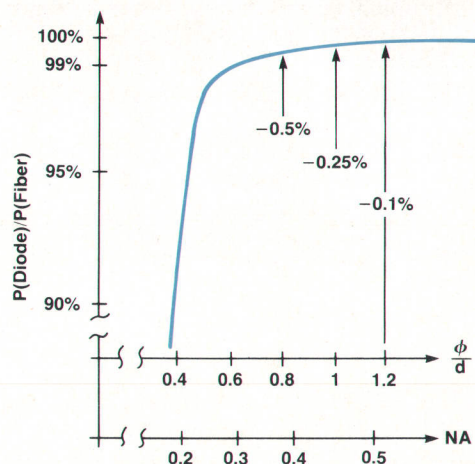

Fig. 7. *Percentage of light reaching the detector from a graded-index fiber with NA = 0.2. ϕ = lens or detector diameter. d = distance of lens or detector from fiber end. NA = sin tan^{-1} (ϕ/2d).*

In this mode, neglecting the voltage drop across R_s, the short-circuit current ($i_{short} = i$ for $R_l = 0$) increases linearly with incident radiation power P_r, that is, $i_{short} = i_p$. With a high-impedance load, $i_D = i_p$, and the detector voltage varies logarithmically with light intensity:

$$V_{open} = \frac{kT}{q} \ln \frac{i_p + I_s}{I_s} \approx 26\,mV \times \ln \frac{i_p}{I_s} \text{ at room temperature.}$$

Photographic exposure meters make use of this operating mode. For solar energy conversion, R_l is chosen to make vi a maximum at a given light level.

In optical power meters, photodiodes are loaded with a virtual short by a transimpedance amplifier to provide a linear response to light intensity. V_D is always very small, so we can represent the diode by its small-signal parameters, R_D and C_D, where

$$\frac{1}{R_D} = \left(\frac{di_D}{dV_D} \right)_{V_D=0} = \left(\frac{q}{kT} I_s \exp \frac{qV_D}{kT} \right)_{V_D=0} = \frac{qI_s}{kT}$$

or $R_D = \frac{kT}{qI_s} \approx \frac{26\,mV}{I_s}.$

From analysis of the linearized circuit (Fig. 10), we learn that diode dynamic resistance R_D is the key parameter that determines the noise level and dc error of the detector unit. Diode noise is essentially shot noise, not thermal (Johnson) noise. But a short-circuited diode generates an amount of shot noise equal to the thermal noise produced by a resistor of magnitude R_D.

Response linearity at high light-power levels is limited by R_s:

$$i_{short} = i_p - i_D = i_p - I_s \left(\exp \frac{qR_s i_{short}}{kT} - 1 \right)$$

To extend the range of linear response of a Ge diode from a few milliwatts to several tens of milliwatts, it has been proposed to measure high intensities with the detector slightly biased (about $-1V$). The argument of the exponential is thereby shifted far to the negative, thus making the diode current term i_D negligible.

i_D is strongly dependent on temperature and bandgap, since

$$I_s = \frac{kT}{qR_D} \approx Constant \times T^3 \exp \left(-\frac{q}{kT} V_{BG} \right).$$
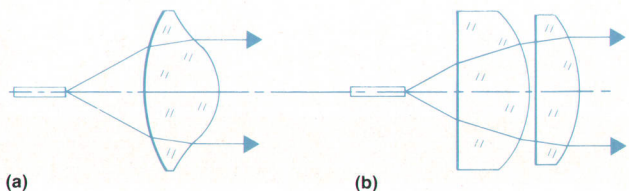
Fig. 8. Two collimators for higher apertures. (a) Molded aspherical lens. (b) Two ground spherical lenses.
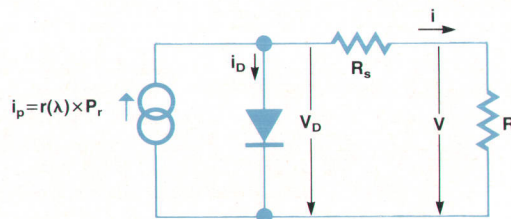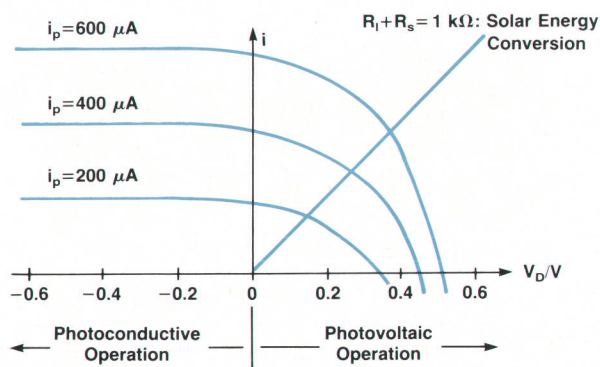
Fig. 9. (a) Photodiode equivalent circuit. (b) v-i characteristics of a silicon photodiode.

Typical R_D values at room temperature are 500 MΩ and 5 kΩ for Si and Ge diodes, respectively, of 5-mm diameter. From this, we calculate that with bandgap voltages of 1.2V and 0.7V, respectively, the Ge detector would have to be cooled down to approximately $-60°C$ to perform as well as its silicon counterpart does at $+23°C$, or room temperature. Practical results are even worse for the Ge diode because of surface effects that have been neglected in this estimation.

DC Stability and Noise Level

The low end of the useful dynamic range is reached at a radiation power level that produces an output signal V_o (Fig. 10) equal to either dc drift or to the rms noise voltage produced at the output of the amplifier.

With $R_D = 100\,k\Omega$ in Fig. 10 (Ge, 5-mm diameter, $-10°C$),
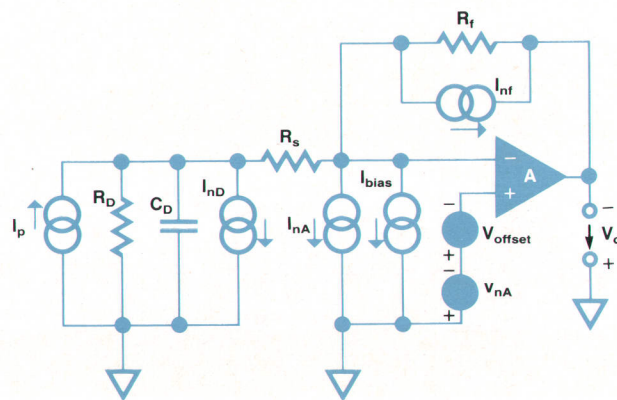
Fig. 10. Linearized photodiode with transimpedance amplifier, including dc and noise error equivalent sources.

$R_f = 50\,M\Omega$, and an OPA111BM operational amplifier, the drift over 0 to 55°C is

$$V_{o\,drift} \leq 55K(1\,\mu V/K)(1+\frac{R_f}{R_D})+(1\,pA)(R_f)(2^{\frac{55-25}{10}}+2^{\frac{0-25}{10}})$$

$$V_{o\,drift} = 27.56\,mV + (50\,\mu V)(8+0.16) = 28\,mV\ max.$$

(14 mV is typical.)

Offset voltage is the predominant error source with the Ge detector. If the responsivity is $r(\lambda) = 0.5 A/W$, this corresponds to a drift equivalent power of

$$\frac{28\,mV}{50\,M\Omega} \times \frac{1}{0.5 A/W} = 1.12\,nW\ maximum.$$

Zeroing the instrument after warm-up will depress this error below the fluctuations caused by flicker noise.

If any leakage current has a chance to reach the summing node, it might increase the effective bias current from femtoamps to nanoamps. Careful guarding on the printed circuit board will prevent this.

The noise voltage at the output is (for low frequencies):

$$v_{no}^2 = (I_{nD}^2 + I_{nf}^2 + I_{nA}^2)R_f^2 + v_{nA}^2\left(1+\frac{R_f}{R_D}\right)^2$$

With the same circuit elements as above, and substituting 6 times the rms value for the peak-to-peak noise of the "white" resistive sources, peak-to-peak noise at the output measured over 0.1 to 10 Hz comes out as

$$v_{no\,p-p}^2 \leq \left[\left(\frac{4\,kT}{R_D}+\frac{4\,kT}{R_f}\right)(9.9\,Hz)(6^2)+(12\,fA)^2\right](50\,M\Omega)^2$$
$$+ (2.5\,\mu V)^2(501)^2$$
$$= (7.64\,pA)^2(50\,M\Omega)^2+(1.25\,mV)^2$$

$$= (1.253\,mV)^2\ max.$$

(0.60 mV is typical.)

The peak-to-peak noise output of 1.25 mV corresponds to an input signal fluctuation of

$$P_{n\,p-p} \leq \frac{1.25\,mV}{50\,M\Omega}\left(\frac{1}{0.5\,A/W}\right) = 50\,pW\ max.$$

(24 pW is typical.)

Noise equivalent power (NEP) is usually measured with a chopping arrangement at 1-kHz chopping frequency and 1-Hz bandwidth. The circuit of Fig. 10 then delivers

$$\frac{v_{no\,rms}^2}{\Delta f} = \left[\frac{4\,kT}{R_D}+\frac{4\,kT}{R_f}+\left(0.4\,\frac{fA}{\sqrt{Hz}}\right)^2\right](50\,M\Omega)^2 +$$
$$\left(7\,\frac{nV}{\sqrt{Hz}}\right)^2(501)^2 = \left(20.54\,\frac{\mu V}{\sqrt{Hz}}\right)^2$$

The rms noise of 20.54 μV corresponds to a noise equivalent power of

$$NEP = \frac{20.54\,\mu V}{50\,M\Omega}\left(\frac{1}{0.5\,A/W}\right) = 0.82\,pW$$

$$= -90.9\,dBm\ typical.$$

The noise levels calculated above are in full agreement with measured results. They reveal that NEP specifications may be misleading when the real resolution of an optical dc power meter has to be determined. The performance of nonchopped long-wave detectors with large-area diodes having low R_D is limited by amplifier flicker noise voltage.

The circuit of Fig. 10 will resolve radiation powers down to the detector NEP, if $I_{nD}R_f$ is the predominant noise term
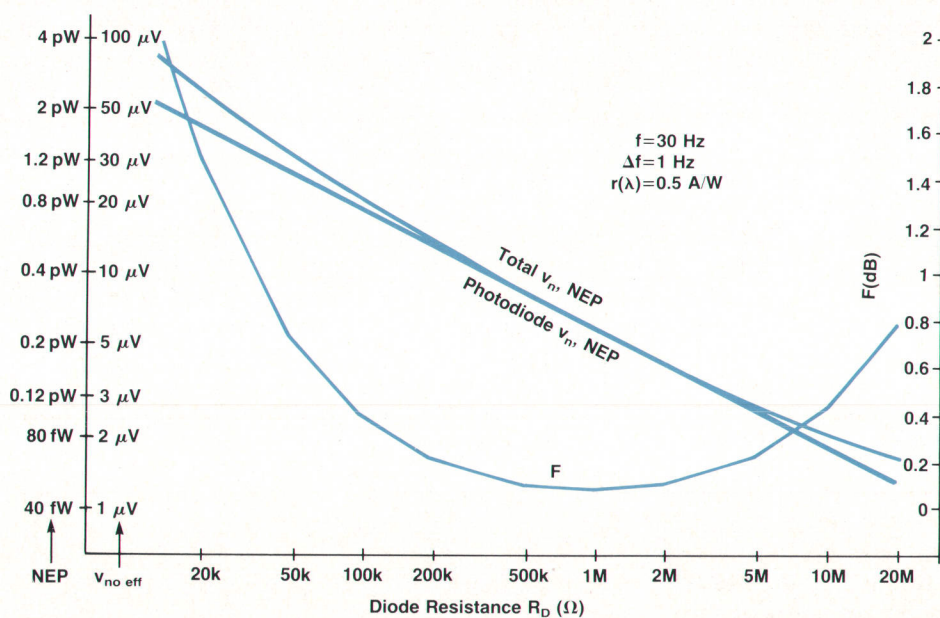

Fig. 11. Noise equivalent power (NEP) and noise figure F of photodiode detector circuits.

Fig. 12 diagram:

Facility:	National Standards Office	Manufacturer's Standards Lab	Production or Service Station	Customers' Applications	
Equipment:	Primary Standard: ESR with Thermopile	Transfer Standard: ESR Pryoelectric or Si or Ge Diode	Working Standard: Si or Ge Diode	Measuring Instrument	Displayed Value
Real Value (Never Known)					
Error Sources:	• Physical Standard Realization Uncertainty • Measurement Variance	• Aging of Transfer Standard • Tolerance of Monochromator, Diaphragms, Electronics	• Aging and TC of Working Standard • Wavelength and Beam Profile Variations	• Aging, TC, Linearity, Noise, Quantization, Beam Geometry, Wavelength Dependence	
Environment:	• P_r=10 μW, T_{amb}=23°C	• P_r=10 μW, T_{amb}=23°C	• P_r=10 μW, T=15 to 35°C	• P_r=1 pW to 2 mW, T =0 to 55°C	

Total Uncertainty at

	Traceability →		Uncertainty →
λ=850 nm:	±1.1% →	±1.7% →	±2.7% → For P_r ≥ 100 pW: ± 6.2% →
λ=1300 nm:	±1.7% →	±2.5% →	±4.2% → For P_r ≥ 10 nW: ± 7.7% →

Without Working Standard: Traceability →

Uncertainty →
λ=850 nm P_r ≥ 100 pW: ± 5.2% →
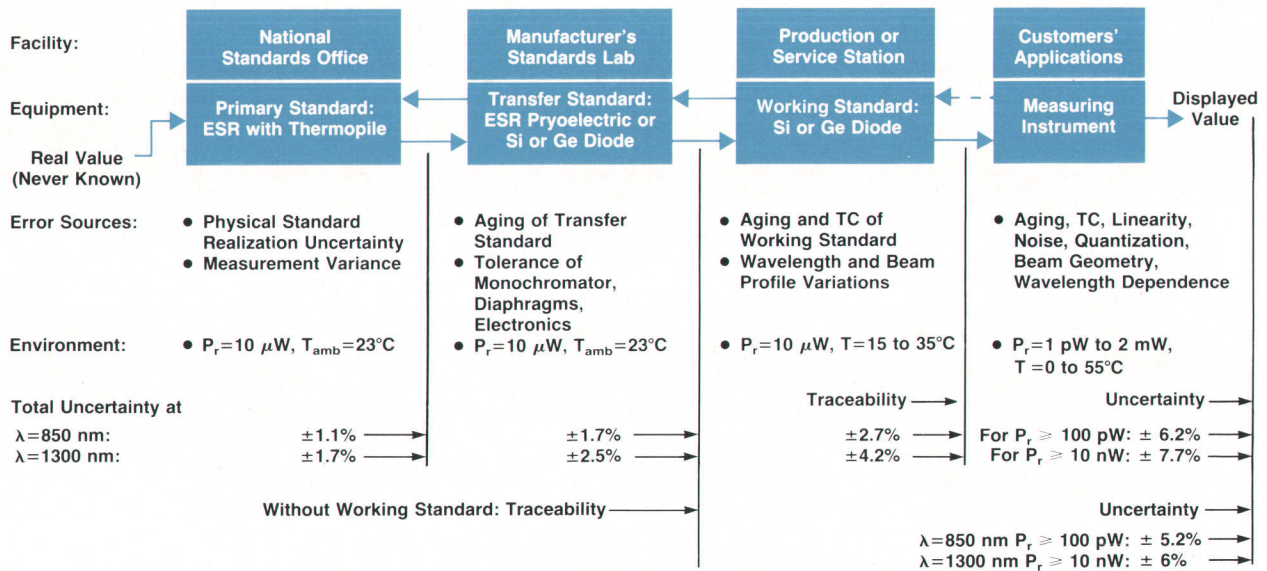λ=1300 nm P_r ≥ 10 nW: ± 6% →

Fig. 12. *Measurement uncertainty is the sum of instrument inaccuracy and calibration uncertainty (traceability).*

in the rms noise formula. This can be achieved, even with large-area Ge detectors, using a chopper. Fig. 11 shows the NEP of the whole circuit and of the detector alone (with an ideal noise-free circuit) as a function of diode impedance R_D. The modulation (chopper) frequency is 30 Hz. Noise figure, F, is the ratio of total NEP to detector NEP.

Calibration and Standards

The total uncertainty of a value displayed by a measuring instrument is composed of the instrument's inaccuracy plus the absolute uncertainty of its calibration.

Instrument inaccuracy includes variations of its transducer gain with intensity and other input signal parameters, temperature dependence, aging, noise, and errors introduced by digitizing and processing.

Calibration uncertainty, often called traceability, usually refers to a specified signal level at fixed environmental conditions. Fig. 12 explains its meaning for radiation power measurements. Listed numbers are tolerance limits, or 3σ statistical uncertainties, which correspond to a 99.7% confidence level.

One step in the calibration chain—the working standard—can be eliminated if all instruments are (re)calibrated in the manufacturer's standards laboratory. This procedure, used within HP, reduces the traceability and the uncertainty specifications of the instrument to ±1.7% and ±5.2% for 850-nm wavelength and to ±2.5% and ±6.0% for 1300-nm wavelength.

Lowest possible uncertainty is achieved if the power meter itself is used as a secondary (transfer) standard and has a calibration certificate from a national bureau of standards. The uncertainty margins in Fig. 12 then shrink from ±6.2% and ±7.7% for 850 and 1300 nm, respectively, to ±4.6% and ±5.2% over the full specified operating range.

Primary standards for radiation power measurements today are blackened absorber discs with a thin-film heater network added for electrical simulation of the radiation power. This element is coupled to a thermopile or a pyroelectric crystal to detect equality of absorbed radiation and electrical heating power. Sophisticated but bulky and slow-reacting constructions, at high power levels, are estimated to yield uncertainties down to 0.2%. Practical calibration procedures at national standards laboratories require one or more copying steps, so the calibration certificate comes out with about ±1% uncertainty, based on a 95% confidence level.

Conclusion

Today's fiber optic links use one or more of the three near infrared bands around wavelengths of 850, 1300, and 1550 nm. A universal power meter transducer with adequate sensitivity and spectral range for these applications can be built with a large-area Ge detector.

For applications in the short-wavelength band only ($\lambda \leq 1$ μm), a silicon diode offers broader dynamic range.

A drawback of both detectors in broadband applications is the considerable and nonlinear variation of their responsivity with wavelength. For instance, when measuring the total radiation of an LED source at 1300 nm ±50 nm, the spectral response curve of Ge and GaInAs may introduce inaccuracies of several percent. A thermal detector, with its inherently flat response, seems preferable. However, the sensitivity and dynamic range of these detectors are 100 to 10,000 times worse than those of the quantum detectors.

Acknowledgments

Precision Optical Heads for 850 to 1700 and 450 to 1020 Nanometers

by Hans Huning, Emmerich Müller, Siegmar Schmidt, and Michael Fleischer-Reumann

THERE ARE TWO OPTICAL HEADS for the HP 8152A Optical Power Meter. Depending on the wavelength of the optical source, either the HP 81521B, for 850 to 1700 nanometers, or the HP 81520A, for 450 to 1020 nanometers, can be used.

HP 81521B Optical Head

The HP 81521B Optical Head is characterized by a wide dynamic range for average power measurements from +3 dBm to −80 dBm, wide spectral responsivity individually measured in 10-nm steps from 850 nm to 1700 nm and the values stored in each optical head, high stability over a temperature range from 0°C to 40°C, a well-cooled detector chip for operation up to 55°C, a noise floor well below −70 dBm, user-friendly optical interfacing, and availability of a large variety of optical adapters and other accessories including a filter holder, a beam splitter, and a bare fiber adapter.

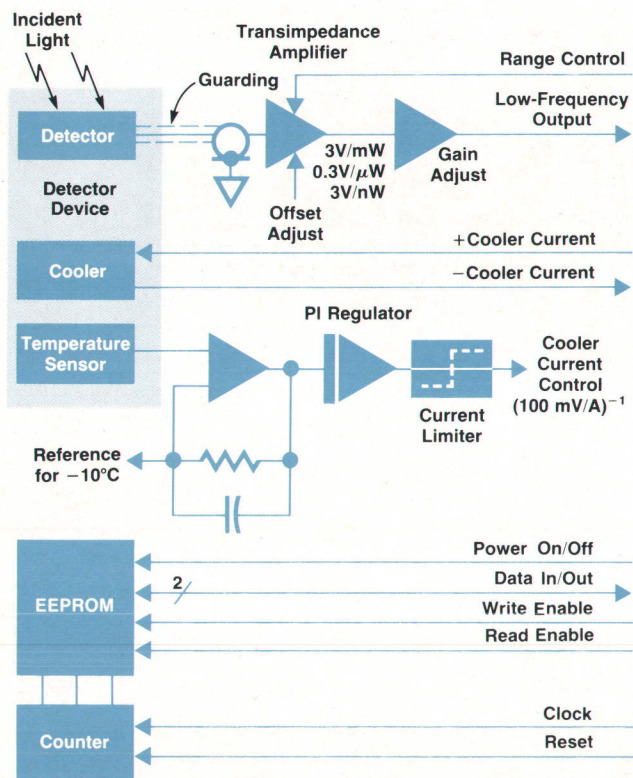The head consists of three main functional blocks, as shown in Fig. 1. The optical detector device includes a two-stage Peltier cooler, a temperature sensing device, and a transimpedance amplifier. A Wheatstone bridge for temperature measurement is followed by a PI (proportional integral) regulator and a current limiter. An EEPROM stores head specific data and calibration factors. The cooler current control and the EEPROM are included in the head to guarantee maximum flexibility in future heads.

The germanium photodiode has an active area of 5-mm diameter. When struck by incident light it generates a current proportional to the absolute optical power with a conversion factor of typically 0.6A/W at 1300 nm. It operates in the photoconductive mode, as described in the article on page 16.

The transimpedance amplifier, Fig. 2, converts this current into an equivalent voltage depending on the selected feedback resistor. The amplifier chosen for this application is the OPA111BM, which exhibits very small input offset voltage drift (maximum 1 μV/K).

Depending on the mainframe gain ($\times 100$, $\times 10$, $\times 1$), the head has to deliver a full-scale input voltage of 0.08V, 0.8V, or 8V to the mainframe.

The following table shows the head gain, feedback resistor (R_f), mainframe gain, and switch positions (Fig. 2) for each input power range. Total gain is the product of head gain and mainframe gain.
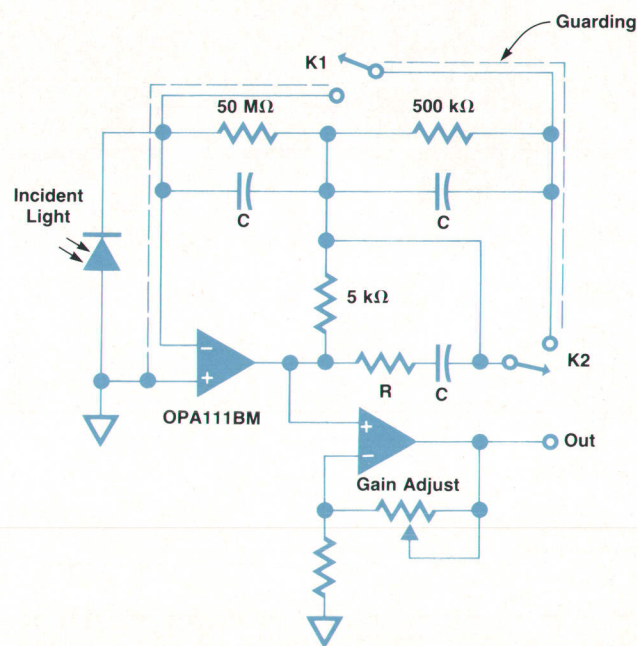

Fig. 1. Block diagram of the HP 81521B Optical Head. The HP 81520A is similar.

Fig. 2. Transimpedance amplifier of the HP 81521B Optical Head. R_f, the effective feedback resistance, depends on the settings of K1 and K2.

Range	R_f	Head Gain	K1	K2	Mainframe Gain
0 dBm	5 kΩ	3V/mW	1	1	1
−10 dBm	5 kΩ	3V/mW	1	1	10
−20 dBm	500 kΩ	0.3V/μW	1	0	1
−30 dBm	500 kΩ	0.3V/μW	1	0	10
−40 dBm	500 kΩ	0.3V/μW	1	0	100
−50 dBm	50 MΩ	0.03V/nW	0	0	10

With the internal gain adjust control, each head is individually adjusted so that its gain is 0.400V/μW at −20 dBm. In the lowest range (full scale = −47 dBm = 19.99 nW) the feedback resistor is 50 MΩ and the photocurrent at −80 dBm is 6 pA. At −47 dBm the photocurrent is 12 nA. Surface leakage currents caused by contaminated surfaces will produce offset errors, so guarding is used to prevent this kind of failure.

HP 81521B Detector Temperature Control

As described in the article on page 16, the absolute temperature is the dominant parameter influencing the noise behavior and parallel impedance of a Ge detector. The heat pumping capacity of the two-stage Peltier cooler required a trade-off between achieving the lowest possible chip temperature and a maximum ambient operating temperature of 55°C. The operating chip temperature selected is −10°C.

The temperature regulator consists of two parts, a driver and a regulator. The driver is installed in the mainframe and supplies the head with a current of +1.5A maximum for cooling or −0.8A for heating. The mainframe also has a slew rate limiter to increase the lifetime of the cooler element.

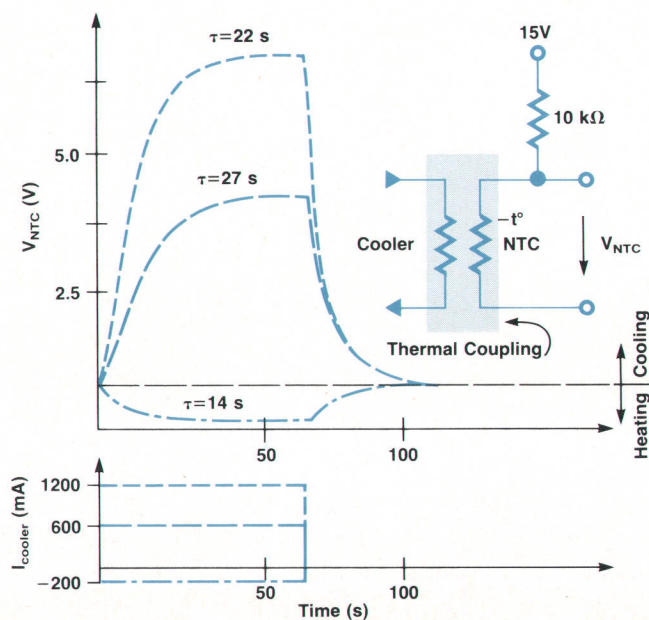The dominant time constant of the regulator, which con-

Fig. 3. The dominant time constant of the temperature regulator is fixed by the thermal coupling between the cooler and the thermal sensor (NTC). This diagram shows typical sensor response to a step change in cooler current at 40°C.
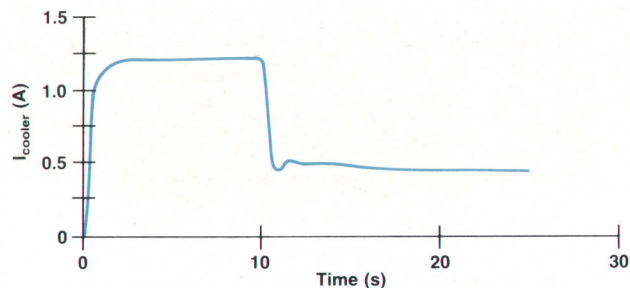
Fig. 4. Typical temperature regulator settling behavior at 25°C.

sists of the resistor bridge, the PI regulator, and the current limiter, is fixed by the thermal coupling between the cooler stage and the thermal sensor, which has a negative temperature coefficient (NTC). This time constant is typically 25 seconds at 25°C ambient temperature. Fig. 3 shows typical behavior at 40°C ambient temperature. The whole system is optimized for minimum overshoot and ringing, and stabilizes the chip temperature within a few hundredths of a degree Celsius.

Settling behavior at 25°C is shown in Fig. 4. Typical cooler current and offset are shown in Fig. 5 as functions of the ambient temperature.

HP 81520A Optical Head

The HP 81520A Optical Head is designed for optical average power measurements at shorter wavelengths, including the spectral window from 450 nm to 1020 nm. A wide dynamic range from +10 dBm down to −100 dBm for average power measurements, spectral responsivity individually measured in 10-nm steps from 450 nm to 1020 nm and the values stored in each head, high stability over a temperature range from 0°C to +55°C, and a noise floor well below −90 dBm are features of this head.

The detector device of the HP 81520A, in contrast to the HP 81521B, is a silicon chip. However, it has the same active area of 5-mm diameter. When struck by incident light, it generates a current proportional to the absolute
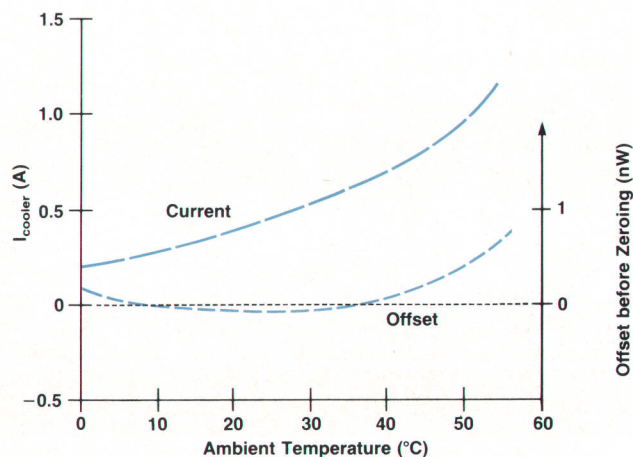
Fig. 5. Typical cooler current and offset as functions of ambient temperature.

optical power with a conversion factor of typically 0.5A/W at 850 nm. It operates in the photoconductive mode.

The HP 81520A Optical Head has the same three main functional blocks as the HP 81521B. Fig. 6 shows the transimpedance amplifier of the HP 81520A.

Depending on the mainframe gain ($\times 100$, $\times 10$, $\times 1$) the head has to deliver a full scale input voltage of 0.08V, 0.8V, or 8V at the mainframe input. The following table shows the head gain, feedback resistor (R_f), mainframe gain, and switch positions (Fig. 6) for each input power range. Total gain is the product of head gain and mainframe gain.

Range	R_f	Head Gain	K1	K2	K3	K4	Main-frame Gain
+10 dBm	1.01 kΩ	0.5V/mW	1	1	1	1	1
0 dBm	1.01 kΩ	0.5V/mW	1	1	1	1	10
−10 dBm	100 kΩ	50 V/mW	1	1	0	1	1
−20 dBm	100 kΩ	50 V/mW	1	1	0	1	10
−30 dBm	10 MΩ	5V/µW	1	0	0	1	1
−40 dBm	10 MΩ	5V/µW	1	0	0	1	10
−50 dBm	10 MΩ	5V/µW	1	0	0	1	100
−60 dBm	1 GΩ	500V/µW	0	0	0	0	10
−70 dBm	1 GΩ	500V/µW	0	0	0	0	100

With the internal gain adjust control, each head is individually adjusted so that its gain is 0.04V/W at −20 dBm. Because of the large tolerance of the 1-GΩ chip resistor (±10%), it is also necessary to adjust this head in the lowest two ranges to get the specified accuracy.

To reach a resolution of −100 dBm (that is, 0.1 pW or 10^{-13} watt) with acceptable stability and noise floor, the detector chip and other parts are enclosed in a hermetically sealed TO-8 housing filled with dry argon. To achieve a constant, controlled temperature of 20°C, the package includes a one-stage Peltier cooler and a temperature sensing resistor (NTC). Also in the package are the detecting and amplifying devices that are sensitive to temperature. These include the silicon detector chip, whose dynamic resis-
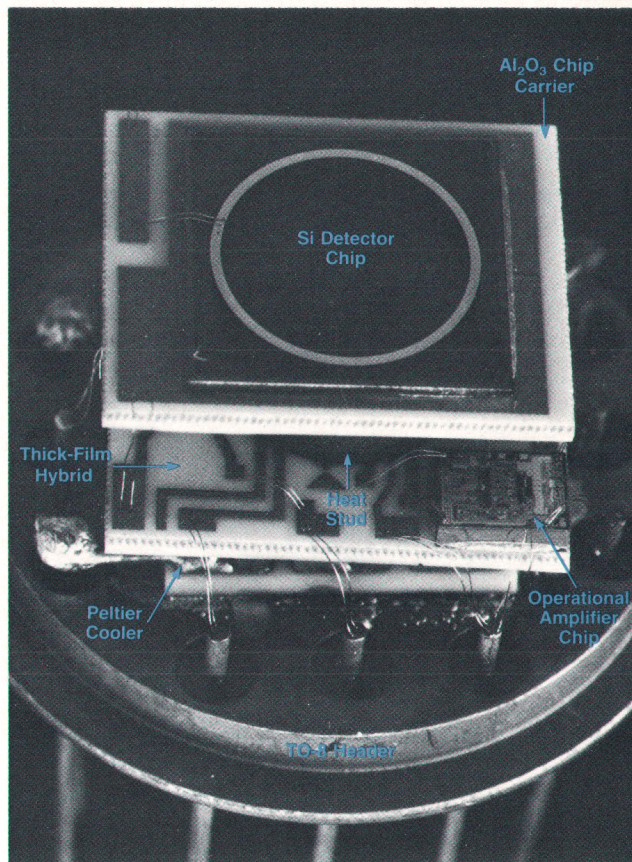
Fig. 7. *HP 81520A Optical Head detector assembly.*

tance changes with temperature, the 10^9-ohm chip resistor (R_f), and the operational amplifier, whose offset voltage drifts with temperature. The chip resistor is also sensitive to contamination and humidity, and is protected from these influences by the package.

The one-stage thermoelectric cooler is soldered onto a standard TO-8 header at 125°C using In-Sn solder paste.

Fig. 6. *Transimpedance amplifier of the HP 81520A Optical Head. The effective R_f is a combination of the four resistors so labeled, depending on the switch positions.*

Optical Power Splitter

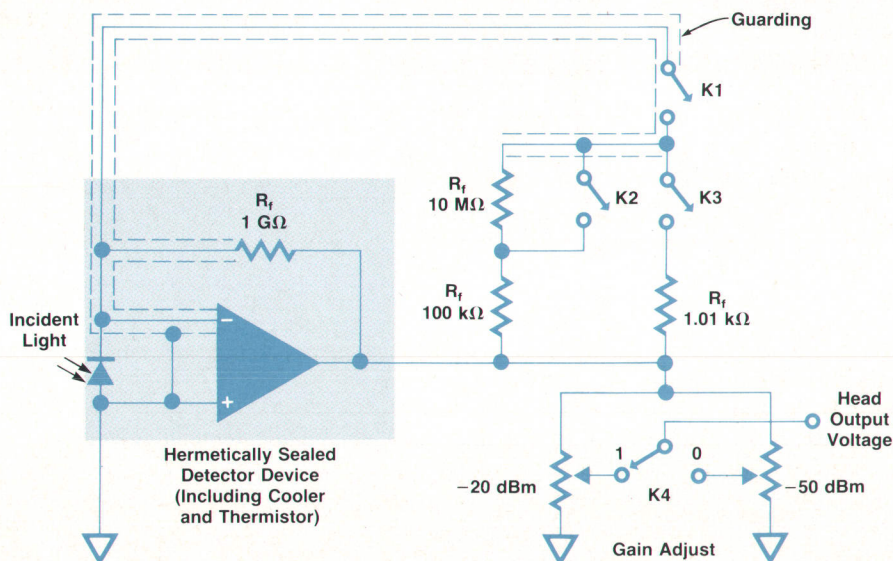The HP 81000AS/BS Optical Power Splitters are used in combination with the HP 8152A Optical Power Meter to measure insertion loss and attenuation of passive optical components or to control power levels.

The HP 81000AS/BS power splitters are three-port devices. They have one fiber connector input, one fiber connector output, and one parallel beam output to the optical head of the HP 8152A. A conventional optical beamsplitting technique is used. A high-precision optical system with the same objective lens as in the HP 8158B Optical Attenuator collimates the divergent light of the input fiber to an expanded parallel beam and refocuses it into the output fiber. A beamsplitter plate, located between the two lens systems, reflects one part of the light intensity to the photodiode of the optical head. The beamsplitter is low-angled to the optical axis to reduce the polarization sensitivity of its reflection factor to less than ±4%. Physical beamsplitting ensures that there is no mode selectivity in multimode applications.

Fig. 1 shows the optical system of the splitter. The light is not fiber guided and so different fiber types with numerical aperture NA less than or equal to 0.3 can be used. The HP 81000AS is designed for multimode applications and accepts fiber core diameters from 50 μm to 100 μm. The HP 81000BS is designed for single-mode and multimode applications and accepts fiber core diameters from 9 μm to 100 μm. The HP 81000AS covers the first fiber optic window, that is, the wavelength range from 600 nm to 1200 nm, and the HP 81000BS covers the second and third fiber optic windows, the wavelength range from 1200 to 1650 nm.

The optical splitters combine the advantages of low insertion loss, stable splitting ratio, and good environmental characteristics. The typical insertion loss, including the two Diamond® HMS-10/HP connectors, is 1 dB for multimode and 2.5 dB for single-mode operation. The splitting ratio depends on the insertion loss of the fiber input to fiber output coupling and is about 10 dB for single-mode and 12 dB for multimode. Thermal stability of the splitting ratio within a ±2°C temperature window is better than +0.06 dB for single-mode and +0.01 dB for multimode.

Siegmar Schmidt
Development Engineer
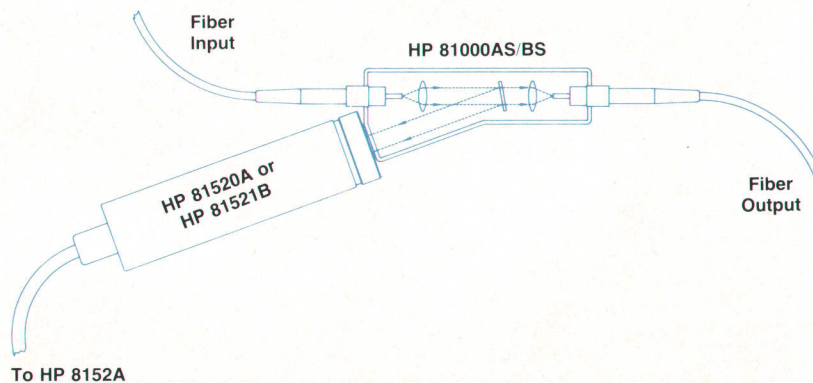Böblingen Instruments Division

Fig. 1. *Optical system of the HP 81000AS/BS Optical Power Splitters with the HP 81520A and HP 81521B Optical Heads.*

The top of the Peltier cooler serves as a mounting base for all the temperature stabilized detector parts (Fig. 7). A thick-film hybrid on an Al_2O_3 ceramic substrate is glued to the cooler with heat-conductive epoxy. The hybrid contains the op amp IC chip, the 1-GΩ chip resistor, and the thermal sensor (NTC chip), which are attached with conductive epoxy. All of these chips are connected with wedge-wedge bonds to the substrate or to the TO-8 header pins.

To achieve more component mounting space, a second floor is generated by mounting the detector chip carrier hybrid on a ceramic heat stud. This design provides a very good temperature stabilized environment for the electrical and optical components, which are responsible for the high stability and sensitivity of this detector assembly. To achieve the MTBF design goal, the whole assembly is hermetically sealed with a laser-welded window cap under an argon atmosphere.

EEPROM

To give the system the flexibility to accept different heads, head specific data is included in the head and not in the mainframe.

Each head contains an electrically erasable programmable read-only memory (EEPROM) that has a capacity of $2K \times 8$ bits, although only $2K \times 2$ bits are used. The amount of memory used represents a compromise between short reading time and a minimum of head-mainframe connections. This memory is split into 512 head bytes of 4×2 bits each.

Fig. 8 shows the memory map. The control bytes include checksum bytes to detect errors and prevent data manipulation, a data valid byte, and a compatibility identifier indicating which mainframes the head is compatible with. There are pointers to several start locations, and head specific data consisting of the following:

- Head specials: zero repetition times, chopper wait time, shutter wait times, etc.
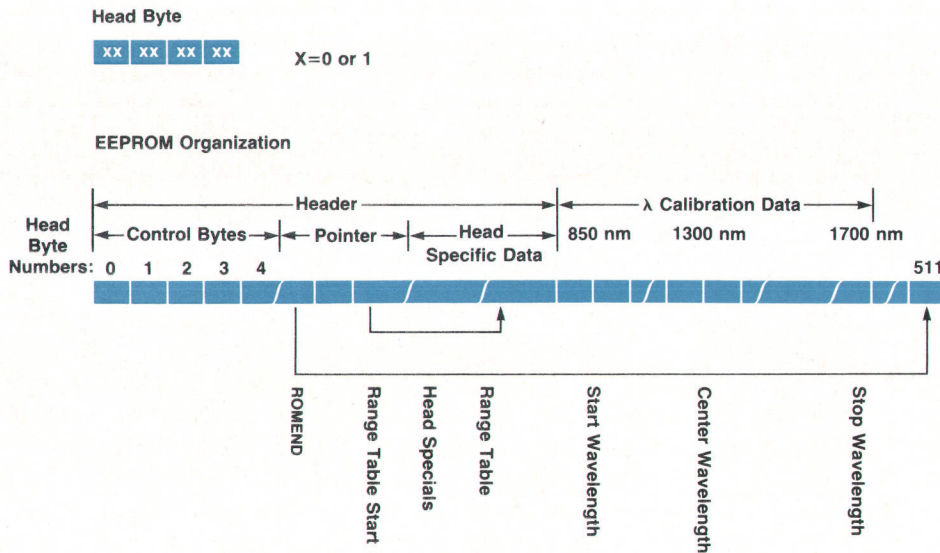- Range table: gain factors for the head and the mainframe

Head Byte

| xx | xx | xx | xx | X=0 or 1

EEPROM Organization

Fig. 8. *Organization of the EEPROM containing head specific data in the HP 81520A and 81521B Optical Heads.*

- Calibration identifier: head serial number, date of calibration, calibration channel, etc.
- Calibration description: start wavelength, center wavelength, stop wavelength, number of calibration points, distance between two calibration points, field length
- Calibration data: individually measured gain factors depending on the wavelength (see article, page 8).

Calibration

Each head is calibrated in a homogeneous, parallel beam with a spot of 2.5-mm diameter at −20 dBm. Spectral responsivity is measured with a high-resolution monochromator in 10-nm steps using a pyroelectric detector as a standard.

Precision Optical Interface

The HP 81520A and 81521B Optical Heads are precision optical-to-electrical converters. To maintain their high overall accuracy, a precise optical interface had to be established between the detector surface and the point at which the power of the incoming light is to be measured.
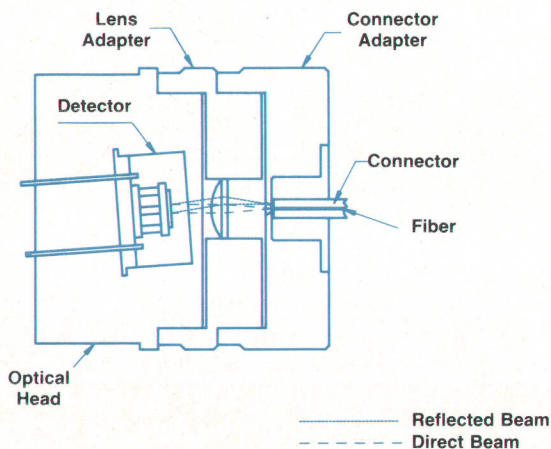
The first design goal was to gather onto the detector a certain (and constant with temperature, mechanical tolerances, and other parameters) amount of power from the user's light emitting device, regardless of the nature of this light, whether it be spatial or fiber guided. In the latter case, the power has to be independent of fiber type and core diameter, and connector type, if any. With spatial light of unknown beam diameter, the "certain amount" mentioned above is 100% of all the light it is possible to capture.

The second design goal was to minimize the interference between the measurement instrument and the system to be measured. This means that neither the optical head nor the optical interface should produce reflections back into the system or device under test. This system or device might be a light source in a parallel beam system on an optical bench, which is typically rather uncritical, or the end of a fiber connected to a laser diode, which, especially in a single-mode system, can be very sensitive.

The third goal was to make accurate absolute calibration possible in spite of the wavelength dependence of the chosen detectors (Ge and Si pin diodes).

The best trade-off between the desired sensitivity and versatility was a 5-mm diameter for the pin diode detectors. But once these semiconductor detector types were chosen, it was necessary to deal with their high reflection factor of about 20%.
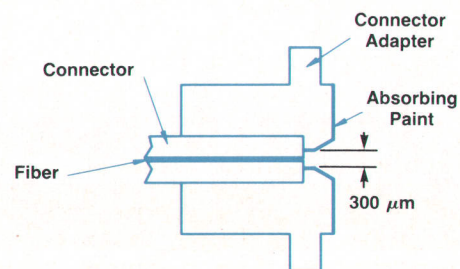
Fig. 9. *Diagram of the precision optical interface for the HP 81520A and 81521B Optical Heads, showing detector tilt angle.*

Fig. 10. *Reflection-reducing inner surface design of the connector adapter.*

In terms of calibration this is no problem, because the light that hits the detector surface and is reflected does not generate electron/hole pairs inside the detector or a voltage at the output of the optical head, and can be calibrated out as long as the amount is constant and the light never returns to the detector surface again. For calibration with spatial light in a parallel beam system, we only had to prevent reflections back into the light source or any optical component, which was easy to achieve by slightly tilting the detector, as can be seen in Fig. 9.

When dealing with fibers, a category that includes the main applications of this instrument, some different requirements arise. First, as described in the article on page 16, a collimating lens system between the fiber end and the detector surface is necessary. This is to ensure that nearly 100% of the light reaches the detector with reasonable distance between fiber and detector, and that the illuminated spot on the detector surface is independent of fiber type and core diameter. The collimating lens system also ensures the same conditions—angle and spot diameter—in actual service as during calibration, either in-house or at the German PTB or other standards laboratory.

Another requirement in a fiber optic system is that the optical system be closed, so that no ambient light reaches the detector. This includes the requirement that the 20% of the incident light that is reflected from the detector surface never return to the surface again in any nonnegligible amount. Surrounding parts have to be highly absorbing, and return to the detector must only be possible after several reflections to reduce the returning power to a negligible value. Coating with optical absorbing paint is one way to achieve this, and again, angling the detector is another. By these methods, not only is instrument accuracy improved by avoiding internal back reflections to the detector, but also reflection back into a connected fiber is totally avoided, so interference between the device under test and the measurement instrument is no longer a problem.

The last remaining location of reflections is the front surface of the customer's connector. Its reflection coefficient is unknown and totally out of the instrument designer's control. The tilting angle would have to be larger than 13° for a 3.5-mm diameter connector to ensure that reflected light misses the connector. Such a large angle is not practicable because it reduces the efficiency of the detector in terms of conversion factor (A/W). It also decreases
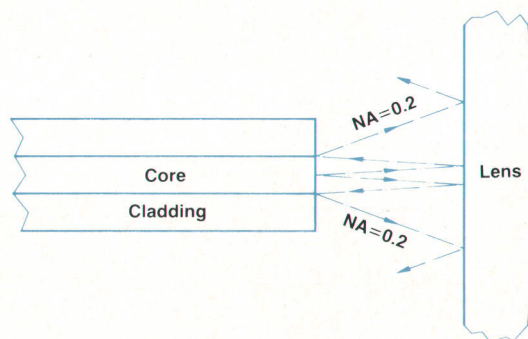

Fig. 12. *Possible back reflection into the fiber.*

the usable parallel beam diameter and thereby increases the sensitivity to mechanical tolerances. This is because:

$$d_{eff} = d_D \cos \alpha,$$

where d_D is the diameter of the detector and α is the tilting angle.

With reasonable angles ($<5°$) the only way to avoid possible inaccuracies is to shade the (unknown and reflecting) front surface of the connector with a specially shaped, absorptive painted surface inside each connector adapter (see Fig. 10).

Uncoated glass lenses usually reflect about 4% of the light at each surface (Fig. 11), so that an optical nonreflective coating is necessary. This can reduce reflections well below 0.5%, so the power reflected back into the fiber is small enough not to be a problem.

Fig. 12 shows a simple approach for estimating the percentage of power that might return into the fiber. Let's assume the typical multimode case with a fiber-core diameter D = 50 μm and a distance between the fiber and the front surface of the lens system of s = 2.5 mm (not the focal length). Then the cone angle for possible back reflections into the fiber core, according to the formula arctan (0.5D/2s), is about 0.28°. With the NA of this fiber being 0.2, the 95% power radiation angle is 11.5°. Assuming a Gaussian power distribution, less than 3.5% of the emitted power has to be taken into account. Since the lens only reflects 0.5% of this power, direct back reflection is really negligible (<200 ppm).

Nevertheless, although negligible in terms of back reflection, this reflection has to be taken into account for the measured power, because 0.5% reflection at each surface means 99% transmittance for a single lens, or 0.04-dB attenuation. This value is not negligible. Therefore, each lens is delivered with a calibration factor, which easily can be entered into the HP 8152A Optical Power Meter mainframe. Because of possible variations of the nonreflective coating, the transmittance of each lens is measured individually and is engraved as a calibration factor on the lens housing (for example, -0.04 dB for a single-mode HP 81010BL).
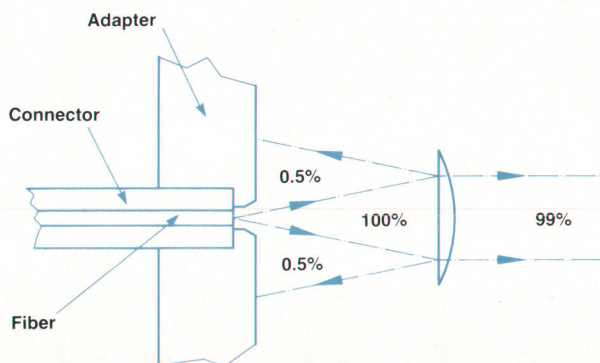
Acknowledgments

Fig. 11. *Nonideal transmittance of a coated lens. Reflections are about 4% for an uncoated lens, 0.5% for coated.*

A High-Precision Optical Connector for Optical Test and Instrumentation

by Wilhelm Radermacher

HIGH-PERFORMANCE CONNECTORS are an important part of fiber optic test instrumentation and systems. The performance of fiber optic instruments and systems depends to a large extent on the performance of the optical connectors. In fact, in many cases the specifications of instruments depend more on the connectors than on other factors. For example, the stability of a source depends more on the stability of the connection than on the stability of the emitting device if the circuitry is designed properly.

High-performance fiber optic connectors are used not only in a direct connector-to-connector scheme like a utility connector, but also as an interface to instrumentation containing bulk optical modules. What are the requirements for a high-performance optical connector for instrumentation and why is a high-performance connector different from a utility connector?

Utility connectors are used in large quanities in optical links. Therefore, they should be small and inexpensive, and have low insertion loss. It is an advantage if they are field-installable, especially in single-mode applications. High-performance connectors, on the other hand, require careful optical alignment which cannot be done in the field and is expensive.

The key characteristics of an optical connector for instrumentation are:

High reliability and long lifetime. Utility connectors are specified for 500 to 1000 cycles. In an optical communications link, this is more than sufficient, because connections occur only during manufacturing, installation, and occasional maintenance. In instrumentation, especially in a production environment, connecting cycles occur very often, perhaps as many as 100 times per day on one instrument. Lifetimes of 500 or 1000 cycles are not acceptable in this application.

- Repeatability of insertion loss on successive connecting cycles. Although the overall insertion loss of a connection can be calibrated out in many applications, it is essential that a measurement that is repeated lead to the same result each time.
- Temperature stability of the insertion loss must be excellent to ensure repeatable measurements, especially during environmental testing of modules and components.
- Overall insertion loss is important to maintain the power budget of a measurement. Since 1-dB maximum insertion loss is a common specification for good single-mode connectors this is seldom a problem.

Need for Physical Fiber Contact

The insertion loss of an optical connector is caused by two main factors. One is misalignment of the fiber cores. The use of good high-quality parts with tight tolerances and good workmanship in the connector production process can reduce the influence of core misalignment to a minimum. The other main influence on the insertion loss is the spacing between the ends of the glass fibers if they are not in physical contact. At the wavelengths of coherent infrared light used for information transfer in the fiber, standing waves are caused by distances between fiber ends of more than one tenth of the wavelength, which can be as little as 100 nm. Minimal changes in this distance, which are mostly caused by ambient temperature changes or mechanical stress in the connectors, will cause large variations in insertion loss (see Fig. 1).

The only solution to this problem is a connector scheme that assures physical contact between the fiber ends under all circumstances. Only a physical-contact connector makes it possible to reach low insertion loss under the
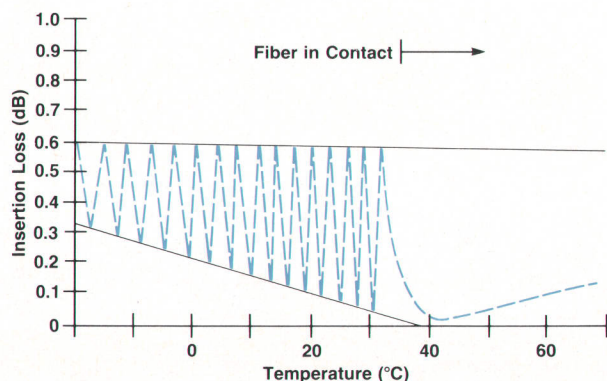
Fig. 1. *Temperature sensitivity of a connector without physical contact. At approximately 35°, the fiber has expanded enough to make contact.*

| | Spec | Measured Values | |
		Average	Variance
Insertion Loss (dB)	1 0.6	0.2 0.1	0.1 0.05
Temperature Stability 0 to 60°C (dB)	0.5 0.3	0.15 0.1	0.05 0.03
Repeatability (dB)	0.2 0.1	0.08 0.03	/ /

Fig. 2. *Specifications and measured values for the main performance characteristics of Diamond® HMS-10/HP connectors. Top number in each box is for single-mode operation; bottom number is for multimode.*

following conditions:

- Changes of ambient temperature of the connection. This is very important if one connector is built into an instrument and exposed to the internal temperature rise caused by power dissipation.
- Variations of insertion loss between connector pairs if a large number of connector combinations are tested.

A number of precautions are necessary to ensure physical contact:

- The front face of the connector must be polished at a very precise 90° angle to the connector ferrule.
- The diameter of the mating surfaces must be small enough to ensure that resilient deformation of the material leads to physical contact, and must be large enough to ensure that no permanent deformation of the material occurs. A well-defined spring force can ensure physical contact and prevent permanent damage.
- A loose connector sleeve bushing is needed to prevent mechanical stresses in the connector ferrule and bushing when the connector is tightened.

The Diamond® HMS-10/HP Connector

The high-precision, high-performance connector used in the new family of fiber optic instruments described in this

issue is the Diamond HMS-10/HP, developed jointly by Diamond and HP, and assembled by HP. This connector meets all of the requirements discussed above. Also, since many of the instruments described in this issue are intended for use in single-mode as well as multimode applications, it is necessary that the connector meet the requirements of both applications and that single-mode and multimode connectors are fully compatible. The Diamond HMS-10/HP also meets this requirement.

Both the connector ferrule and the connector bushing are made of tungsten carbide. Tungsten carbide is a very hard material and it was expected that in spite of the very tight tolerances involved it would wear less than any other material. Extensive lifetime tests of more than 10,000 cycles have shown that the connector has a very long lifetime. All connectors tested were well within specifications after these tests.

Connector Characterization

A major problem that every manufacturer of optical connectors faces is the definition of a worst-case specification of the insertion loss and other parameters. This is because only a small number of connectors are available and can be characterized at any time, since most connectors from previous production lots are at customer locations and not available. The insertion loss is a characteristic of a particular connector pair, not of one connector only. The only way to guarantee quality is to make measurements on a limited sample base using statistical methods.

The margin between the average measured insertion loss and the maximum specification depends on the variance and the desired probability of meeting the specifications. It was our goal to reach a probability of 99.7% that any HMS-10/HP connector would meet the specified insertion loss measured with any other HMS-10/HP connector. Assuming that the measured values fit a Gaussian distribution, this means that desired maximum specification is equal to the average value plus three standard deviations.

Fig. 2 shows the main performance characteristics of the HMS-10/HP connector, comparing measured values with maximum specifications. Fig. 3 shows the distribution of insertion loss measurements and compares it with a Gaussian distribution. Fig. 4 shows the temperature sensitivity of a typical HMS-10/HP connector.
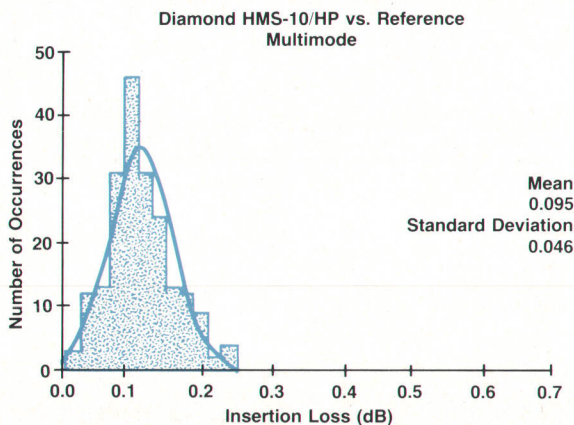

Diamond HMS-10/HP vs. Reference
Single-Mode

Mean 0.204
Standard Deviation 0.100

Diamond HMS-10/HP vs. Reference
Multimode

Mean 0.095
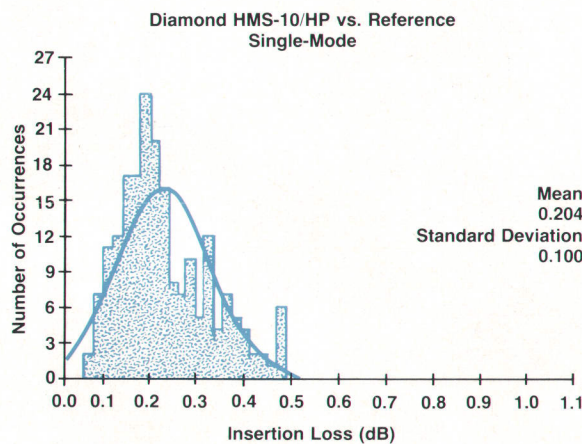Standard Deviation 0.046

Fig. 3. *Typical distributions of measured Diamond® HMS-10/HP insertion loss.*
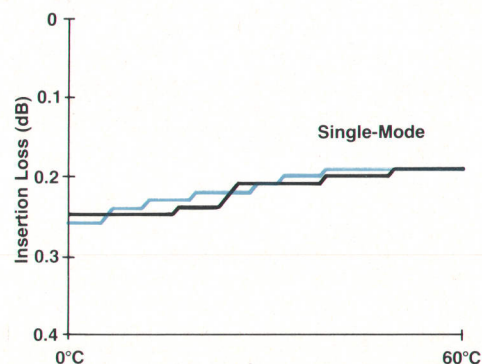

Fig. 4. *Temperature sensitivity of a typical Diamond® HMS-10/HP connector. The two curves are the results of cycling up and down.*
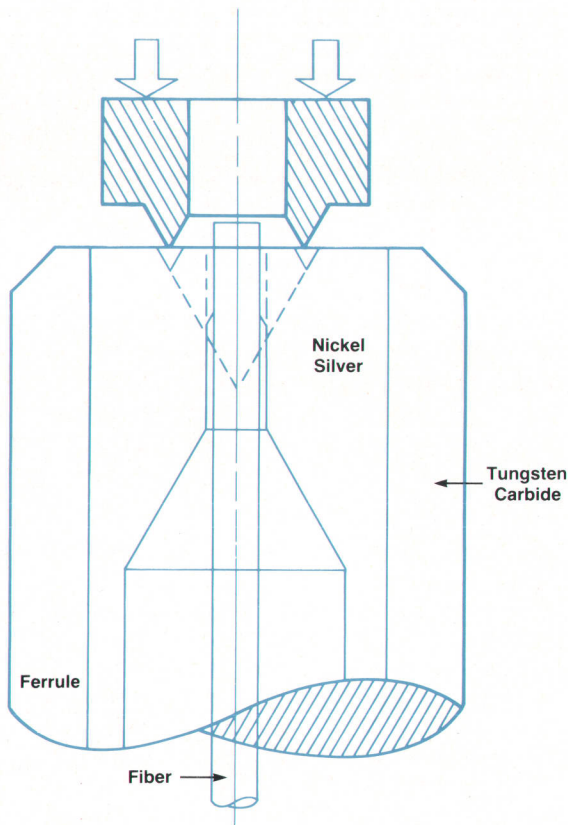
Fig. 5. *Principal fiber core alignment procedure.*

Fig. 6. *Fine fiber core alignment procedure.*

Core-to-Core Alignment

Although the characteristics of single-mode optical fibers have been improved over the last few years, eccentricity of the core can lead to excess insertion loss unless a core-to-core alignment is done. The production process of the HMS-10/HP includes this alignment.

The principal method of core alignment is as follows. The hole in the ferrule, which will eventually hold the fiber, has a diameter of nominally 135 μm. It is, therefore, quite easy to insert the fiber, which has a cladding diameter of nominally 125 μm. Another advantage of this connector is that only one type of ferrule is used for different cladding diameters (they can vary approximately ± 2 μm even within one batch of fibers). The fiber is centered in the hole by applying force on the front face of the connector with a special tool, which stamps a circular V-groove into the front face of the nickel-silver insert of the tungsten carbide ferrule (Fig. 5). After this, however, the core of the fiber may be slightly out of center.

The eccentricity of the fiber core is then measured using a TV camera and visible light. An adjustment tool then stamps a larger V-groove into a segment of the previously stamped groove and moves the fiber such than the core is exactly centered (Fig. 6).

The area inside the circular V-groove is later polished and used as the contact area. This ensures a reproducible diameter and consequently a reproducible size of the contact area.
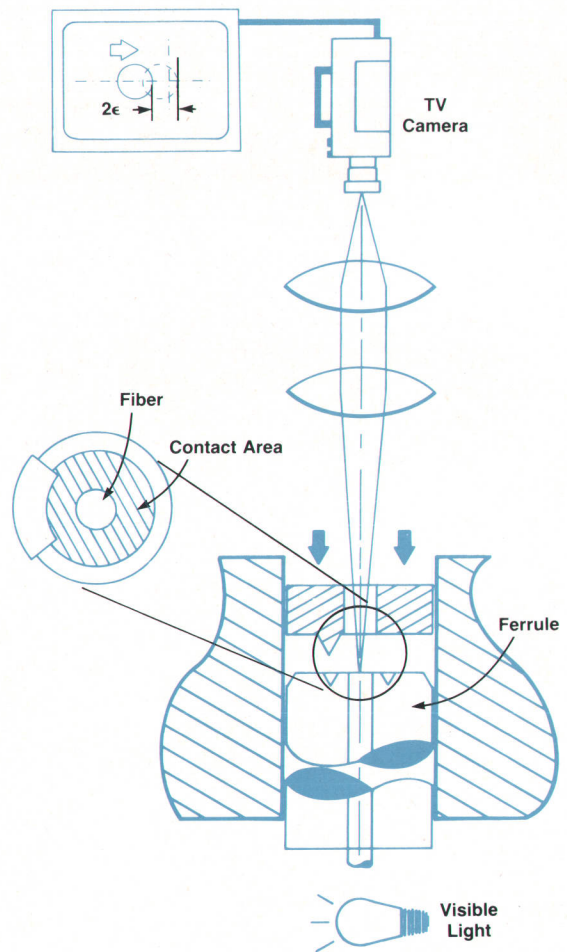
Design Approach for a Programmable Optical Attenuator

by Bernd Maisenbacher, Siegmar Schmidt, and Michael Schlicker

WITH INCREASING DATA RATES and wider repeater spacing, requirements on optical fiber transmission systems have become more stringent and tolerances have become smaller. Better test equipment, especially on the optical side, is needed to measure performance and ensure that specifications are met.

At the same time, the demand for high-performance transmission equipment grows rapidly. Production capacities must be built up and test procedures generated. Shorter testing times are needed to keep up with demand. One strategy for achieving these goals has been the increasing use of computer control and automation. Computer-aided testing and HP-IB (IEEE 488/IEC 625) programmable test equipment are solutions to the problem of long test times.

In general, electrical test instrumentation can be operated under computer control. This trend, however, has not yet penetrated the area of optical measurement equipment to the same extent. In the case of optical attenuators, there is quite a variety of manual attenuators available, but only a handful of programmable models for single-mode applications. This availability is important for high-performance transmission systems, which are now almost exclusively implemented with single-mode technology.

The new HP 8158B Option 002 Optical Attenuator (Fig. 1) is believed to be the first variable optical attenuator suitable for both single-mode and multimode applications. It handles all fiber core diameters from 9 to 100 μm and is calibrated at both 1300 nm and 1550 nm. For other wavelengths between 1200 nm and 1650 nm, it automatically calculates adjustment factors.

The HP 8158B Option 001 Optical Attenuator is designed for the wavelength range from 600 to 1200 nm and is calibrated at 850 nm. It handles fiber core diameters from 50 to 100 μm.

The maximum attenuation range of both attenuators is 60 dB. Resolution is 0.01 dB and typical insertion loss is 1.0 dB for multimode and 2.0 dB for single-mode. Precise calibration and a digital display ensure repeatability within 0.04 dB over a temperature range of 0 to 55°C.

The HP 8158B has high-precision Diamond® HMS-10/HP connectors (see article, page 28) and is fully programmable via the HP-IB.

Optical System

Commercially available fiber optic attenuators, both programmable and manual, use a range of techniques for achieving the optical attenuation. Many use a technique based on some angular, lateral, or axial displacement between the two fiber ends. Others use some sort of filter or dispersive element. The HP 8158B uses two filter wheels and various bulk optical components.

As shown in Fig. 2, a high-precision optical system collimates the light of the input to an expanded parallel beam and refocuses it onto the output fiber. Fixed filters, a reflection prism, and a continuously variable 0-to-10-dB circular filter are located between the two lens systems. Fig. 3 shows the optical block.

There are five fixed filters in 10-dB steps from 10 to 50 dB to cover the attenuation range up to 60 dB. These filters are coated with a metallic neutral density layer, which reduces the wavelength dependency of the optical density of the filters.

All optical surfaces are coated with multilayer broadband antireflection coatings to prevent interference modulation and to achieve low insertion loss. The filters are angled to the optical axis to prevent back reflection into the fibers. The expanded-beam technology with attenuation filters ensures that there is no mode selectivity in the case of multimode fiber applications, and reduces the sensitivity of the instrument's performance to dust particles. In addition, the attenuator optical blocks are produced and mechanically adjusted in a flow box and are sealed under this same condition to ensure a high level of dust-free air inside the blocks.

Both filters are aligned in the optical path, and each has its own drive motor and optical encoder.

The digital design of the motor control circuits guarantees fast realignment for any change in attenuation setting. Realignment time is typically 50 ms, so short measurement cycles can be achieved with automatic test systems.

Fig. 1. *The programmable HP 8158B Option 002 Optical Attenuator is designed for multimode and single-mode applications and is calibrated at 1300 and 1550 nm. Another model, the HP 8158B Option 001, is calibrated at 700, 850, and 950 nm.*

Automated Calibration with Wavelength Correction

Linearity of attenuation characteristics is achieved by

individual calibration in production. Using an HP 9000 Series 200 Computer, an automatic calibration program is run on each unit. The attenuation of the fixed filters for a given setting is measured at 1300 and 1550 nm for the HP 8158B Option 002 and at 700, 850, and 950 nm for the HP 8158B Option 001. Within the same measurement cycle, the dynamic attenuation of the circular filter is also measured.

The measured data is processed by the computer and transferred via the HP-IB to an EEPROM in the attenuator. Any errors caused by the manufacturing tolerances of the optical filters are calibrated out. In addition, the wavelength characteristics for the metallic filter coatings are stored in the EEPROM. This permits the microprocessor to calculate correction factors for each wavelength/attenuation combination. As a result, automatic correction is performed for the wavelength and attenuation settings made by the user.

Connector Considerations

In a sense, this approach to designing an optical attenuator can be described as an optical feedthrough connector with attenuating filters located along the optical path. With single-mode operation selected, the optical coupling is approximately characterized by a Gaussian distribution curve.

Fig. 4 shows how the coupling loss varies with misalignment of two fibers. To minimize connector loss, the fiber ends must be exactly positioned in the X, Y, and Z axes. The HP 8158B uses connector adapters that can be precisely adjusted at the focal point of the lens system with better than 0.2-μm repeatability. To maintain this precision over the instrument's operating life, a hard metal bushing and a hard metal Diamond HMS-10/HP connector are used for each part. This approach minimizes wear and resultant misadjustment.

Loss resulting from off-axis connector coupling can be evaluated quantitatively. Two Gaussian beams can be coupled without loss when they have identical beam shapes. This means that the propagation axes must coincide and that the spot radii must be the same. These conditions must be fulfilled in all directions perpendicular to the prop-
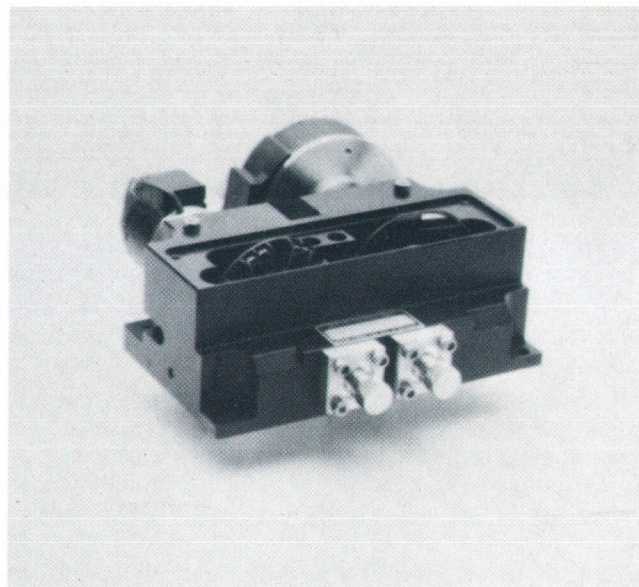

Fig. 3. *The optical block of the HP 8158B Optical Attenuator has two connectors, each with a lens system.*

agation axis. If these conditions are not fulfilled, the loss can be calculated as follows:[1,2]

$$V_{kx} = 10 \log \left\{ k_x \cdot \exp \left(-k_x^2 \left[\frac{\Delta x^2}{2} \left(\frac{1}{W_{o1x}^2} + \frac{1}{W_{o2x}^2} \right) + \right. \right. \right.$$

$$\left. \left. \left. \frac{K^2 \alpha_x^2}{8} \left(W_{1x}^2 + W_{o2x}^2 \right) - \frac{\Delta x \, \alpha_x \, \Delta Z_x}{W_{o1x}^2} \right] \right) \right\}$$

$$k_x = \frac{2 \, W_{o1x} \, W_{o2x}}{\sqrt{(W_{o1x}^2 + W_{o2x}^2)^2 + \frac{4 \Delta Z_x^2}{K^2}}}$$

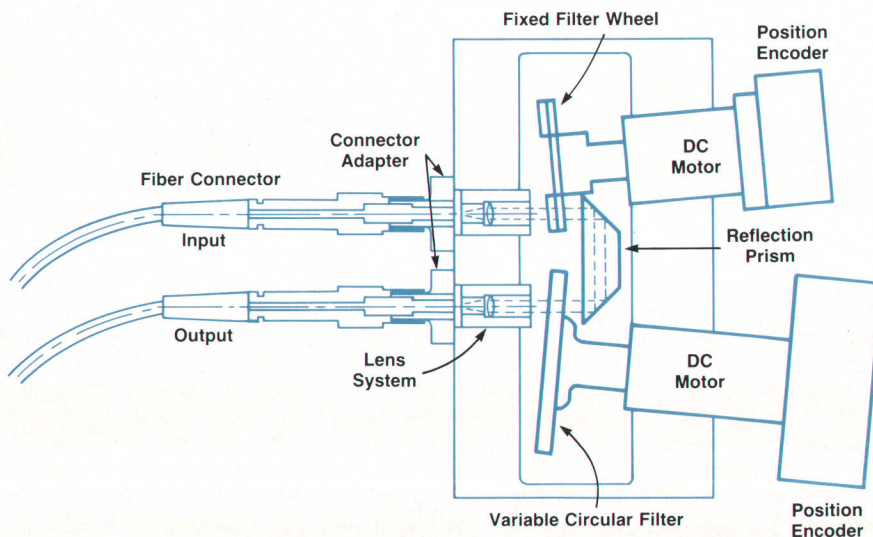$$W_{1x}^2 = W_{o1x}^2 \left(1 + S_x^2 \right)$$

Fig. 2. *The optical system of the variable attenuator includes a fixed filter wheel with 10-dB increments, and a continuously variable filter wheel.*

$$K = \frac{2\pi}{\lambda}$$

$$S_x = 2 \frac{\Delta Z}{K W_{o1x}^2}$$

where:
W_{o1x} = spot radius after optical imaging in the X direction
W_{o2x} = spot radius of the fiber in the X direction
ΔZ_x = separation of the spot from the fiber
Δx = misalignment of the optical axes of the two fibers (X component)
α_x = angular misalignment between the fibers in the X direction.

The above formulas also apply to the Y direction, so that the total loss then can be determined by the formula:

$$V_k = V_{kx} + V_{ky}.$$

Hardware

Both servo loops are closed in one of the two microprocessors of the HP 8158B (Fig. 5). The other microprocessor controls the display and the keyboard, handles the HP-IB, and calculates and transmits the positions for the motor controller via the device bus.

Microprocessor. The heart of the digital motor controller is an 8-bit CMOS microprocessor with 128-byte internal RAM and a 16-bit internal timer. The firmware is resident in a standard EPROM.

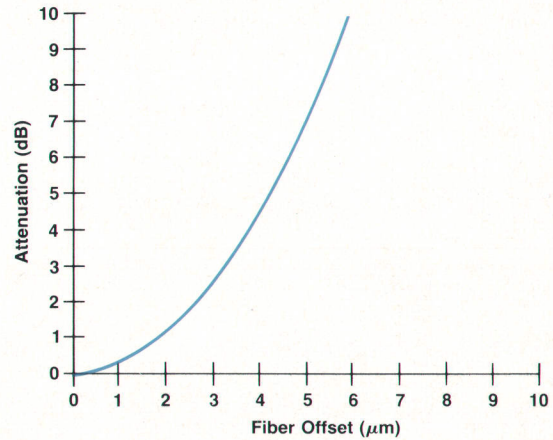**Pulse Width Modulator and Motor Driver.** To extract the

Fig. 4. *Plot of coupling loss versus misalignment of two fibers follows a Gaussian distribution.*

best possible performance at minimum cost, the digital-to-analog converter for the motor driver is a simple pulse width modulator and the motor driver itself consists of an inexpensive transistor full bridge. Therefore, the HP 8158B needs only a unipolar 15V power supply for the motors and a 5V supply for the digital logic. Fig. 6 shows the design of the motor driver circuitry.

The control processor sets the PWM register. A 7-bit comparator compares the content of the PWM register with a 7-bit free-running counter. Whenever the PWM register value is higher than the value of the free-running counter
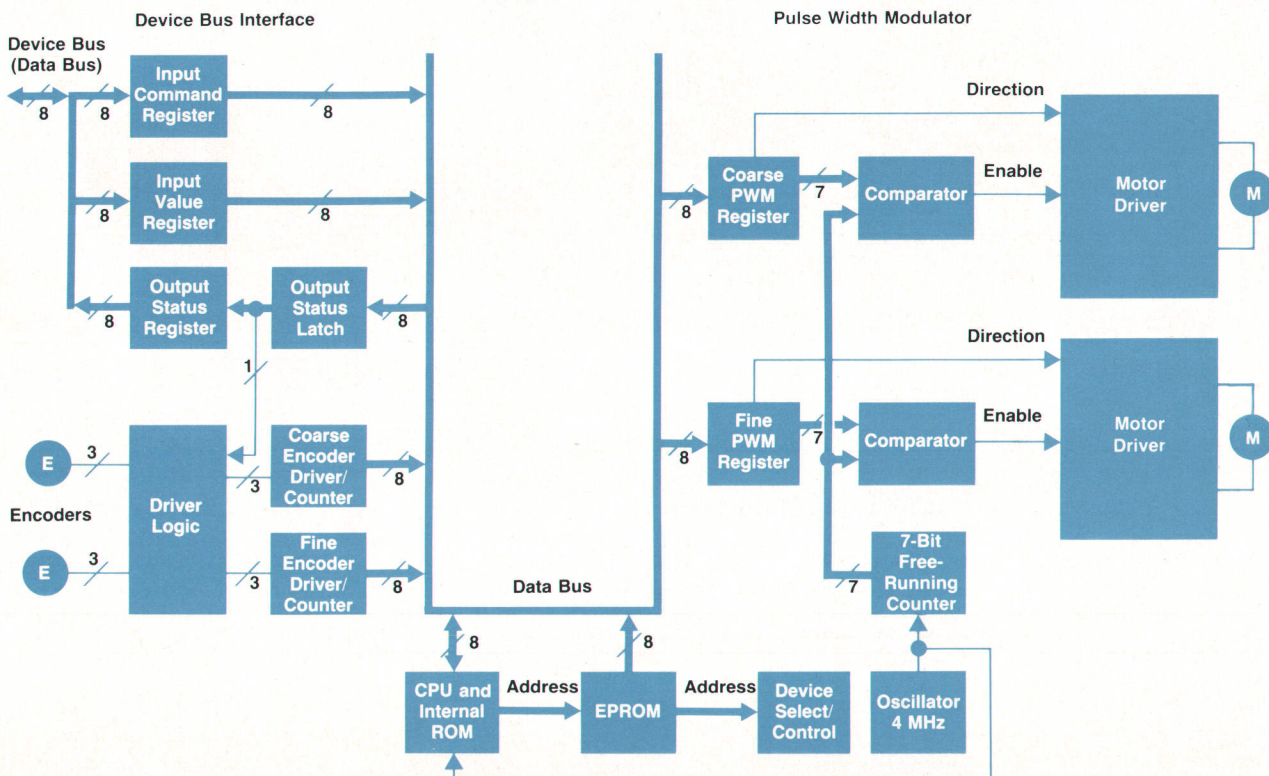

Fig. 5. *HP 8158B digital motor controller diagram.*

the transistor bridge is enabled. The high-order bit of the PWM register determines the turn direction for the motors. The period of the PWM is 31.25 kHz, high enough to prevent audible noise.

Position Sensing System. The optical filter wheels are fixed on the front of the motor shaft, so no mismatch between the filter position and the position sensing system is possible. For the variable filter wheel, a 1024-track incremental encoder is used, and for the fixed filter wheel, a 512-track incremental encoder is used. Both encoders are standard HP products. To get better resolution, the encoders are driven in quadrature mode. In this mode, the effective resolution is 4096 (2048) tracks per revolution. This technique is explained in the *HP Optoelectronic Designer's Catalog*. The complete logic for the encoder driver including the microprocessor interface is integrated in a gate-array-based VLSI IC.

Device Bus Interface. The interface between the two microprocessors consists of three 8-bit latches. Two latches are used by the main microprocessor to transfer a command and if necessary a bit value to the motor controller. The third latch indicates the status of the motor controller and is readable by the main microprocessor. It is also used to acknowledge receipt of a command on the device bus. The latches are software debounced.

Software

The software is designed to reduce the hardware requirements wherever possible. For this reason, a very simple device bus interface and an inexpensive motor driver interface were possible. The test hardware was also reduced by intelligent software design.

Self-Test. The self-test is divided into two sections. The first section verifies the internal RAM after a power-on reset. If this test fails, the motor controller tries to go into a defined EXIT condition. Otherwise, the second section of the self-test checks the internal timer of the CPU, the timer compare register of the CPU, the external EPROM, the PWM, motor, and encoder of the fixed filter wheel, the PWM, motor, and encoder of the variable filter wheel, and the initial position logic of both encoders.

If an error occurs during the self-test, the motor controller indicates the error and transmits the errors by way of the status latch to the main microprocessor to aid effective troubleshooting. In this case the motors are disabled to prevent damage to the optical system.

Initialization of the Position Sensing System. Since both encoders are incremental encoders, the HP 8158B does not know its position at power-on. Therefore, the software enables the initial channel of the encoders, and turns the motors for a maximum of one revolution. When the index pulse occurs, the 16-bit position counter is cleared and an interrupt tells the motor controller that the encoders are initialized.

Synchronization. After completion of the self-test, or after an error, the motor controller waits for synchronization with the main processor. The main processor starts the synchronization with a special POWER ON keyword in the command register and the value register. The motor controller acknowledges receipt of this keyword by a specific flag combination in the status register. The main processor then sends the TRANSFER FINISH command, which is answered by the READY flag from the motor controller. After this synchronization procedure, the main processor can transfer commands and values to the motor controller.

Transfer of a New Command. A command transfer is similar to synchronization. Normally, the main processor sends TRANSFER FINISH to the command register. The motor controller polls the contents of the command register, waiting for another command. When it finds a stable command in the command register, the motor controller fetches the value register. To acknowledge receipt of the command, it sends BUSY by way of the status register. The main processor then sends TRANSFER FINISH again and the motor controller sets the BUSY flag to READY when it completes execution of the command.

Motor Control Algorithm

Since the motor has practically no friction, the device under control is an extremely unstable third-order system. The transfer function is given by equation 1.

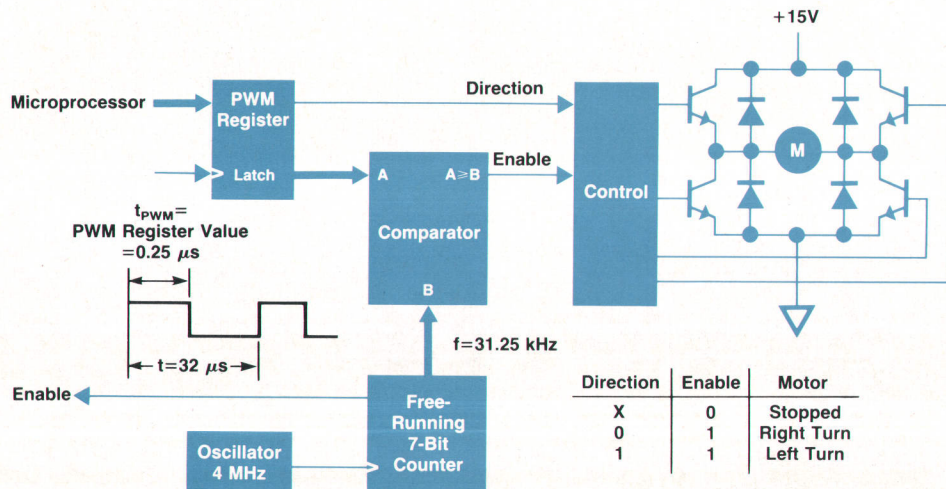$$F(s) = \frac{G}{s(s + \omega_1)(s + \omega_2)}. \tag{1}$$
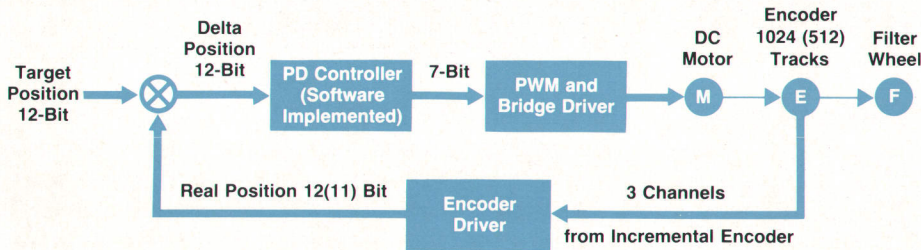

Fig. 6. *Motor drive circuitry.*

Direction	Enable	Motor
X	0	Stopped
0	1	Right Turn
1	1	Left Turn

Fig. 7. *Motor servo loop.*

where G is the gain, ω_1 is the mechanical pole frequency (2 to 8 Hz), and ω_2 is the electrical pole frequency (16.5 kHz).

Different control algorithms were investigated to find a solution that could guarantee a step accuracy of ±1 step of the encoders, a short settling time, and an overshoot less than 1%. One of these algorithms, the deadbeat controller,[3] is very fast and simple, but extremely sensitive to parameter changes. If the temperature changes over a 50° range, the position error resulting from the corresponding change in the motor resistance is 25%.

Another algorithm investigated, the state-variable controller,[4] is an accurate algorithm, but requires one division, six multiplications, and four additions per sample and motor. This needs higher performance than an 8-bit CPU can offer.

A third algorithm, the standard PD controller, is an accurate solution,[5] but it tends towards some instabilities on a third-order system, such as large overshoot and long settling times. For the CPU it is not a problem, requiring only two multiplications and one addition per sample and motor. The HP 8158B uses a standard PD controller, but the software changes the controller gain depending on the actual position. Equation 2 shows the transfer function of an ideal PD controller, while equation 3 gives the corresponding output of a PD controller for a time discrete solution.

$$F_R(s) = G_R \left(1 + \frac{\omega_R}{G_R} \, s\right) \tag{2}$$

$$y_R(n) = G_R x_n + \omega_R \frac{x_n - x_{n-1}}{T_{sample}} \tag{3}$$

where:

$F_R(s)$ = PD controller transfer function
s = Laplace operator
G_R = Gain of PD controller
ω_R = Compensation pole frequency of PD controller
$y_R(n)$ = Output of PD controller at sampling time n
x_n = Input of PD controller at sampling time n
= Delta position.

Every 1.048 ms, the CPU timer produces a timer interrupt. On each interrupt, the interrupt service routine TIMER alternately calls the motor controller routine for the variable filter wheel or the motor controller routine for the fixed filter wheel. These motor controller routines, MOTOR FINE CONTROL and MOTOR COARSE CONTROL, sample the motor positions and calculate the delta position by forming the difference between the target position and the real position. Depending on these delta positions, the control algorithm selects the PD controller gain. For small delta positions, the PD controller shows aperiodic behavior, so the system response is free of overshoot. Otherwise, the controller works with low velocity feedback. This would normally produce a large overshoot but a fast rise time. If the delta position reaches the band with the aperiodic behavior, the higher velocity feedback brakes the motor and prevents a large overshoot.

Fig. 7 shows the schematic of the motor servo loop.

To minimize the dead time between sampling and stimulating the system, the motor controller precalculates the terms involving only the preceding sample.

Acknowledgments

References

1. M. Saruwatari and K. Nowata, "Semiconductor Laser to Single-Mode Fiber Coupler," *Applied Optics*, Vol. 18, 1979, p. 1847.
2. P. Lecoy and H. Richter, *Berechung der Transmission von elliptischen Mikrolinsen zur Optimierung der Kopplung zwischen Halbleiterlaser und Monomodefaser*, Deutsche and Bundespost FTZ, 1979.
3. H.P. Becker, "Entwurf und Realisierung digitaler Regler mit Mikroprozessoren," *Elektronik*, no. 5, March 9, 1984.
4. O. Foellinger, *Lineare Abtastsysteme*, Oldenburg Verlag, 1974.
5. D.C. Tribolet, K.A. Regas, and T.J. Halpenny, "The HP 7550A X-Y Servo: State-of-the-Art Performance on a Budget," *Hewlett-Packard Journal*, Vol. 36, no. 4, April 1985.

A Programmable Fiber Optic Switch

by Michael Fleischer-Reumann

The HP 8159A Optical Switch is a fiber optic switch designed to simplify measurement systems in production and R&D environments. The main feature of the switch is its good repeatability, which means that once its three optical paths are characterized in terms of insertion loss, many reliable measurements can be performed without having to do a recalibration cycle.

The HP 8159A is designed for applications at 850 and 1300 nm with 50-μm graded-index fibers. It has two inputs, **A** and **B**, and two outputs, **C** and **D**. Three optical paths are possible, as shown symbolically on the front panel (Fig. 1): **AC**, **BD**, or **AD**.

The switch has repeatability of 0.2 dB, low insertion loss, HP-IB programmability, and high-precision Diamond® HMS-10/HP connectors that can be taken apart for cleaning.
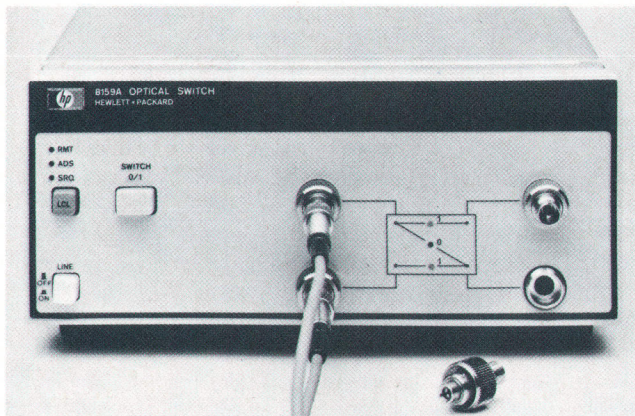

Fig. 1. *The HP 8159A Optical Switch is designed for applications at 850 and 1300 nm with 50-μm graded-index fibers.*

Typical Applications

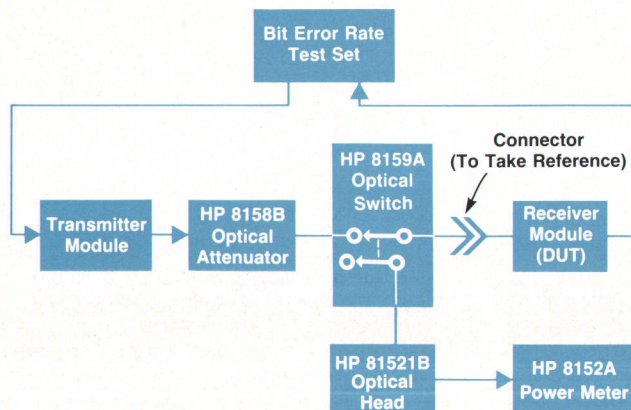Fig. 2 shows a test setup that might be used by a manufacturer of fiber optic links to test the sensitivity of receiver
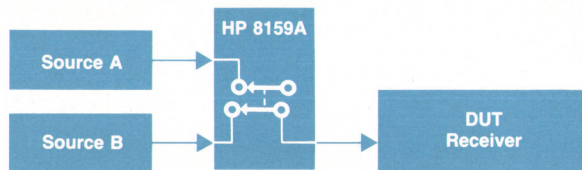

Fig. 2. *Receiver sensitivity test setup.*

Fig. 3. *Testing a receiving element with different sources.*

modules. The manufacturer's own transmitter is driven with the output of a BER (bit error rate) test set, and the electrical output of the receiver under test is the input for the BER test set. The purpose of the programmable attenuator is to find the power level where the BER begins to increase over specified limits.

Since transmitter modules often are not very stable in terms of output power (not temperature stabilized), the source might be drifting. Therefore, after finding the attenuation setting where the BER begins to increase, output power of the transmitter is to be measured. This is easily done by simply switching the transmitter output to a power meter (e.g., HP 8152A) using the HP 8159A Optical Switch. In this application, a power splitter like the HP 81000BS would also be helpful.

In Fig. 3, the reaction of a receiving element (for example, a pin diode or a receiver module) to different types of sources (a laser and an LED or sources of different wavelengths) is being tested. The HP 8159A is used to switch the two sources.

Fig. 4 shows a test setup for a completely optical device (for example, an attenuator). The HP 8159A makes it easy to measure power with and without this device in the optical path.
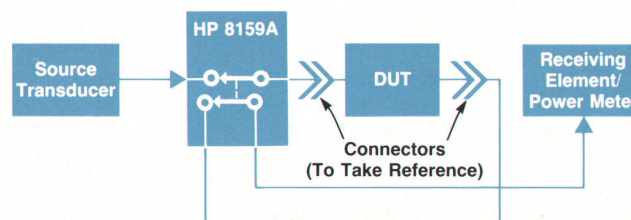

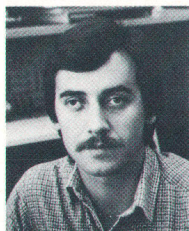**Fig. 4.** *Test setup for an optical device such as an attenuator.*

Acknowledgments

Authors

Michael Fleischer-Reumann

With HP since 1980, Michael Fleischer-Reumann is an R&D project manager at the Böblingen Instruments Division. He was project manager or project leader for several of the fiber optic products described in this issue and continues to manage work on other fiber optic products. Earlier, he contributed to hardware design for the HP 8112A Pulse Generator. He's named inventor on a patent related to pulse generator timing and is author or coauthor of several *HP Journal* articles. Michael was born in Essen and attended the Ruhr University of Bochum, from which he received his Diplom Ingenieur. He and his wife are residents of Nufringen and he teaches electronics at a Stuttgart college. His outside interests include backpacking, hiking, kayaking, playing guitar, and almost all kinds of music.

Horst Schweikardt

An R&D project leader at the Böblingen Instruments Division, Horst Schweikardt has been with HP since 1972. In addition to leading work on the HP 8152A Optical Power Meter and the HP 81521B Optical Head, he has headed project teams for the HP 214B Pulse Generator and other products. He received his Diplom Ingenieur in electrical engineering from the University of Stuttgart in 1972. A native of Baden-Württemberg, he was born in Schwäbisch Gmünd. He and his wife and daughter now live in Herrenberg. His hobbies include bowling, mountaineering, and photography.
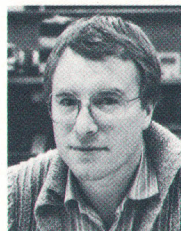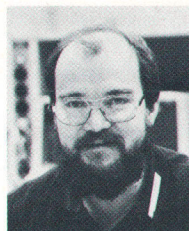
Michael Goder

A native of Wesel am Rhein, Michael Goder studied electronics at Duisburg and received his Diplom Ingenieur in 1979. He joined the Böblingen Instruments Division the same year and has developed HP-IB software for the HP 8152A Power Meter, the HP 8158A Attenuator, and the HP 8154B LED Source. He's coauthor of a 1985 *HP Journal* article on the HP 8151A Power Meter. Michael is married and lives in Gäufelden. He enjoys skiing, photography, and motorcycling.

Bernhard Flade

Bernhard Flade first worked at HP from 1967 to 1970 as an apprentice electrician. He returned to the company in 1981 after earning a degree in communication engineering from the University of Karlsruhe. He has contributed to firmware development for the HP 8150A Optical Signal Source, the HP 8152A Power Meter, the HP 8154A LED Source, and the HP 8158A Attenuator. He's coauthor of a January 1985 *HP Journal* article. Born in Dresden, Bernhard is a resident of Böblingen, is married, and has two children. He's a member of the German and the international associations of ski instructors and a member of a German technical relief organization. When he's not skiing, he may be found riding his Italian motorcycle or working with his home computer.

Josef Becker

With HP since 1979, Jo Becker designed the detector heads for the HP 8152A Power Meter and was responsible for the design of the HP 8180A Data Generator output amplifiers. Before coming to HP he was a biomedical engineer at the University of Stuttgart. He holds a 1969 Diplom Ingenieur in electrical engineering from the University of Karlsruhe. His work on a programmable pulse generator is the subject of a patent and he's the author of over 25 papers on electronic circuits and automated analyses for clinical laboratories. He also lectures on electrical engineering at a local university. Jo was born in Hoengen, Aachen, lives in Sindelfingen, and has three sons. He enjoys astronomy and amateur radio.

Johannes Huning

With HP since 1982, Hans Huning has contributed to the development of the HP 8151A Power Meter and the HP 8150A Optical Signal Source. He also developed a pulsed-laser source for testing the HP 81512A Optical Head. Born in Vreden, he earned his Diplom Ingenieur from the Reinisch Westfälisch Technische Hochschule at Aachen and then joined HP. Hans and his wife and two children are residents of Herrenberg. He likes bicycling with his family, playing chess, and flying gliders.
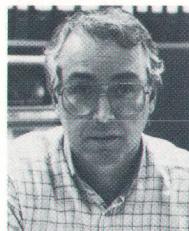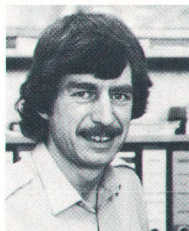
Siegmar Schmidt

With HP since 1984, Siegmar Schmidt has a degree in physics from the Friedrich Schiller University at Jena. He's an optics specialist and worked in that field before coming to HP. He contributed to the development of the HP 8158A/B Attenuators and the HP 81000AS/BS Optical Power Splitters. He's the author of a *Laser Focus* article on the design of the HP 8158B. Born in Jena, Thüringen, Siegmar and his wife and two sons live in Wildberg in the Black Forest region. His hobbies include fishing, windsurfing, and swimming.

Emmerich Müller

With HP since 1981, Emmerich Müller is responsible for hybrid and fiber optic prototypes at the Böblingen Instruments Division. He was born in Villingen and attended the Engineering School in Furtwangen (Black Forest), from which he received his Diplom Ingenieur (FH). He's a coauthor of several *HP Journal* articles and a member of the International Society for Hybrid Microelectronics. Emmerich and his wife and two children live in Gärtringen. His outside interests include cycling and all kinds of skiing.

28 ▭ Optical Connector ▭

### Wilhelm Radermacher

With HP's Böblingen Instrument Division since 1985, Wilhelm Radermacher worked on the Diamond® HMS-10/HP Connector and has contributed to the development of the HP 8154B LED Source and the HP 8159A Optical Switch. Before coming to HP he designed microwave integrated circuits for satellite applications. His Diplom Ingenieur (FH) was awarded in 1978 by the Jülich Engineering School and he earned his Diplom Ingenieur in electronic communications from the Rheinisch Westfälisch Technische Hochschule at Aachen in 1982. Wilhelm was born near Cologne and lives in Sindelfingen. Newly married, he enjoys sailing.

31 ▭ Optical Attenuator ▭

Michael Schlicker

Michael Schlicker was born near Saarbrücken and studied at the Engineering School of Saarland and at the University of Metz in France. He joined HP in 1982 and after working as a materials engineer, he contributed to the development of the HP 8158B Optical Attenuator and other fiber optic products. He has recently left the company. Michael and his wife and two children live in Wildberg, on the edge of the Black Forest. He spends much of his spare time building a house.

Bernd Maisenbacher
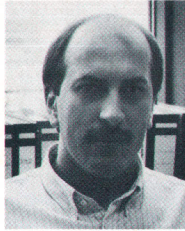
Bernd Maisenbacher was project leader for the HP 8158B Attenuator and is now a project manager with responsibility for fiber optic laboratory instrumentation, including cable and adapter accessories, at the Böblingen Instruments Division. He received his Diplom Ingenieur from the University of Stuttgart and has been with HP since 1981. He's named inventor on two patent applications related to fiber optics. Born in Pforzheim, Bernd is now a resident of Schömberg in the Black Forest region. His outside interests include skiing, dancing, and stamp collecting.

36 ▭ Fiber Optic Switch ▭

Michael Fleischer-Reumann

Author's biography appears elsewhere in this section.

39 ▭ De-Embedding Active Devices ▭

Louis J. Salz

Lou Salz was born in Waterloo, Iowa and completed work for his BS degree in computer engineering from Iowa State University in 1981. He started at HP the same year for the Microwave Technology Division. Recently he has developed computer-aided test software for HP network analyzers. He has also written software for other computer-aided testing tools to support R&D and manufacturing efforts. His professional interests include real-time operating systems and automated test equipment. A resident of Santa Rosa, California, he enjoys bicycling, backpacking, and skiing.

Glenn E. Elmore

Glenn Elmore is an R&D engineer at the Network Measurements Division who has been with HP since 1972. He has worked on various test sets for the HP 8510 family of network analyzers and on the HP 8620 and HP 8350 families of sweep oscillators. His work on test set firmware for the HP 8510A is the subject of a patent and he is coauthor of a 1982 *HP Journal* article on the HP 83500 series plug-ins for the HP 8350A Sweep Oscillator. A California native, Glenn was born in Sebastopol and now lives in nearby Santa Rosa. He's married and has two children. An amateur radio operator (N6GN), his interests include packet and microwave radio communications.

Quality Microwave Measurement of Packaged Active Devices

A special fixture, the HP 8510 Microwave Network Analyzer, and the concept of de-embedding provide a solution to a formerly difficult measurement problem.

by Glenn E. Elmore and Louis J. Salz

COMPONENTS AND DEVICES become more difficult to measure directly at microwave frequencies. Although automatic network analyzers such as the HP 8510 can make direct measurements when used with calibration standards that have the same connector type as the device under test, many times the device cannot be connected directly to the calibration plane of the analyzer. This is the case with packaged transistors. In the past there has been no uniform way to measure such devices to provide useful and accurate data that can be verified by measurements made at different times and places by different operators. As a result, circuits designed using measured data did not always operate as expected. This was for two primary reasons: the measurements were not sufficiently accurate because of instrumentation errors or limitations, and the device environments (the fixtures) were not alike and were often different from the application.

With the advent of the HP 8510 Microwave Network Analyzer, instrumentation to make accurate and rapid error-corrected measurements is available. The need for a standard fixture in which to make packaged transistor measurements for a variety of package styles has become apparent. Accurate calibration of such a fixture is necessary to provide repeatable and accurate device data.

The HP 85014A Active Device Measurements Pac responds to this need by adapting a suitable fixture for optimum operation with the HP 8510 and providing data output formats and archiving capabilities to meet the needs of those involved in measuring and using packaged active devices in the microwave region. The fixture allows the measurement of the two most common package styles through the use of specific fixture inserts for each style of package. Accurate data is provided through the use of the precision coaxial calibration standards available with the HP 8510, together with careful fixture characterization and a technique called de-embedding. De-embedding combines the information a network analyzer obtains from measuring known standards at the analyzer's calibration plane with known fixture characteristics to allow fully error-corrected measurements right at the desired measurement location inside the fixture.

The HP 85014A Active Device Measurements Pac is a software and hardware applications product designed to harness the speed, power, and accuracy of the HP 8510 for the measurement of active devices mounted in the HP 85041A Transistor Test Fixture, Fig. 1 (next page) shows the active device measurement system block diagram.

De-embedding

Conventional calibration standards could be used to allow fixtured device measurements with the HP 8510. For packaged device measurement, such standards would have to be device-like, that is, small packaged opens, shorts, and loads for each type of device to be measured. They should be of quality similar to available coaxial standards. Such standards would cause additional expense and require particular care to use and protect if accuracy were to be maintained. To avoid these difficulties, a different approach was taken.

To allow the HP 8510 to make error-corrected measurements without using in-fixture calibration standards, a process called de-embedding is provided.[1,2,3] After the HP 8510 is calibrated with precision coaxial standards, the software modifies the HP 8510 error-correction process. The analyzer then operates in a normal manner, as if a conventional calibration had been performed at the desired device measurement plane within the fixture.

After measurement, the software acquires the fully error-corrected data from the analyzer and provides a variety of output formats that are specific to active device measurement and design. The resulting data can also be archived in formats compatible with computer circuit analysis programs. This ability provides a vital connection between real device measurement and application product design or transistor fabrication process engineering. Examples of some of the available output formats are shown in Fig. 2.

Distributed Processing

Like many of today's newer instruments, the HP 8510 performs a complex measurement process internally. It is therefore necessary to use new methods to interface the complex system software within the instrument with additional external software. The approach taken with the HP 85014A Active Device Measurement Pac was to use the capabilities of the HP 8510 whenever possible. This approach has resulted in a number of advantages.

The first and most obvious advantage is vastly improved performance of the overall system. By taking advantage of the HP 8510's ability to perform high-speed measurements and error correction in real time, the HP 85014A software is able to eliminate the need for any postprocessing of the data before fully corrected s-parameter data can be displayed. The HP 85014A software only jumps into the measurement process when the instrument cannot perform the needed operations. The modification of the HP 8510's internal error correction is an example of this approach.
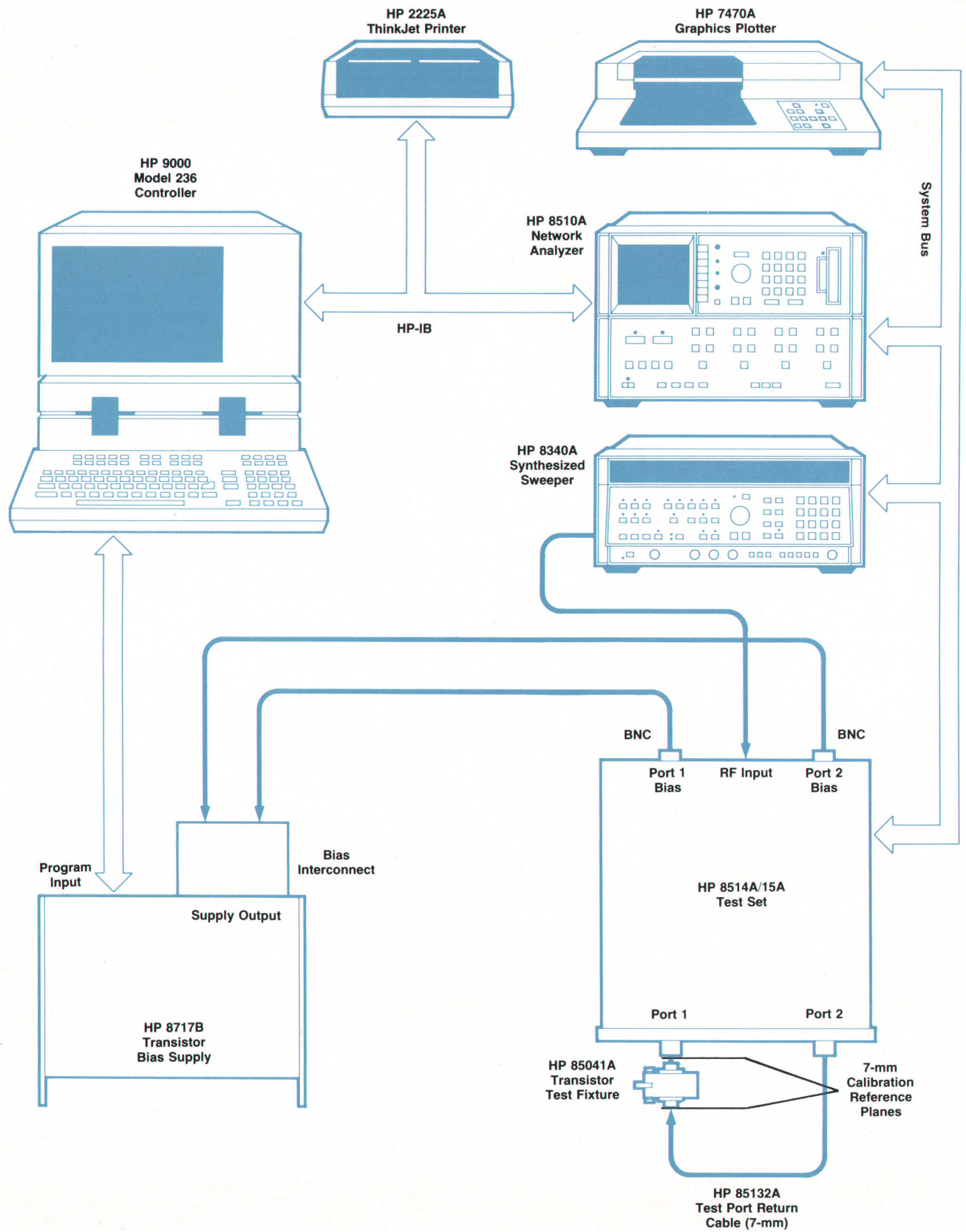
Fig. 1. *Block diagram of a typical system for transistor measurements using the HP 85041A Transistor Test Fixture and the HP 85014A Active Device Measurements Pac.*

The HP 85014A uses the HP 8510's internal error-correction algorithms to measure coaxial standards and produce an error-correction data set that removes the systematic errors in the HP 8510. The HP 85014A software then intervenes by reading these error terms from the HP 8510 and modifying them to include modeled errors introduced by the HP 85041A test fixture. These modified error terms are then returned to the HP 8510 so that the analyzer can perform a fully error-corrected measurement using its built-in algorithms and high-speed processing capabilities. The HP 85014A software from this point on only directs the measurement process within the HP 8510 and reads data from the instrument after the data has been corrected.

A second advantage of the distributed processing approach is the reduced complexity of the HP 85014A software package relative to what would have resulted if more of the measurement process had been included in the external computer. All measurement parameters are set within the measurement package and sent to the HP 8510 to be checked for validity. They are then adjusted to values the HP 8510 can use.

Another benefit is consistency between the HP 8510 and the HP 85014A. Since the measurement pac uses much of the analyzer's system software directly, the feature set of the particular HP 8510 configuration in use is directly apparent to the user of the measurement pac.

Measurement Pac Contributions

Contributions and benefits of the HP 85014A Active Device Measurement Pac include the following:

- Improved HP 85041A Test Fixture designed for more accurate, repeatable, and verifiable measurements. Improvements in fixture repeatability allow precise, controlled measurements to be made to 18 GHz. By controlling fixturing variations the quality of the measured data is improved. Reduction of fixture losses also allows more accurate measurement of devices with high reflection. Another result is improved measurement verification, assuring that measurements made are correct.

- More accurate transistor measurement because of calibration by de-embedding. The use of de-embedding allows precision coaxial standards to be used for calibration. Such standards, along with a carefully controlled and verifiable fixture, yield precision measurements. This allows leveraging available high-quality coaxial standards to provide the best available measurement data.

- Common verifiable measurement environment for industry-wide standardization of transistor measurements. The controlled and modeled characteristics of the fixture and verification device permit rapid verification of the entire measurement system. Data taken with one pac can be verified and directly compared with data taken at other times and places to allow meaningful analysis. This allows device manufacturers and users to communicate more effectively. Better correlation between manufacturers' data sheets and user designs may be obtained.

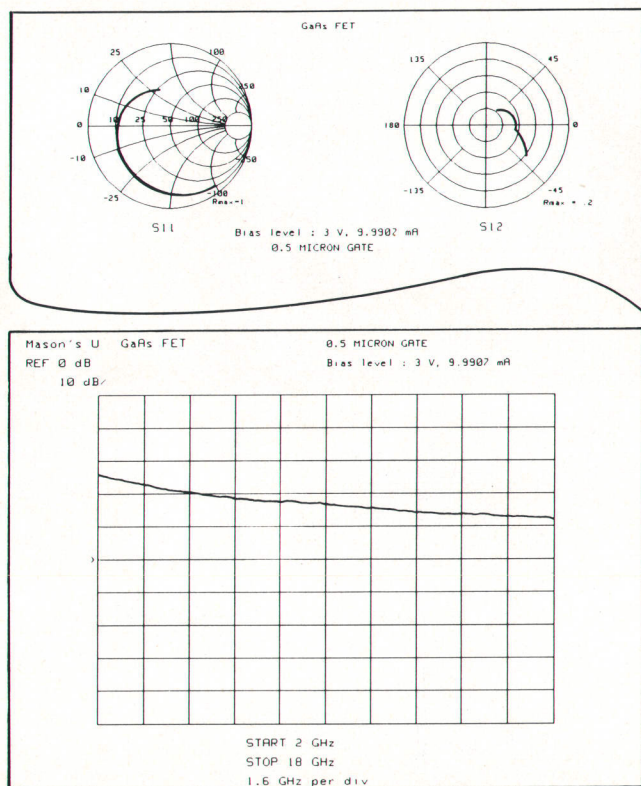- Real-time fully error-corrected display of measured data.

DEMO FET

FREQUENCY MHz	GUmax dB	GAmax dB	|S21|^2 dB	|S12|^2 dB	K	Delay nsec	Mason's U dB	G1 dB	G2 dB
4700.0000	14.42	16.90	7.66	-27.41	1.01	.037	20.653	2.68	4.08
4730.0000	14.38	16.76	7.69	-27.43	1.02	.037	20.803	2.66	4.03
4760.0000	14.35	16.36	7.70	-27.60	1.04	.042	20.506	2.65	4.00
4790.0000	14.29	16.33	7.69	-27.40	1.04	.040	20.371	2.61	4.00
4820.0000	14.25	16.02	7.68	-27.66	1.07	.042	20.061	2.59	3.98
4850.0000	14.18	16.07	7.68	-27.57	1.07	.019	20.314	2.56	3.94
4880.0000	14.19	16.35	7.69	-27.34	1.04	.061	20.906	2.54	3.96
4910.0000	14.14	15.87	7.69	-27.62	1.09	.043	20.077	2.53	3.93
4940.0000	14.10	16.03	7.68	-27.43	1.06	.039	20.611	2.51	3.92
4970.0000	14.10	15.97	7.70	-27.44	1.07	.032	20.413	2.48	3.93
5000.0000	14.03	15.79	7.66	-27.48	1.09	.041	20.253	2.46	3.91

DEMO FET

FREQUENCY MHz	GAMMAm1 MAG	GAMMAm1 ANG	GAMMAm2 MAG	GAMMAm2 ANG	1/S11 MAG	1/S11 ANG	1/S22 MAG	1/S22 ANG
4700.0000	.949	120.1	.966	48.72	1.473	103.9	1.281	39.5
4730.0000	.936	120.3	.957	48.89	1.478	104.5	1.286	39.8
4760.0000	.901	120.5	.933	48.70	1.481	105.0	1.289	39.8
4790.0000	.904	121.6	.936	49.00	1.489	105.6	1.289	40.0
4820.0000	.874	121.8	.916	48.82	1.492	106.4	1.291	40.2
4850.0000	.881	122.3	.920	49.12	1.498	107.1	1.295	40.5
4880.0000	.908	123.2	.939	49.33	1.502	107.5	1.293	40.6
4910.0000	.865	123.5	.909	49.41	1.505	108.1	1.296	40.9
4940.0000	.883	124.3	.922	49.50	1.510	108.9	1.297	41.0
4970.0000	.876	125.1	.918	49.63	1.517	109.6	1.296	41.2
5000.0000	.864	125.5	.910	49.52	1.522	110.2	1.298	41.2

DEMO FET

FREQUENCY MHz	S11 MAG	S11 ANG	S21 MAG	S21 ANG	S12 MAG	S12 ANG	S22 MAG	S22 ANG
4700.0000	.679	-103.9	2.414	86.4	.043	47.1	.781	-39.5
4730.0000	.677	-104.5	2.424	86.0	.043	47.9	.777	-39.8
4760.0000	.675	-105.0	2.426	85.6	.042	48.0	.776	-39.8
4790.0000	.672	-105.6	2.423	85.1	.043	46.9	.776	-40.0
4820.0000	.670	-106.4	2.421	84.7	.041	47.1	.775	-40.2
4850.0000	.668	-107.1	2.421	84.5	.042	47.9	.772	-40.5
4880.0000	.666	-107.5	2.424	83.8	.043	48.3	.773	-40.6
4910.0000	.664	-108.3	2.424	83.4	.042	47.2	.771	-40.9
4940.0000	.662	-108.9	2.420	82.9	.042	48.2	.771	-41.0
4970.0000	.659	-109.6	2.426	82.6	.042	47.3	.771	-41.2
5000.0000	.657	-110.2	2.416	82.2	.042	47.6	.770	-41.2

Fig. 2. *The HP 80514A measurement software offers a variety of output formats. It provides data specific to the design and analysis of transistor amplifiers and oscillators and more conventional s, h, y, and z device parameters.*

Since the desired device data is presented in real time with the errors of the fixture removed from the data, the effects of varying device parameters such as bias or temperature can be directly observed. This direct observation, along with the human ability to synthesize information, allows fundamentally new information about device performance to be obtained. This is of importance in, for example, the design of low-phase-noise oscillators where knowledge of parameter changes as a function of bias may be useful in determining optimum resonator design or coupling.

■ Output formats appropriate to active device measurements. Although the HP 8510 Microwave Network Analyzer can, by itself, provide several different formats of data output, active devices are frequently characterized in additional ways. The active device measurement pac provides amplifier parameters including unilateral, transducer, conjugately matched, and Mason's gain values. Mismatch gain, group delay, and amplifier stability are also available. In addition, termination parameters, useful for amplifier and oscillator design, are provided. These include optimum source and load terminations (to provide maximum available gain) and $1/s_{11}$
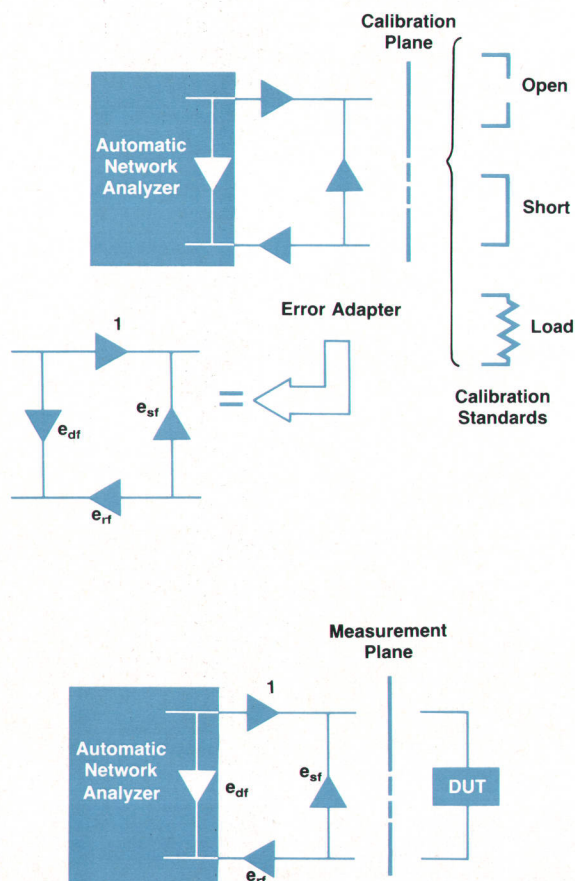
and $1/s_{22}$ for oscillator design. Unformatted output data can be stored for later retrieval and comparison by the measurement pac or stored in a format compatible with circuit analysis and optimization programs.

Automatic Network Analyzer Error Correction

Normally, an automatic network analyzer makes measurements by first going through a process called calibration. This process consists of measuring a number of known devices called calibration standards.

Based on the resulting data and a model of how the characteristics of the microwave hardware in the measurement system contribute to errors in measurement, called an error model or error adapter, the analyzer corrects future measurements to remove the systematic measurement errors. Device measurements are then made as though an errorless network analyzer were located right at the location
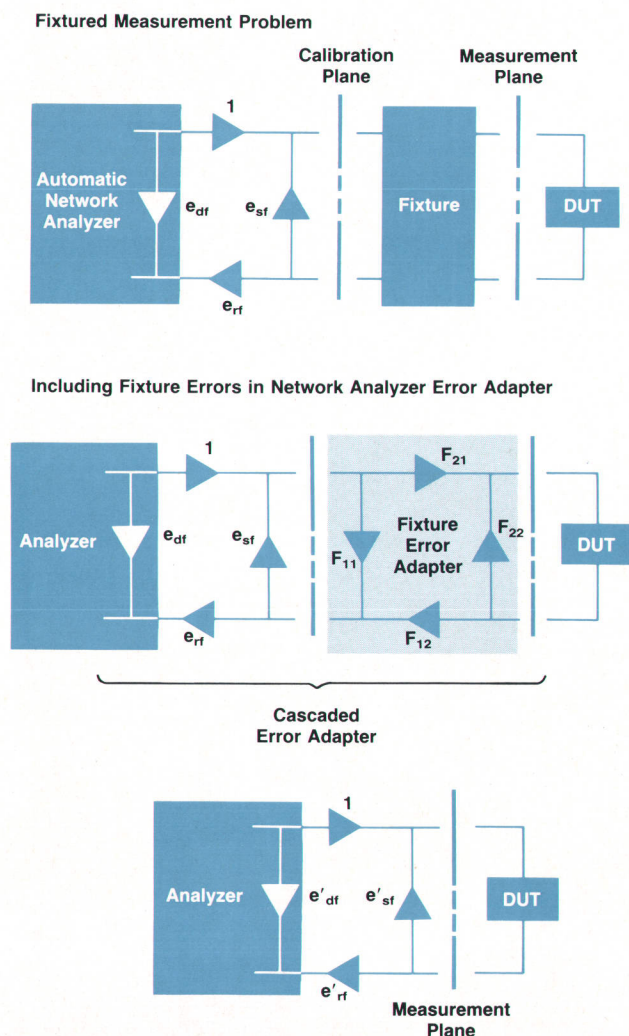

Fig. 3. For one-port error correction when the measurement plane is the same as the calibration plane, known calibration standards are measured first (top) and error-term values for an error adapter are automatically computed by the automatic network analyzer. When the DUT is connected (bottom), these error-term values are used by the analyzer to produce error-corrected data.

Fig. 4. In many cases the device to be measured is not located at the calibration plane. Rather, it is separated by a fixture consisting of adapters, transitions, or other kinds of connecting networks. If these fixture effects are included with the original error terms obtained from calibration and the results returned to the network analyzer, direct measurement of devices embedded within the fixture can be achieved. This is termed a de-embedded measurement.

where the calibration standards were connected.

Fig. 3 shows the network analyzer calibration and measurement process for a one-port test device. The calibration process provides values for an error model of the network analyzer hardware characteristics. Imperfections in connectors and the analyzer's directional device are included here. The error-correction software in the automatic network analyzer then adjusts the measured data to remove the effects of these system imperfections.

For an error-corrected one-port measurement, the network analyzer solves the following equation. Since each term has both magnitude and phase (or alternatively, real and imaginary) components, the solution is performed in the complex domain.

$$s_{11a} = \frac{(s_{11m} - e_{df})}{e_{rf} + e_{sf}(s_{11m} - e_{df})}$$

where s_{11a} = actual s-parameter of the device being measured
s_{11m} = measured (uncorrected) value
e_{df} = error caused by the directional device in the system
e_{rf} = transmission characteristics of the hardware
e_{sf} = error attributable to source match of the system hardware.

Calibration for measurement of two-port devices requires additional calibration standards and a more complex error model. Commonly an open, a short, and a load on each port, as well as a through connection are used. Nine additional error terms are used for a total of twelve error terms in the error model.

For a description of software signal processing in the HP 8510, including error correction, see the box on page 47.

De-embedding Concepts

Conventional calibration and measurement provides the desired data as long as standards that can be attached right at the measurement point are available. For many microwave measurements, calibration cannot be performed at the precise location where data is desired. This is the situation addressed by de-embedding. De-embedding consists of modifying the normal error-correction process of the automatic network analyzer so that the errors introduced by the hardware between the point at which calibration was performed and the desired measurement location can be removed by the error-correction process of the analyzer.

Referring to Fig. 4 and "Automatic Network Analyzer Error Correction" above, the necessary error term modification for de-embedding a one-port measurement can be described. In Fig. 4, F_{11}, F_{21} and F_{22}, F_{12} represent the fixture reflection and transmission s-parameters for port 1 and port 2, respectively. To allow the network analyzer to make the de-embedded measurements, new error terms, e', must be calculated:

$$e'_{df} = e_{df} + \frac{(e_{rf}F_{11})}{(1 - e_{sf}F_{11})}$$

$$e'_{rf} = \frac{(e_{rf}F_{12}F_{21})}{(1 - e_{sf}F_{11})^2}$$

$$e'_{sf} = F_{22} + \frac{(e_{sf}F_{12}F_{21})}{(1 - e_{sf}F_{11})}$$

Here e'_{rf} is set to the product of the forward and reverse terms of the combined network to put the error matrix into the normalized form required by the error analyzer.

These new error terms must be put into the network analyzer for use by its error-correction algorithm. Real-time display of the de-embedded measurement is the result. In the two-port measurement case, nine additional terms must be calculated.

For de-embedded measurements to be possible, errors caused by the intervening hardware must be known at the time of measurement.

The HP 85041A Transistor Test Fixture is designed to play the role of accurately known hardware to make de-em-
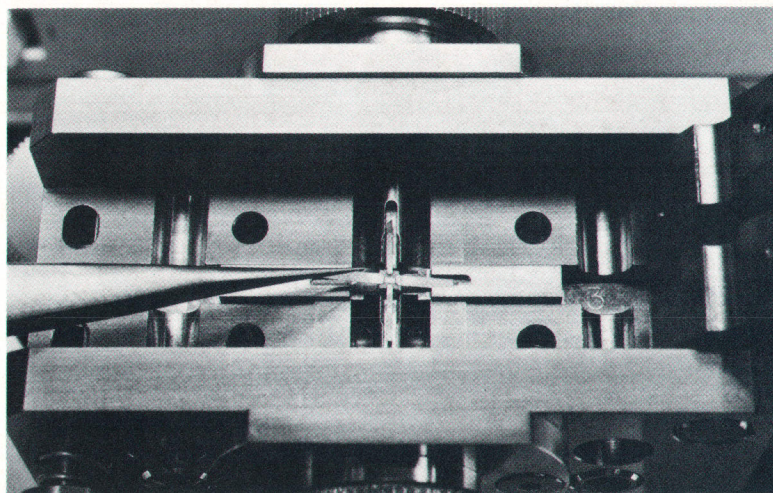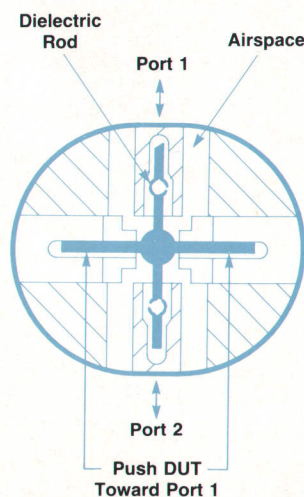

Fig. 5. In the HP 85041A Transistor Test Fixture, the transistor leads fit into troughs to determine the device location accurately.
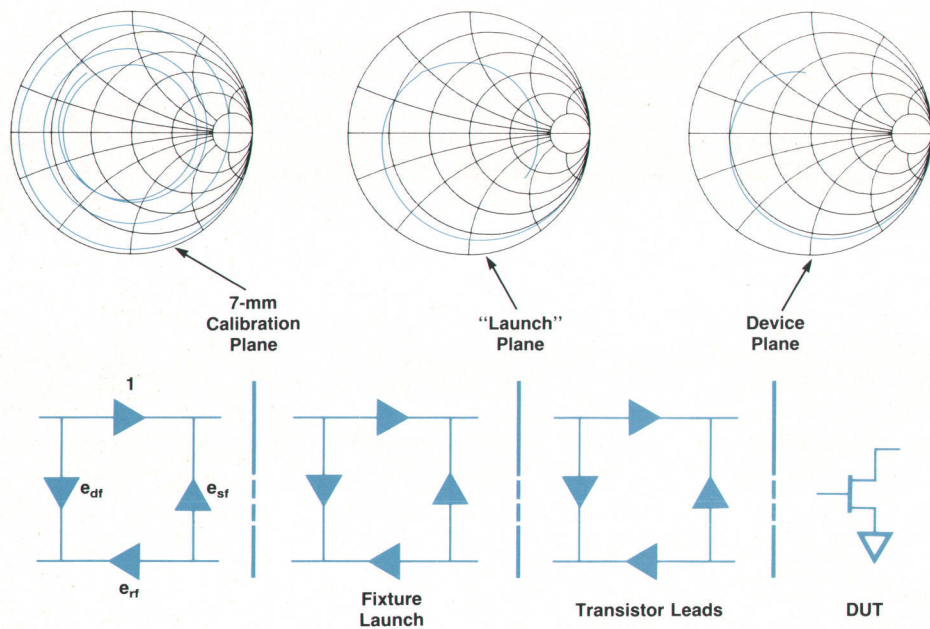
Fig. 7. Measurement of s_{11} of a 0.5-μm gallium arsenide field effect transistor. *(left) A measurement without de-embedding includes losses and reflections introduced by the entire fixture. (center) The measurement with the effects of errors caused by the fixture body halves removed. (right) Errors caused by the entire fixture—body halves, leads, and parasitics—removed by de-embedding.*

bedding possible. The fixture is shown in Figs. 5 and 6.

Fig. 7 shows the results, as first the fixture effects and then the transistor leads themselves are removed from the measured data by de-embedding. The device is a 0.5-μm gate length GaAs FET.

Fixture Characterization for Accurate De-embedding

The function of a fixture is to provide a convenient connection to the measurement system. Often a fixture is used to provide information about how a device will perform in a proposed application. In such a situation, it is important that a fixtured measurement be nondestructive of the device under test and relatable to the application.

A fixture used for network measurement should transmit energy from the network analyzer to the device under test with minimum loss and reflection. If the characteristic impedance of the device to be measured is greatly different from that of the network analyzer, it may be necessary for the fixture to provide impedance transformation. In any case the fixture must efficiently couple the device to the analyzer while perturbing the measurement as little as possible.

For an error-corrected measurement, careful hardware characterization is necessary to allow the errors to be removed from the measurement, leaving only device data. In any measurement, it is desirable to understand not only the numerical value of errors introduced by the measurement process, but also the fundamental causes of errors and how they relate to the application as well as the measurement.

This characterization can be performed in a number of ways. The most common way is through the conventional calibration process already described. Various types of standards can be used with a variety of techniques to quantify the errors in the system hardware including the fixture. An alternative is to calibrate (characterize) the system
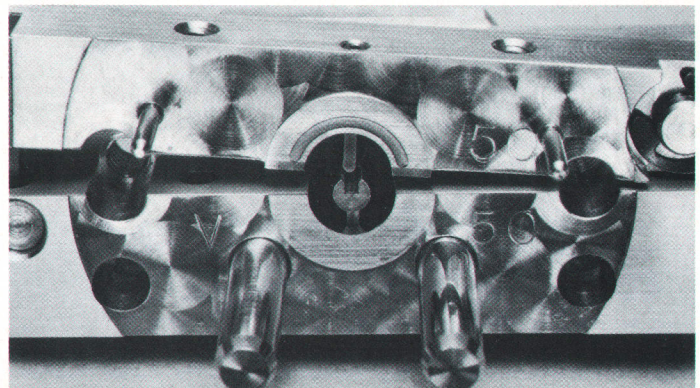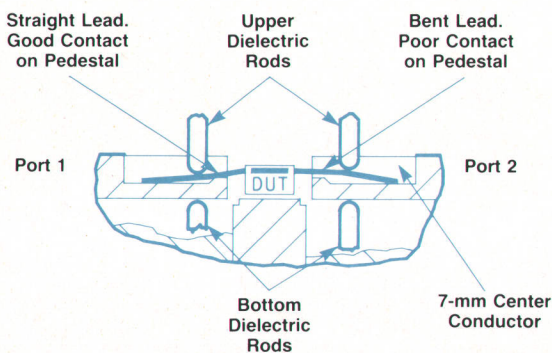

Fig. 6. *(a) Dielectric rods ensure well-defined connection to the through leads in the HP 85041A fixture. Common leads are grounded very close to the transistor package by sandwiching them between the top and bottom halves of the fixture insert. Inserts can be changed to accommodate different package styles. (b) One body half, showing dielectric rods, center conductor, and conductive elastomer.*
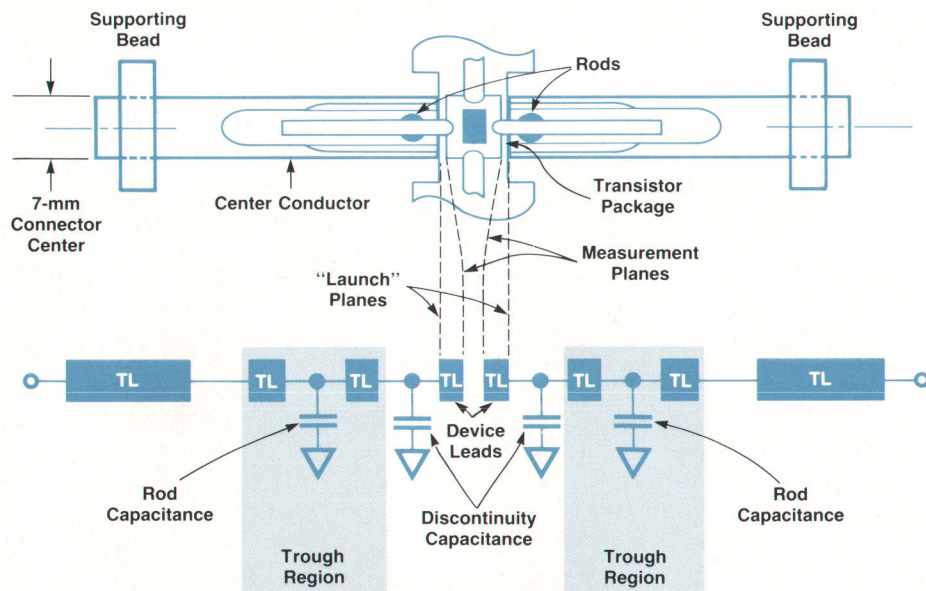
Fig. 8. The final fixture model has good correlation with the physical fixture and its measured electrical characteristics. (TL indicates transmission line with impedance, length, and loss.)

hardware excluding the fixture with the conventional process and available precision standards. The fixture can then be separately characterized and the two characterizations combined to allow error-corrected measurements inside the fixture. This alternative is termed de-embedding.

In a sense, the fixture offsets the calibration standards used to characterize the rest of the microwave hardware just before the time measurements are to be made. For the measurement to be accurate, the description (model) of this offsetting network must reflect reality at the time of measurement. The fixture essentially becomes part of the calibration standards used to arrive at the device measurement. For high-quality measurements, whether de-embedded or not, the fixture must be well-controlled and have known, repeatable characteristics.

The fixture itself can be characterized for de-embedding in more than one way. Direct measurement is one obvious method. However, direct measurement of the fixture implies the availability of calibration standards that might be used to characterize the entire system in a more conventional manner not requiring de-embedding. Also, this approach requires either that the measurements always be at the same frequencies as the original fixture measurements or that some kind of interpolation be performed to provide values based on the original data points. Such interpolation generally requires smooth, well-behaved performance between the original data points.

Another method is to use a model of the fixture to calculate fixture parameters. This model can be an equivalent circuit model or an analysis based on physical dimensions. In any case the modeling must produce a sufficiently accurate representation of the fixture's actual performance at the time it is used for device measurement. Representing a fixture in this way has the advantage of automatically providing values at arbitrary frequencies within the valid range. Additionally, the modeling process may help to uncover discrepancies between intended fixture operation and actual performance, which simple measurement may not reveal. This is of great importance in understanding

the overall measurement process and applying the results to any final application.

The second approach, that of using a circuit model to represent the fixture, was used with the HP 85041A Transistor Test Fixture.

Fixture Development and Characterization

At the outset of the project, a commercially available fixture was selected. This fixture provided a degree of device package flexibility and manufacturing precision important for the project. As can be seen in Fig. 5, the fixture consists of symmetrical body halves between which is sandwiched an insert. The transistor or other device to be tested rests in the insert, which is tailored for the particular device package style. The through leads of the device contact the coaxial center conductor of the body halves. These halves effectively act as adapters between 7-mm coaxial connectors and the device package leads.

The common leads of the device are sandwiched between the top and bottom halves of the insert to provide a low-impedance ground connection. Good contact to the through leads is assured by spring-loaded dielectric rods in the lid. Each rod holds a through lead against the bottom of a trough in the end of the coaxial center conductor (Fig. 6a).

The top portion of the insert and the top part of the coaxial body half are hinged. This allows access for device insertion and removal by simply opening the lid.

Very soon after we set out to characterize (model) the fixture, the real-time measurement ability of the HP 8510 revealed that there were some fixture nonrepeatabilities. The connections made by the lid to the fixture body were not consistent and could result in considerable reflection and loss. To combat this problem, a cylindrical conductive elastomer was installed in grooves in the four mating surfaces of the lid to act as microwave gaskets. This significantly improved the fixture repeatability and also reduced insertion loss.

Fig. 6b shows one body half without insert. The conductive elastomer is visible in the lid.

To begin the modeling process, the fixture was considered in smaller sections rather than as a whole. One half of the body of the fixture, without insert, was examined first. Special coaxial devices that attached at the plane of the insert were available. Although these devices were not in themselves of sufficient quality and design to characterize the fixture adequately, they did provide a starting point. Problems not only with the devices but with providing reliable connection to the fixture were obvious and gave insight about how a better characterization might be performed. Best results were finally achieved by measuring a short made from thin shim brass. The flexibility of this material allowed good contact to be made to the ends of the coaxial center and outer conductors. Repeatability of measurement not only for a given fixture half but also from half to half was ascertained. This was possible since the entire fixture is symmetrical. These measurements indicated that differences between shim-shorted half fixtures were at least 40 dB down (less than 1%).

Once a good-quality short and high fixture repeatability were obtained, as evidenced by smooth, near-unity reflection coefficient across the entire 45-MHz-to-18-GHz range, further measurements were made. An open-circuit measurement was made using one of the special coaxial devices as a shield for the open. This shielding was necessary to prevent radiation from the open end of the fixture. A two-port measurement was made of the two body halves connected together with no insert. A small shim was placed between the center conductors to assure good contact. The outer conductor contact was already assured by the conductive elastomer. The data from these measurements was read by a computer and a circuit analysis and optimization program was used. This program allowed a tentative circuit model of the fixture half to be developed and provided circuit values that best fit the measured data for all three measurements. Initial topology for the circuit model came from physical examination of the fixture. The coaxial structure was represented as series-connected lossy transmis-

sion lines with discontinuities at their junctures represented by a fringing capacitance, which was allowed to be frequency dependent.

The model for the open half-fixture includes an unknown fringing capacitance at its end in addition to internal capacitances which were common to all three models. Initial values, as well as limits for these values, were obtained through physical examination of the fixture. For example, the overall physical length of the body half and the locations of discontinuities resulting from supporting beads, the slotted center conductor, and the dielectric were easily measured. Allowing the optimizer to select values for line impedance, loss, and discontinuity capacitance yielded a circuit model that is a good fit to all three sets of measured data. Examining and optimizing a portion of the complete fixture instead of the entire fixture as a whole speeded up the process and gave results that more nearly matched physical reality. Solutions that fit the data but were not physically accurate were avoided. Additionally, greater understanding of the nature of the fixture was obtained.

Final results for modeling two connected fixture halves yielded a model that fits the measured data within better than -40 dB (1%) for all measurements.

Along the way it was possible to use the current best model to perform a de-embedded measurement of the two fixture halves connected together without insert. This, along with measurement of the shim short, gave a direct indication of the quality of the model, since residue or error in the model was directly visible in real time. The through connection looked very nearly like a zero-length, lossless, reflectionless transmission line. Similarly, the short appeared as a near-unity reflection at 180° on the Smith chart over the entire frequency range.

Corresponding calibrations performed with the special coaxial standards mentioned above were typically 15 dB worse than this. Thus, the effort to characterize and understand the fixture resulted in a considerable improvement in measurement accuracy and, perhaps as important, a
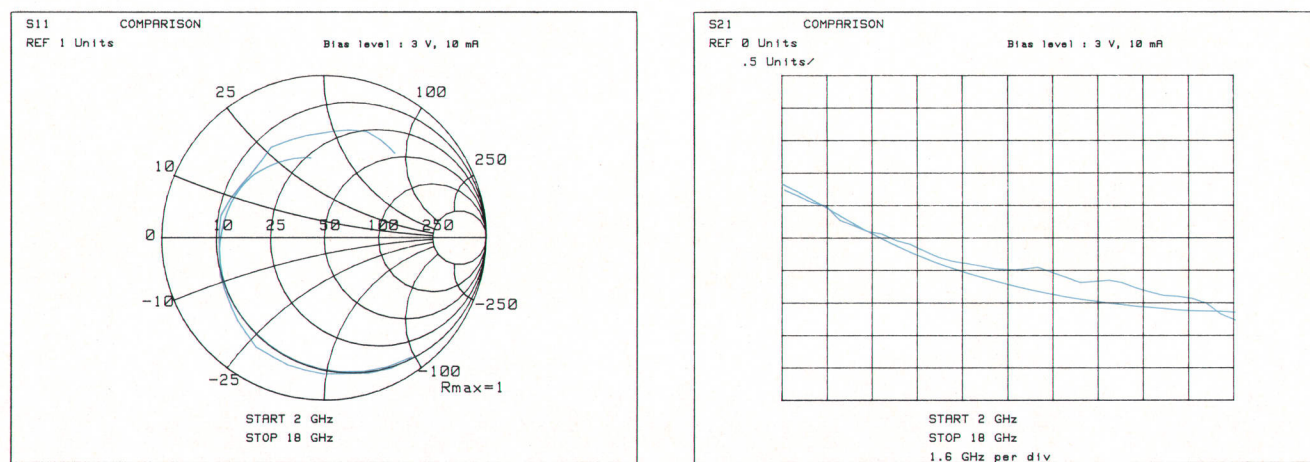

Fig. 9. *Modeling and de-embedding along with improvements in the fixture result in a significant improvement in transistor measurements. Improvements in trace smoothness over previous measurements[4] (black trace) are evident with the HP 85014A (color trace). The same packaged GaAs FET with the same bias conditions is being measured in both examples. The transistor, which is small in terms of measurement wavelengths and has a relatively simple structure, can be expected to have a smoothly varying response as a function of frequency.*

commensurate improvement in understanding of the fixture's operation, its limitations, and areas where additional work might provide maximum return.

Once a good model for the body was obtained (residue more than 40 dB below unity reflection for both short and through connection), the insert and transistor characteristics and parasitics were arrived at in a similar iterative manner, but this time using special transistor-like standards inside the inserts. Here again the process involved using measurements of the best characteristics of available standards and using an analysis/optimization program to generate a circuit and values to fit. As before, this iterative process yielded new understanding of the operation, which led to modification of the measurement process and reoptimization of the circuit model topology and values.

Fig. 8 shows the final model used for the transistor test

HP 8510 Software Signal Processing

Digital signal processing in the HP 8510 Microwave Network Analyzer (Fig. 1) begins at the output of the synchronous detector pair, which provides the real (X) and imaginary (Y) parts of the test and reference signals. Offset, gain, and quadrature errors are corrected for both of the IF/detector chains before the test vector is ratioed against the reference vector. The result is an unprocessed s-parameter stored into the raw array. If requested by the HP 8510 user, subsequent data points taken at the same frequency are averaged together using a stable averaging technique, thus enhancing the HP 8510's dynamic range.

While the raw array is continually filled under control of the data acquisition software, the data processing software concurrently removes data from the raw array and controls additional signal processing. Using error coefficients that model the microwave measurement hardware, the data is further corrected through a set of vector math operations. This corrected data can be converted from the frequency domain to the time domain using the chirp z-transform technique. Storage into a data array allows quick response to the user when making format or trace math changes.

Data can be stored into memory and used in vector computations with data from a second device. Comparison is accomplished through vector division, subtraction, or simultaneous display of data and memory.

The vector data is reformatted into magnitude, phase, group delay, or other formats. It is stored into the format array, which provides convenient access for scale and offset changes. Scaled data is stored into a display list, from which the display generator hardware repetitively creates a plot on the CRT for a flicker-free display.

Input and output access is provided to all the arrays via the HP-IB (IEEE 488/IEC 625). S-parameters can be obtained from the data array. Direct plotter output is from the format array.

The user can trade off the data update rate against the number of data points by selecting resolutions from 50 to 400 points.

A multitasking software architecture provides the fastest possible update rate by allowing data processing to take place when the data acquisition software is not busy. Overlying command and control tasks interleave data processing with acquisition cycles for two-port error correction and dual-channel display modes.

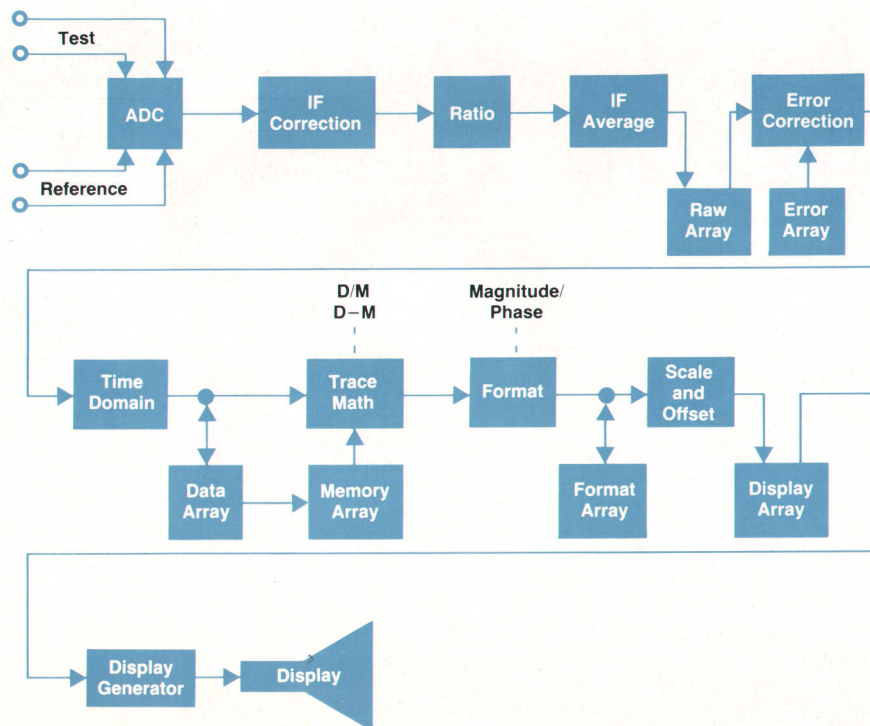*Michael Neering*
Project Manager
Network Measurements Division

Fig. 1. HP 8510 Automatic Network Analyzer software signal processing.

fixture.

Application of the Data

Since the transistor or other active device is not generally mounted in the application as it is in the fixture, some correcting network may be desirable to correlate fixture-measured device parameters with those of an application. A correlating network can be obtained using techniques similar to those described above. Such networks depend upon the application. For example, in a microstrip application, the board thickness and common lead grounding techniques can affect device operation. Once the differences between the test fixture and the application are known, these differences can be included with fixture-measured data to predict the performance of the device in the application accurately. Such fixture/application differences are of most concern at higher frequencies and for devices with impedances greatly different from 50Ω.

The de-embedded measurements that result from the models developed have proven themselves to be considerably better than any available before. Fig. 9 demonstrates the results of fixture improvements and de-embedding calibration techniques.

Even without accounting for differences in mounting technique in the application, data from the HP 85014A Active Device Measurements Pac has been used to achieve finished amplifier results very close to computer predicted values at 10 GHz. Constructed amplifiers have been measured with results within a few tenths of a dB of those predicted by fixture-measured data and a circuit analysis program. It is believed that the dominant sources of variation in measurements are operator technique and package characteristics. Bent leads, variations in plating, and the positioning of the device in the fixture are critical parameters, particularly above 12 GHz. This is to be expected when one considers that a few thousandths of an inch variation in package position can easily cause several degrees of error in the phase of a reflection measurement.

Verification

For the HP 85041A Transistor Test Fixture, the verification standard is a small planar cross similar in dimension to a packaged transistor. Using such a device allows the fixture's common lead characteristics to be verified also. This verification or check device is mechanically simple

and provides a good way to verify system performance. Although this device is a good conductor, it is not a perfect short from the point of view of the measurement planes, having both length and loss. To make the verification process easier, a special model was developed to de-embed the check device's nonideal characteristics from the verification measurement. Doing this effectively normalizes the check device to appear very nearly like an ideal short, although it in fact has some reactance and loss. The actual value of the measurement is not of importance, since the goal is only to verify that the proper data is obtained and that a calibration is good. This normalization by de-embedding the measurement calibration using the check short normalizer model and measuring the check short allows quick and easy verification of the system. The transmission characteristics of the fixture are effectively verified by the two one-port reflection measurements, since the stimulus signal must travel from the connectors to the center and back for such measurements. Although use of a single standard does not completely characterize (verify) a two-port fixture, experience has shown that a broadband measurement of the check device provides a high degree of certainty of fixture performance.

References

1. R.F. Bauer and P. Penfield, Jr., "De-embedding and Unterminating," *IEEE Transactions on Microwave Theory and Techniques*, Vol. MTT-22, March 1974, pp. 282-288.
2. G. Elmore, "De-embedded Measurements Using the HP 8510 Microwave Network Analyzer," Hewlett-Packard RF and Microwave Symposium, 1985.
3. G. Elmore, "De-embed Device Data with a Network Analyzer," *Microwaves and RF*, November 1985, pp. 144-146.
4. R. Lane, R. Pollard, M. Maury, and J. Fitzpatrick, "Broadband Fixture Characterizes Any Packaged Transistor," *Microwave Journal*, October 1982, p. 104.